Aus der Klinik für Innere Medizin – Kardiologie
des Deutschen Herzzentrums Berlin

DISSERTATION

Über die Differenzierung verschiedener Herzinsuffizienzentitäten mittels neuer Bildgebungsparameter der kardialen Magnetresonanztomographie

zur Erlangung des akademischen Grades
Doctor medicinae (Dr. med.)

vorgelegt der Medizinischen Fakultät
Charité – Universitätsmedizin Berlin

von

Moritz Daniel Blum

aus Stuttgart

Datum der Promotion: 04.03.2022

Inhaltsverzeichnis

1. Abstracts auf Deutsch und Englisch **4**

1.1 Abstract (Deutsch) **4**

1.2 Abstract (English) **5**

2. Einführung **6**

2.1 Pathophysiologie der Herzinsuffizienz **6**

2.2 Bildgebung in der Diagnostik der Herzinsuffizienz **7**

2.3 Drei potentielle CMR-Parameter für die Diagnostik der Herzinsuffizienz **8**

3. Methoden **10**

3.1 Studienpopulation **10**

3.2 Studienprozeduren **11**

3.3 Fast-SENC-Strainmessung vor und während isometrischer HG-Belastung **12**

3.4 Multilayer-Strainmessung **13**

3.5 Gewebecharakteriserung mittels Tissue-Mapping **13**

3.6 Statistische Methoden **13**

4. Ergebnisse **14**

4.1 Veränderung von Fast-SENC Strain während isometrischer HG-Belastung **15**

4.2 Multilayer-Strain zur Differenzierung von HFpEF und Herzgesunden **16**

4.3 Gewebecharakterisierung mittels Tissue-Mapping **16**

5. Diskussion **17**

5.1 Myokardialer Strain – ein vielversprechender Bildgebungsparameter? **17**

5.2 Der Effekt erhöhter kardialer Nachlast auf myokardiale Kontraktilität **18**

5.3 Heterogene Strainänderung bei HI-PatientInnen in Folge von HG-Belastung **19**

5.4 Multilayer-Strain zur Diagnostik von HFpEF **20**

5.5 Tissue-Mapping zur Gewebecharakterisierung bei HI **21**

5.6 Limitationen **22**

5.7 Fazit **22**

6. Referenzen **24**

7. Eidesstattliche Versicherung und Anteilserklärung **29**

7.1 Eidesstattliche Versicherung **29**

7.2 Anteilserklärung an den erfolgten Publikationen **30**

8. Druckexemplare der ausgewählten Publikationen **32**

9. Lebenslauf **64**

10. Publikationsliste **65**

11. Danksagung **69**

1. Abstracts auf Deutsch und Englisch

1.1 Abstract (Deutsch)

Hintergrund: Innovationen in der kardialen Magnetresonanztomographie (CMR) ermöglichen heute die Messung von myokardialen Verformungsparametern (Strain) und Gewebeeigenschaften. Ziel dieser Studie war die Erprobung neuer CMR-Parameter zur Differenzierung von Herzinsuffizienz (HI) mit reduzierter, mittelgradiger und erhaltener Ejektionsfraktion (HFrEF, HFmrEF, HFpEF) und Herzgesunden.

Methoden: PatientInnen mit etablierter HI-Diagnose sowie Herzgesunde wurden klinisch, labormedizinisch und mittels CMR untersucht. Ausgeschlossen wurden unter anderem Menschen mit CMR-Kontraindikationen und instabilem klinischem Zustand. Linksventrikulärer globaler longitudinaler Strain (LV GLS) wurde vor und während isometrischer Handgrip-Belastung (HG) mittels *fast strain-encoded CMR* (Fast-SENC) bestimmt. Mittels *feature-tracking* wurde der LV GLS für die subendokardiale, intra-myokardiale und subepikardial Myokardschicht bestimmt (Multilayer-Strain). *Tissue-Mapping* zur Bestimmung von nativer T1- und T2-Relaxationszeit sowie extrazellulärem Volumen (ECV) wurde durchgeführt. Zur statistischen Auswertung kamen unter anderem *analysis of variance*, Pearson-Regressionskoeffizienten und die Fläche unter der *receiver operating characteristic*-Kurve (AUC) zum Einsatz.

Ergebnisse: Insgesamt wurden 72 TeilnehmerInnen (Kontrollgruppe: n=19; HFpEF = 17; HFmrEF: n= 18; HFrEF: n=18) in die Studie eingeschlossen.

Die mittlere Änderung des LV GLS während HG betrug +1.2 ± 5.4% in der Kontrollgruppe, −0.6 ± 8.3% bei HFpEF, −1.7 ± 10.7% bei HFmrEF und −3.1 ± 19.4% bei HFrEF ($p = 0.746$). Der Betrag der LV GLS Änderung unabhängig vom Vorzeichen unterschied sich signifikant zwischen den Subgruppen (Kontrollgruppe: 4.4 ± 3.2%; HFpEF: 5.9 ± 5.7%; HFmrEF: 6.8 ± 8.3%; HFrEF 14.1 ± 13.3%; $p = 0.005$) und korrelierte mit NTproBNP und Lebensqualitätsmetriken.

In der Multilayer-Strain-Analyse unterschied sich LV GLS sowohl subendokardial (−20.8 ± 4.0 vs. −23.2 ± 3.4, $p = 0.046$) als auch intra-myokardial (−18.0 ± 3.0 vs. −21.0 ± 2.5, $p = 0.002$) und subepikardial (−12.2 ± 2.0 vs. −16.2 ± 2.5, $p < 0.001$) signifikant zwischen HFpEF und Herzgesunden. Insbesondere subepikardialer LV GLS differenzierte hervorragend zwischen HFpEF und Herzgesunden (AUC 0.90, 95% Confidence Interval 0.81-1).

Die per Tissue-Mapping bestimmte native T1-Relaxationszeit war bei HFrEF (1033 ± 54 ms) und HFmrEF (1027 ± 40 ms) im Vergleich zu HFpEF (985 ± 32 ms) und Kontrollgruppe (972

± 31 ms) angehoben, ebenso die T2-Relaxationszeit (Kontrollgruppe: 50.6 ± 2.1 ms; HFpEF: 52.6 ± 3.6 ms; HFmrEF: 55.4 ± 3.4 ms; HFrEF 56.0 ± 6.0 ms). ECV unterschied sich hingegen nicht signifikant.

Fazit: Fast-SENC Strainmessung während HG liefert nur begrenzt diagnostisch verwertbare Informationen. Tissue-Mapping lässt strukturelle Ähnlichkeit von HFmrEF und HFrEF erkennen. Subepikardialer LV GLS ist ein vielversprechender diagnostischer Parameter zur Differenzierung von HFpEF und Herzgesunden.

1.2 Abstract (English)

Background: Novel developments in cardiac magnetic resonance imaging (CMR) allow for quantification of myocardial strain and tissue characteristics. In this study we sought to evaluate the diagnostic utility of novel CMR parameters in heart failure (HF) with reduced, mid-range and preserved ejection fraction (HFrEF, HFmrEF, HFpEF) and healthy controls.

Methods: Patients with an established diagnosis of HF and controls underwent physical examination, lab work and CMR. Exclusion criteria included CMR contraindications and unstable clinical status. Left ventricular global longitudinal strain (LV GLS) was measured before and during isometric handgrip (HG) using fast strain-encoded CMR. LV GLS was quantified on a subendocardial, mid-myocardial and subepicardial level employing feature tracking (multilayer strain). Using tissue mapping, native T1 and T2 relaxation times and extracellular volume (ECV) were quantified. Statistical methods included analysis of variance, Pearson's coefficients and the area under the receiver operating characteristic curve (AUC).

Results: The study comprised 72 subjects (Controls: n=19; HFpEF = 17; HFmrEF: n= 18; HFrEF: n=18).

Mean change of LV GLS during HG was +1.2 ± 5.4%, −0.6 ± 8.3%, −1.7 ± 10.7% and −3.1 ± 19.4% in controls, HFpEF, HFmrEF and HFrEF, respectively (p = 0.746). The absolute value of LV GLS change differed significantly between subgroups. (Controls: 4.4 ± 3.2%; HFpEF: 5.9 ± 5.7%; HFmrEF: 6.8 ± 8.3%; HFrEF 14.1 ± 13.3%; p = 0.005) and correlated with NTproBNP and quality-of-life scores.

Multilayer strain analysis showed significant differences in LV GLS between HFpEF and controls on subendocardial (−20.8 ± 4.0 vs. −23.2 ± 3.4, p = 0.046), mid-myocardial (−18.0 ± 3.0 vs. −21.0 ± 2.5, p = 0.002) and subepicardial levels (−12.2 ± 2.0 vs. −16.2 ± 2.5, p < 0.001). Subepicardial LV GLS in particular facilitated excellent discrimination between HFpEF and controls (AUC 0.90, 95% Confidence Interval 0.81-1).

Tissue mapping showed elevated native T1 relaxation times in HFrEF (1033 ± 54 ms) and HFmrEF (1027 ± 40 ms) compared to HFpEF (985 ± 32 ms) und controls (972 ± 31 ms) and a similar pattern regarding T2 relaxation times (controls: 50.6 ± 2.1 ms; HFpEF: 52.6 ± 3.6 ms; HFmrEF: 55.4 ± 3.4 ms; HFrEF 56.0 ± 6.0 ms). ECV did not differ significantly between subgroups.

Conclusion: The diagnostic utility of measuring strain during HG appears to be limited. Tissue mapping reveals structural similarities of HFmrEF and HFrEF. Subepicardial LV GLS is a promising diagnostic parameter discriminating between HFpEF and healthy subjects.

2. Einführung

2.1 Pathophysiologie der Herzinsuffizienz

Der Terminus Herzinsuffizienz (HI) bezeichnet ein klinisches Syndrom, das durch die Symptome Dyspnoe, zunächst bei körperlicher Belastung, und Erschöpfung gekennzeichnet ist und von typischen klinischen Zeichen wie Beinödemen, pulmonalen Rasselgeräuschen oder erhöhtem Jugularvenendruck begleitet wird.[1] Die HI betrifft einen beträchtlichen Teil insbesondere der älteren Bevölkerung westlicher Industrienationen und geht mit einem erheblichen Verlust an Lebensqualität sowie einer Fünf-Jahres-Mortalität nach Erstdiagnose von bis zu 50% einher.[2,3]

Innerhalb der letzten zwei Dekaden haben sich wissenschaftliche Beobachtungen gemehrt, die nahelegen, dass dem einheitlichen klinischen Syndrom der HI separate Krankheitsentitäten zugrunde liegen, die sich pathophysiologisch voneinander unterscheiden.[4] Auffälligstes Unterscheidungskriterium ist zunächst die systolische linksventrikuläre Ejektionsfraktion (LVEF), die bei ungefähr der Hälfte der HI-PatientInnen reduziert, bei der anderen Hälfte jedoch erhalten ist.[1] Bei letzteren PatientInnen sind hingegen vor allem Parameter der Ventikelrelaxation und –füllung gestört, was die Begriffe systolische und diastolische HI nahelegte, bevor 2016 in den Leitlinien der *European Society of Cardiology* (ESC) für den europäischen Raum die Termini *heart failure with reduced ejection fraction* (HFrEF), *heart failure with preserved ejection fraction* (HFpEF) und *heart failure with mid-range ejection fraction* (HFmrEF) etabliert wurden.[1] Ätiologisch wird HFrEF mit einer Schädigung des Myokards in Verbindung gebracht, die regional durch ischämische Ereignisse oder global beispielsweise durch Infektion und Inflammation bei Myokarditis oder genetische Aberrationen im Fall von dilatativen Kardiomyopathien auftreten kann.[1] Bei HFpEF hingegen wird ätiologisch ein Zusammenspiel von metabolischen Veränderungen wie Adipositas, arterieller Hypertonie (HTN) und Diabetes mellitus (DM) angenommen, die durch Induktion von Zytokinausschüttung einen systemischen pro-inflammatorischen Zustand bedingen. Hierdurch wird die Signaltransduktion von myokardialem Endothel auf das Myokard derart moduliert, dass Kardiomyozyten zunehmend hypertrophieren und myokardiale Fibroblasten vermehrt Kollagen produzieren, was zu konzentrischer Hypertrophie und erhöhter Wandsteifigkeit führt.[5] Infolgedessen ist die myokardiale Relaxation gestört, linksventrikuläre Füllungsdrücke steigen und der linke Vorhof wird belastet, was den pathophysiologischen Zustand der diastolischen Dysfunktion (DD) konstituiert.

Auch in Bezug auf therapeutische Möglichkeiten unterscheiden sich HFrEF und HFpEF. Für HFrEF stehen mit Beta-Blockern, Inhibitoren des Renin-Angiotensin-Aldosteron-Systems und in ausgewählten Fällen Neprilysin-Inhibitoren, Ivabradin, implantierbaren Kardioverter-Defibrillatoren (ICD) oder kardialer Resynchronisationstherapie (CRT) diverse Therapien zur Verfügung, die in Studien die Mortalität reduzieren konnten.[1] Bei HFpEF konnte bis zum heutigen Tag für keine therapeutische Intervention ein Überlebensvorteil demonstriert werden. Symptomatisch können Diuretika bei Zeichen der Volumenüberladung eingesetzt werden. Ansonsten sind die therapeutischen Möglichkeiten auf die Kontrolle von Komorbiditäten wie HTN, DM und Adipositas beschränkt. Nicht zuletzt wegen der unterschiedlichen therapeutischen Konsequenzen ist die akkurate und frühzeitige Erkennung und Differenzierung der verschiedenen HI-Entitäten ein wichtiger Bestandteil der kardiologischen Diagnostik.

2.2 Bildgebung in der Diagnostik der Herzinsuffizienz

Bildgebenden Verfahren kommt ein hoher Stellenwert in der diagnostischen Aufarbeitung der HI zu.[1] In der klinischen Praxis spielt die transthorakale Echokardiographie (TTE) als Erstlinienmodalität die größte Rolle. Nachteile der TTE sind allerdings Untersuchervariabilität, die insbesondere durch Variation des Anlotungswinkels und damit verbundener perspektivischer Verkürzung bedingt ist, schlechte Einsehbarkeit des rechten Ventrikels sowie schwierige Untersuchungsbedingungen auf PatientInnenseite wie Luftüberlagerung oder Adipositas.[6]

Bezüglich dieser Nachteile ist die kardiale Magnetresonanztomographie (CMR) der TTE überlegen. Sie stellt den Goldstandard zur akkuraten Quantifizierung kardialer Volumina sowie der LVEF dar. Zudem ermöglicht die CMR die Darstellung myokardialer Fibrose und so eine Einschätzung der Ätiologie einer HI sowie eine Einschätzung der Viabilität einzelner Myokardsegmente vor potentieller Revaskularisierung.[7] Aktuell gehört die CMR allerdings nicht zur Routinediagnostik der HI, was vor allem an den hohen Kosten, der begrenzten

Verfügbarkeit sowie der aktuell häufig noch zeitaufwendigen Untersuchung liegt, die flaches Liegen über längere Zeit sowie Atemhaltemanöver beinhaltet. Zudem gelten für die CMR strenge Kontraindikationen, insbesondere die vorangegangene Implantation eines ferromagnetischen ICD sowie Platzangst.

Ein Bildgebungsparameter, der zunehmend Einzug in die Diagnostik der Herzinsuffizienz erhält ist die myokardiale Verformung (Strain). Das Konzept des Strain entstammt der Kontinuumsmechanik und beschreibt auf das Herz übertragen die lokale Verformung des Myokards während der Herzaktion. Wird das Herz in würfelförmige Myokardsegmente unterteilt, so kann die Verformung jedes dieser Segmente entlang dreier Achsen, der longitudinalen, der circumferentiellen und der radialen, quantifiziert werden. Mittelt man nun die lokalen Strainwerte aller Myokardsegmente, kann ein globaler Strain entlang jeder der drei Achsen angegeben werden, der als quantitatives Maß für die Verformungseigenschaften des Myokards dient.[8] Je nach Ausrichtung der Messachse wird von *global longitudinal strain* (GLS), *global circumferential strain* (GCS), *global radial strain* (GRS) gesprochen.

Die Quantifizierung von Strain in der CMR ist mittels verschiedener technischer Ansätze, wie zum Beispiel *feature tracking* (FT) möglich.[9] Die *fast strain-encoded CMR* (Fast-SENC) hebt sich dadurch von anderen Messmethoden ab, als dass sie es ermöglicht in kürzester Zeit während einer einzigen Herzaktion in freier Atmung Strain zu quantifizieren, was Untersuchungszeit und PatientInnenbelastung durch Atemhaltemanöver minimiert.[10] In früheren Studien konnte unsere Gruppe zeigen, dass Fast-SENC gut reproduzierbare Strainwerte liefert und darüber hinaus auch die schnelle Quantifizierung von linksventrikulären Volumina und LVEF ermöglicht. [11–13]

Eine weitere Innovation auf dem Gebiet der CMR ist das parametrische *Tissue-Mapping*, das es ermöglicht Gewebeeigenschaften des Myokards basierend auf T1- und T2-Relaxationszeit zu quantifizieren. Auch das extrazelluläre Volumen (ECV) kann rechnerisch bestimmt werden. Auf diese Weise können Rückschlüsse auf pathophysiologische Gewebeveränderungen wie Ödem und Entzündung, Fibrose oder Einlagerung von Amyloidprotein oder Eisen gezogen werden.[14]

2.3 Drei potentielle CMR-Parameter für die Diagnostik der Herzinsuffizienz

Die vielen Innovationen auf dem Gebiet der CMR haben großes Potential, die Diagnostik der HI und insbesondere die Unterscheidung von der HI-Entitäten für klinische sowie für Forschungszwecke zu optimieren. Im Rahmen der *Study to analyze parameters of internal and external cardiac power, cardiac output and aortic compliance using cardiac magnet resonance* *imaging in patients with heart failure* rekrutierten wir TeilnehmerInnen mit HFrEF, HFmrEF und HFpEF sowie Herzgesunde, die sich freiwillig einer CMR unterzogen, um Unterschiede in Bezug auf potentiell diagnostische Bildgebungsparameter zu untersuchen. Für die vorliegende Dissertation werden drei Analysen experimenteller diagnostischer Ansätze vorgestellt, deren Rationale im Folgenden kurz erörtert werden soll:

Dyspnoe und Ermüdung sind Symptome der HI, die in frühen Stadien der Erkrankung zunächst nur bei körperlicher Anstrengung auftreten. Daher ist es wenig überraschend, dass Untersuchungen unter physischer Belastung bei der Diagnose der HI eine wichtige Rolle spielen, um Funktionsstörungen am Myokard aufzudecken. Insbesondere bei der Diagnose von HFpEF kommen Stressuntersuchungen zum Einsatz, um eine DD zu demaskieren.[1,15] Eine simple und breit verfügbare, klinisch jedoch selten eingesetzte Methode zur Induktion kardiovaskulärer Belastung ist die Handgrip-Untersuchung (HG), bei der ein Handdynamometer über einige Minuten durch isometrische Muskelkontraktion komprimiert wird.[16] HG führt zu einem akuten Anstieg der kardialen Nachlast und stellt so einen hämodynamischen Stressor dar, der myokardiale Dysfunktion aufdecken könnte.[17] Mittels Fast-SENC lässt sich Strain schnell und reproduzierbar innerhalb eines einzigen Herzschlages in freier Atembewegung quantifizieren.[10,11]

In der Studie *Variability of Myocardial Strain During Isometric Exercise in Subjects With and Without Heart Failure*[18] untersuchten wir daher, inwieweit sich die Veränderung des myokardialen Fast-SENC-Strain während HG-Belastung zwischen PatientInnen mit HFrEF, HFmrEF und HFpEF und Herzgesunden unterscheidet und diagnostisch nutzen lässt.

Die Architektur der myokardialen Muskelfasern ist komplex und variiert innerhalb der Herzwand: Während die epikardialen Fasern diagonal orientiert sind, verlaufen intra-myokardiale Fasern eher circumferentiell und subendokardiale Fasern longitudinal entlang der Herzachse.[19,20] Mittels FT-CMR ist eine hochauflösende Erfassung des Strains innerhalb der einzelnen Wandschichten möglich (Multilayer-Strain).

In der Studie *Multilayer myocardial strain improves the diagnosis of heart failure with preserved ejection fraction*[21] untersuchten wir, ob die differenzierte Erfassung von subendokardialem, intra-myokardialem und subepikardialem Strain die diagnostische Unterscheidung von PatientInnen mit HFpEF und Herzgesunden verbessert.

Unterschiede in der Pathophysiologie legen die Hypothese nahe, dass sich die verschiedenen HI-Entitäten auch in Bezug auf die myokardialen Gewebeeigenschaften unterscheiden

könnten. Parametrisches Tissue-Mapping mittels CMR ermöglicht es, Myokardgewebeeigenschaften quantitativ zu charakterisieren und könnte so auch die diagnostische Differenzierung unterstützen sowie Einblicke in die Pathophysiologie geben.[14] Insbesondere die myokardialen Gewebeeigenschaften bei HFmrEF, welches als HI-Entität explizit definiert wurde, um eine intensivere Beforschung dieses Begriffes anzuregen, könnten hier von Interesse sein.
In der Studie *CMR Tissue characterization in patients with HFmrEF*[22] untersuchten wir daher, inwieweit PatientInnen mit HFrEF, HFmrEF und HFpEF sowie Herzgesunde im Hinblick auf ihre Gewebeeigenschaften mittels CMR-basiertem Tissue-Mapping besser charakterisiert werden können.

3. Methoden

Die *Study to analyze parameters of internal and external cardiac power, cardiac output and aortic compliance using cardiac magnet resonance imaging in patients with heart failure* (EMPATHY-HF) war eine prospektive, *single-center* Querschnittsstudie. Das Studienprotokoll wurde vom Ethikausschuss 4 am Campus Benjamin Franklin der Charité Universitätsmedizin Berlin am 28. Oktober 2016 genehmigt und die Studie beim Deutschen Register Klinischer Studien angemeldet (ID: DRKS00015615). Alle TeilnehmerInnen gaben nach einem ausführlichen Informationsgespräch und ausreichender Bedenkzeit ihre schriftliche Einwilligung. Die Studie wurde unter Einhaltung der Deklaration von Helsinki sowie der Satzung der Charité – Universitätsmedizin Berlin zur Sicherung Guter Wissenschaftlicher Praxis vom 20.06.2012 durchgeführt.

3.1 Studienpopulation

Die TeilnehmerInnenrekrutierung fand von April 2017 bis November 2018 in der Kardiologischen Studienambulanz der Charité Universitätsmedizin, Campus Virchow Klinikum am Augustenburger Platz 1, 13353 Berlin statt. Die Einschlusskriterien richteten sich nach der jeweiligen Subgruppe, in die die TeilnehmerInnen aufgenommen werden sollten und forderten die Erfüllung aller Kriterien der aktuellsten HI-Leitlinie der ESC.[1] Alle TeilnehmerInnen mussten mindestens 45 Jahre alt und krankenversichert sein. HI-PatientInnen mussten seit mindestens sieben Tagen unverändert mit leitliniengerechter Medikation behandelt und in klinisch stabilem Zustand sein (keine intravenöse Diuretikagabe, keine Inotropikatherapie, keine Hospitalisierung), des Weiteren unter symptomatischer Dyspnoe Klasse II oder III nach New York Heart Association (NYHA) leiden und zudem im Labor ein

NTproBNP von ≥220 pg/ml aufweisen. Für TeilnehmerInnen mit HFrEF war eine LVEF <40% gefordert, für TeilnehmerInnen mit HFmrEF und HFpEF der Nachweis einer LV Hypertrophie (Septumdicke >12 mm) oder einer DD (E/e' >13 oder Linksatrialer Volumenindex >34ml/m^2) sowie eine LVEF von 40-49% für HFmrEF, beziehungsweise ≥50% für HFpEF.
Für einen Einschluss in die Kontrollgruppe, die im Verlauf auch als Herzgesunde bezeichnet wird, war der Ausschluss von strukturellen Herzerkrankungen, höhergradigen Klappenvitien und relevanten Herzrhythmusstörungen sowie die Freiheit von Symptomen der HI und der koronaren Herzerkrankung (KHK) gefordert.
Ausschlusskriterien für alle Subgruppen umfassten: Geschäftsunfähigkeit, Vorhofflimmern, höhergradige Klappenvitien, Angina-Pectoris-Symptome, hypertroph-obstruktive oder infiltrative Kardiomyopathien, komplexe kongenitale Vitien, aktive Myokarditis, höhergradige Herzrhythmusstörungen, höhergradige Lungenerkrankungen, eine vor weniger als vier Monaten stattgehabte oder geplante Koronarintervention oder Koronararterien-Bypass-Operation, ein vor weniger als drei Monaten stattgehabter Myokardinfarkt oder Schlaganfall, stattgehabte oder geplante Herztransplantation, geplante Änderung der Medikation, eine innerhalb der letzten vier Monate stattgehabte Implantation eines ICD oder eines Herzschrittmachers, eine innerhalb der letzten drei Monate stattgehabte Implantation einer CRT, unkontrollierte systolische Hypertension (>180 mmHg) oder Hypotension (<95 mmHg), eingeschränkte Nierenfunktion mit einer geschätzten glomerulären Filtrationsrate <40 ml/min, eine unbehandelte Schilddrüsenerkrankung, eine Anämie (Hämoglobin <10mg/dl), Platzangst in der Vorgeschichte sowie jegliche Implantate, die eine CMR Kontraindikation darstellen.

3.2 Studienprozeduren

Alle StudienteilnehmerInnen wurden zunächst umfassend zur medizinischen Vorgeschichte sowie zu Symptomen der HI befragt, körperlich untersucht und zur Gewinnung von venösem Blut für Laboruntersuchungen punktiert. Auch ein Elektrokardiogramm (EKG) wurde abgeleitet. Alle TeilnehmerInnen füllten außerdem den *Minnesota Living With Heart Failure Questionnaire* (MLHQ) aus und wurden einem Sechs-Minuten-Gehtest unterzogen. Im weiteren Verlauf erfolgte bei allen StudienteilnehmerInnen eine Echokardiographie sowie eine CMR-Untersuchung.
Die CMR wurden in einem 1.5 Tesla Scanner (Achieva, Philips Healthcare, Best, Niederlande) durchgeführt. Cine-Aufnahmen wurden in der Kurz-Achsen-Ebene (SA), Zwei-Kammer-Blick (2Ch), Drei-Kammer-Blick (3Ch) und Vier-Kammer-Blick (4Ch) in balancierter Steady-State-Free-Precession-Technik (bSSFP) mit retrospektivem EKG-Gating aufgenommen. Alle

aufgezeichneten CMR Sequenzen wurden im CMR-Corelab des Deutschen Herzzentrum Berlin von speziell trainierten Mitarbeitern zentral ausgewertet. Kardiale Volumina und Dimensionen wurden mit der Software Medis® Suite 3.1.16.8 (Medis medical imaging systems, Leiden, Niederlande) bestimmt.

3.3 Fast-SENC-Strainmessung vor und während isometrischer HG-Belastung

Im Rahmen des HG-Experiments wurden zusätzlich Fast-SENC-Sequenzen in SA-, 2Ch-, 3Ch- und 4Ch-Ebene in freier Atmung aufgenommen.[10] Hierzu wurden bei den TeilnehmerInnen nach 15 Minuten Ruhe in Rückenlage zunächst Blutdruck (RR) und Herzfrequenz (HF) gemessen. Dann wurde die Fast-SENC-Sequenz in körperlicher Ruhe aufgenommen. Als nächstes wurden die StudienteilnehmerInnen gebeten, ein MRT-sicheres Handdynamometer (Stoelting, Wood Dale, Illinois) für 3 Minuten mit 30% der Maximalkraft ihrer dominanten Hand zu komprimieren, die vor Beginn des Experimentes ermittelt worden war. Dabei wurden StudienteilnehmerInnen instruiert, kontinuierlich weiter zu atmen, um valsalvamanöverbedingte Änderungen der kardialen Vorlast und konsekutiv der Herzfrequenz zu vermeiden. Sodann wurden RR und HF erneut gemessen und die Fast-SENC Sequenz unter HG-Bedingungen aufgezeichnet.

Für die Fast-SENC Strain Messung wurde die Software MyoStrain 5.0 (Myocardial Solutions, Inc., Morrisville, North Carolina, USA) verwendet. Die Verläufe von Endo- und Epikardium wurde manuell sowohl in der End-Systole als auch in der End-Diastole markiert und dann während des Herzzyklus automatisiert nachverfolgt. Zur Quantifizierung von GLS wurden die SA-Aufnahmen auf drei Schnittebenen (apikal, mittig, basal) ausgewertet, der Longitudinalstrain für jedes Segment bestimmt und abschließend zu einem globalen Strain gemittelt. Zur Quantifizierung von GCS wurden 2Ch-, 3Ch- und 4Ch-Aufnahmen ausgewertet und der circumferentielle Strain der einzelnen Segmente gemittelt. Da die Strainmessung mittels Fast-SENC technologisch auf der Aufzeichnung von Magnetisierungssignalen parallel zur Bildebene basiert, wird – anders als bei anderen *Tagging*-Methoden – longitudinaler Strain aus kurzachsigen CMR-Aufnahmen und circumferentieller Strain aus langachsigen CMR-Aufnahmen ermittelt. Als weitere Konsequenz hieraus ergibt sich, dass radialer Strain per Fast-SENC nicht zu bestimmen ist. Eine frühere Studie zu Intra- und Inter-Untersuchervariabilität von Fast-SENC-Strain Messungen zeigte sehr gute Reproduzierbarkeit.[11]

3.4 Multilayer-Strainmessung

Für die Erfassung des Multilayer-Strains wurden bSSFP-Cine-Sequenzen mit Hilfe der Softwarepakete QMass Version 8.1 und QStrain RE (Medis Medical Imaging Systems, Leiden, Niederlande) ausgewertet, die auf FT-Technologie basiert.[9] Endo- und epikardiale Konturen wurden manuell in End-Systole und End-Diastole markiert und automatisiert den Herzzyklus über nachverfolgt. Für die Bestimmung von GCS wurden SA-Aufnahmen auf drei Schnittebenen (apikal, mittig, basal), für GLS die 2Ch-, 3Ch- und 4Ch-Aufnahmen herangezogen und GLS und GCS jeweils für die subendokardiale, intra-myokardiale und subepikardiale Wandschicht quantifiziert.

3.5 Gewebecharakteriserung mittels Tissue-Mapping

Zur Gewebecharakterisierung wurde StudienteilnehmerInnen mit Herzinsuffizienz 0.15 mmol gadoliniumhaltiges Kontrastmittel (KM) pro Kilogramm Körpergewicht appliziert (Gadobutrol 1.0 mmol/ml). T1-Tissue-Mapping wurde nativ sowie 15 min nach KM Applikation mittels *modified look-locker inversion recovery* (MOLLI) durchgeführt.[23] T2-Tissue-Mapping wurde nativ mittels der andernorts beschriebenen *gradient spin echo technique* (GraSE) durchgeführt.[24] Aufgrund kürzlich bekanntgewordener Ablagerungen von gadoliniumhaltigem KM im zentralen Nervensystem mit noch unklarer klinischer Signifikanz wurde bei StudienteilnehmerInnen der Kontrollgruppe aufgrund von Nutzen-Risiko-Abwägungen kein gadoliniumhaltiges KM eingesetzt.

Im Rahmen des Tissue-Mapping kam das Softwarepaket QMap RE Version 2.0 (Medis Medical Imaging Systems, Leiden, Niederlande) zum Einsatz. Native T1- und T2-Relaxationszeit wurden aus MOLLI, beziehungsweise GraSE Sequenzen errechnet. Das ECV wurde aus nativer T1-Relaxationszeit und T1-Relaxationszeit 15 Minuten nach KM Applikation sowie dem Hämatokrit, der bei der vorangegangenen venösen Blutuntersuchung gemessen wurde, bestimmt.[25] Da die StudienteilnehmerInnen der Kontrollgruppe wie oben beschrieben kein KM erhalten hatten, konnte für diese Gruppe kein ECV ermittelt werden. Stattdessen wurden publizierte Werte einer ähnlichen Gruppe gesunder Probanden zum Vergleich verwendet.[26]

3.6 Statistische Methoden

Verteilungen von kontinuierlichen Variablen wurden mit dem Shapiro-Wilk Test auf Normalverteilung überprüft, als arithmetisches Mittel ± Standardabweichung wiedergegeben und Gruppenunterschiede mittels t-Test für unabhängige Stichproben, dem gepaarten T-Test oder *analysis of variance* (ANOVA) auf statistische Signifikanz überprüft. Post-hoc Testung bei signifikanter ANOVA wurde mittels Tukey-Test durchgeführt. Die Verteilungen kategorialer Variablen werden als absolute Häufigkeit (relative Häufigkeit in Prozent) wiedergegeben und mittels Chi-Quadrat-Test auf statistische Signifikanz überprüft. Für lineare Korrelationen zwischen zwei kontinuierlichen Variablen wurde Pearson-Koeffizienten berechnet. Diagnostischer Nutzen wurde anhand der *area under the curve* (AUC) der *receiver operating characteristic* (ROC) Kurve beurteilt. Zweiseitige p-Werte <0.05 wurden als statistisch signifikant erachtet.

Der Stichprobenumfang wurde pragmatisch in Anbetracht verfügbarer CMR-Kapazitäten und ähnlicher Studien gewählt. Die erreichte TeilnehmerInnenzahl pro Subgruppe war im Durchschnitt n=18. Die Standardabweichung der LV GLS Änderung während HG betrug gerundet ±12. Eine Powerberechnung ergab, dass eine ANOVA unter diesen Prämissen einen Subgruppenunterschied in Bezug auf die Strainänderung während HG von ±5 auf einem Signifikanzniveau von 0.05 mit einer Power von 0.83 detektieren konnte.

Kontraktion eines myokardialen Segments ergibt per definitionem negative Strainwerte. Stärkere Kontraktion führt also mathematisch zu einer Abnahme des Strainwertes noch weiter ins Negative. Aus Gründen der besseren Nachvollziehbarkeit wird allerdings im Folgenden stärkere Kontraktion als Strainzunahme bezeichnet, auch wenn der numerische Strainwert abnimmt und vice versa schwächere Kontraktion als Strainabnahme, auch wenn der numerische Strainwert zunimmt.

Statistische Berechnungen wurden mit den Softwares R Version 3.5.1 (2018-07-02) (R Foundation for Statistical Computing, Wien, Österreich) und SPSS 24 (IBM, Armonk, New York, USA) durchgeführt.

4. Ergebnisse

Die präsentierten Ergebnisse sind bereits andernorts publiziert.[18,21,22]

Insgesamt wurden 72 TeilnehmerInnen in die Studie eingeschlossen (HFrEF: n=18; HFmrEF: n= 18; HFpEF = 17; Kontrollen: n=19). Tabelle 1 in Blum et al. 2020 charakterisiert die Studienpopulation im Detail.[18] Aufgrund des Fehlens verwertbarer Messungen mussten für die Multilayer-Strain- und Tissue-Mapping-Experimente teilweise TeilnehmerInnen ausgeschlossen werden, was die leicht variierenden TeilnehmerInnenzahlen in den einzelnen Experimenten erklärt. Die Subgruppen unterschieden sich in Bezug auf demographische und klinische Eigenschaften: In der HFrEF-Gruppe waren Männeranteil, BMI und Raucher-Packyears am höchsten. HFmrEF-PatientInnen waren am häufigsten von KHK betroffen, hatten aber größtenteils nur milde Dyspnoesymptomatik. HFpEF-PatientInnen waren am ältesten, am häufigsten von DM und HTN betroffen und zeigten die stärkste Gehstreckeneinschränkung im Sechs-Minuten-Gehtest.

4.1 Veränderung von Fast-SENC Strain während isometrischer HG-Belastung

Hämodynamische Parameter und Fast-SENC Strain vor und während isometrischer HG-Belastung sind in Tabelle 2 in Blum et al. 2020 detailliert ausgeführt.[18] HG-Belastung führte in allen Subgruppen zu einem Anstieg von systolischem und diastolischem RR, HF und Pulsdruck.

LV GLS und LV GCS waren sowohl vor als auch während HG-Belastung am höchsten in der Kontrollgruppe und nahmen von HFpEF über HFmrEF zu HFrEF stufenweise ab (Tabelle 2, Blum et al. 2020).[18] Die durchschnittliche prozentuale Strainänderung während HG-Belastung unterschied sich nicht nicht signifikant zwischen den Subgruppen, weder für LV GLS (Kontrollen: +1.2 ± 5.4%; HFpEF: −0.6 ± 8.3%; HFmrEF −1.7 ± 10.7%; HFrEF −3.1 ± 19.4%; p = 0.746) noch für LV GCS (Kontrollen: −0.8 ± 11.0%; HFpEF: +3.1 ± 11.6%; HFmrEF +10.8 ± 48.6%; HFrEF −2.4 ± 18.1%; p = 0.467).

Auf individueller Ebene konnte die Strainänderung während HG sowohl positiv als auch negativ sein (Figur 4, Blum et al. 2020).[18] Während sich positive und negative Änderung in allen Subgruppen größtenteils die Balance hielten, wie an den um null rangierenden durchschnittlichen Änderungen ersichtlich, unterschied sich die Spannweite der Strainänderung deutlich zwischen den Subgruppen. Beispielsweise waren Minimum und Maximum der LV GLS Änderung -11.0% und +10.0% in der Kontrollgruppe, im Vergleich zu -42.0% und +32.0% in der HFrEF Gruppe.

Auf Basis dieser Beobachtung untersuchten wir den Betrag der prozentualen Strainänderung während HG, ungeachtet des Vorzeichens der Änderung und fanden signifikante Unterschiede zwischen den Subgruppen für sowohl LV GLS (Kontrollen: 4.4 ± 3.2%; HFpEF: 5.9 ± 5.7%; HFmrEF: 6.8 ± 8.3%; HFrEF 14.1 ± 13.3%; p = 0.005) als auch für LV GCS (Kontrollen: 8.6 ± 6.6%; HFpEF: 9.8 ± 6.6%; HFmrEF: 14.7 ± 10.2%; HFrEF 28.3 ± 40.4%, p = 0.028).

Der Betrag der LV GLS Strainänderung während HG korrelierte signifikant mit der Ruhe-LV EF (r = −0.37, p = 0.001), NTproBNP (r = 0.33, p = 0.004), dem MLHQ Score, der Einschränkungen der Lebensqualität quantifiziert (r = 0.26, p = 0.028), dem LV enddiastolischen Volumen (r = 0.40, p = 0.006) und dem LV endsystolischen Volumen (r = 0.43, p = 0.001).

4.2 Multilayer-Strain zur Differenzierung von HFpEF und Herzgesunden

Im Rahmen der FT-Multilayer-Strainuntersuchung wurden 20 StudienteilnehmerInnen mit HFpEF und 20 TeilnehmerInnen der Kontrollgruppe verglichen. HFpEF PatientInnen zeigten sowohl auf subendokardialer (−20.8 ± 4.0 vs. −23.2 ± 3.4, $p = 0.046$) und intra-myokardialer (−18.0 ± 3.0 vs. −21.0 ± 2.5, $p = 0.002$) und subepikardialer Ebene (12.2 ± 2.0 vs. −16.2 ± 2.5, $p < 0.001$) signifikant reduzierten LV GLS verglichen mit StudienteilnehmerInnen aus der Kontrollgruppe. Bezüglich des LV GLS hingegen unterschieden sich HFpEF und Kontrolle weder auf subendokardialer (−34.9 ± 6.5 vs. −34.0 ± 6.0, $p = 0.72$) noch auf intra-myokardialer (−22.0 ± 3.9 vs. −21.8 ± 3.7, $p = 0.85$) oder subepikardialer Ebene signifikant (−10.9 ± 2.8 vs. −11.8 ± 2.2, $p = 0.30$).
Eine vergleichende Beurteilung der diagnostischen Kapazität mittels ROC zeigte, dass subepikardialer GLS eine größere AUC erreichte (0.90, 95% Confidence Interval 0.81-1) als E/e’ (0.62, 95% Confidence Interval 0.46-0.78) und ähnlichen diagnostischen Nutzen erbrachte wie NTproBNP (Figur 1, Tanacli et al 2020). Eine Kombination von subepikardialem GLS (Cut-off < -13.0) und NTproBNP (Cut-off >220 ng/l) erreichte mit einer Sensitivität von 89% und einer Spezifität von 100% eine ausgezeichnete Differenzierung von Herzgesunden und HFpEF (AUC 0.98, 95% Confidence Interval 0.95–1, $p < 0.001$).

4.3 Gewebecharakterisierung mittels Tissue-Mapping

In die Tissue-Mapping-Analyse wurden 17 PatientInnen mit HFrEF, 18 mit HFmrEF, 17 mit HFpEF und 17 StudienteilnehmerInnen aus der Kontrollgruppe eingeschlossen. Die T2-Relaxationszeit betrug 56.0 ± 6.0 ms, 55.4 ± 3.4 ms, 52.6 ± 3.6 ms und 50.6 ± 2.1 ms in den Gruppen HFrEF, HFmrEF, HFpEF und in der Kontrollgruppe. Während HFrEF und HFmrEF sich in Bezug auf die T2 Relaxationszeit signifikant von der Kontrollgruppe unterschieden ($p=0.005$), war kein signifikanter Unterschied zwischen HFpEF und der Kontrollgruppe feststellbar ($p=0.449$). Die T2-Relaxationszeit korrelierte signifikant mit logNTproBNP ($r=0.64$, $p<0.001$), dem MLHQ Lebensqualitäts-Score ($r=0.48$, $p<0.001$) und der Gehstrecke im Sechs-Minuten-Gehtest ($r=-0.34$, $p=0.004$).
Die native T1-Relaxationszeit betrug 1033 ± 54 ms, 1027 ± 40 ms, 985 ± 32 ms und 972 ± 31 ms in den Gruppen HFrEF, HFmrEF, HFpEF und der Kontrollgruppe. Auch in Bezug auf die T1-Relaxationszeit unterschieden sich HFrEF und HFmrEF signifikant von der Kontrollgruppe ($p<0.001$), während der Unterschied zwischen HFpEF und Kontrollgruppe keine statistische

Signifikanz erreichte (p=0.776). Die native T1-Relaxationszeit korrelierte signifikant mit logNTproBNP (r=0.60, p<0.001) und dem MLHQ Lebensqualitäts-Score (r=0.36, p=0.002). Das errechnete ECV betrug 29.3 ± 3.4 % in der HFrEF-, 29.2 ± 2.6 % in der HFmrEF- und 27.3 ± 2.6 % in der HFpEF-Gruppe. Das ECV der historischen Vergleichskohorte Herzgesunder betrug 27 ± 4 %.[26] Die Unterschiede zwischen den einzelnen Subgruppen erreichten keine statistische Signifikanz. ECV korrelierte leicht mit logNTproBNP (r=0.29, p=0.039). Native T1-Relaxationszeit, T2-Relaxationszeit und ECV korrelierten signifikant untereinander (native T1 ~ T2: r=0.66, p<0.001; T2 ~ ECV: r =0.35, p=0.010; T1 ~ ECV: r=0.47, p<0.001).

5. Diskussion

Die vorliegende Studie zur Evaluation dreier experimenteller CMR-Methoden zur besseren Differenzierung von PatientInnen mit HI untereinander und im Vergleich zu Herzgesunden erbrachte im Wesentlichen die folgenden Ergebnisse:

1. Die durchschnittliche Änderung von Fast-SENC-Strain während HG-Belastung unterschied sich nicht signifikant zwischen den HI-Entitäten und Herzgesunden. Der Betrag der Strainänderung hingegen stieg von Herzgesunden über HFpEF und HFmrEF bis HFrEF signifikant an.
2. In einer FT-Multilayer-Strainanalyse zeigten HFpEF PatientInnen in allen Wandschichten signifikant reduzierten LV GLS verglichen mit Herzgesunden. Insbesondere epikardialer LV GLS eignete sich hervorragend zur Differenzierung zwischen HFpEF und Kontrollgruppe.
3. Im Tissue-Mapping-CMR zeigten PatientInnen mit HFmrEF und HFrEF signifikant angehobene native T1- und T2-Relaxationszeiten verglichen mit Herzgesunden, während PatientInnen mit HFpEF sich nicht signifikant von Herzgesunden unterschieden. ECV variierte nicht signifikant zwischen HI-Entitäten und Kontrollgruppe.

Diese Ergebnisse wurden in einzelnen Publikationen bereits diskutiert und die im Folgenden dargestellten Verortungen und Interpretationen wurden dort bereits elaboriert.[18,21,22]

5.1 Myokardialer Strain – ein vielversprechender Bildgebungsparameter?

Myokardialer Strain – vor wenigen Jahren noch ein rein experimenteller Parameter – hält immer weiter Einzug in die klinische Praxis: Während Strain in den letzten ESC Leitlinien zu Diagnose und Behandlung der HI noch keine einzige Erwähnung fand, wird in den aktuellen

ESC-Leitlinien von 2016 Strain-Messung im Zusammenhang mit der Diagnostik der DD und dem Monitoring während kardiotoxischer Chemotherapie erwähnt und erhält eine Klasse IIa Empfehlung zur Früherkennung myokardialer Funktionsstörungen.[1,27]

Fast-SENC stellt eine Weiterentwicklung der CMR-basierten Strainmessung insbesondere deshalb dar, weil innerhalb eines aufgezeichneten Herzzyklus eine vollständige Strain-Quantifizierung durchgeführt werden kann, ein deutlicher Fortschritt gegenüber FT-basierten Strainmessungen, bei denen für die Aufnahme von bSSFP-Sequenzen längere Atemhaltemanöver notwendig sind, die für dyspnoeische HI-PatientInnen oft eine große körperliche Belastung darstellen.[10]

Die Bedeutung von Stresstests zur Diagnose – insbesondere diastolischer – myokardialer Funktionsstörungen wird in den aktuellen ESC Leitlinien zur Diagnose und Behandlung der HI deutlich betont.[1] Im Rahmen dieser Studie wurde erstmals ein kombinierter diagnostischer Ansatz aus Fast-SENC basierter Strain Messung und HG-Belastung eingesetzt, der sich vor allem deshalb empfiehlt, weil HG eine simple, breit verfügbare Belastungsintervention darstellt, die zudem verspricht, weniger Bewegungsartefakte zu erzeugen als andere Belastungsmodalitäten.

5.2 Der Effekt erhöhter kardialer Nachlast auf myokardiale Kontraktilität

HG führt durch die isometrische Kontraktion einer relativ kleinen Muskelgruppe zu einer kreislaufrelevanten Erhöhung der kardialen Nachlast, in deren Folge systolischer und diastolischer RR sowie die HF ansteigen.[16,17] Eine aktuelle Metaanalyse bestätigte den signifikanten Anstieg der HF während HG und fand, dass Herzzeitvolumen (HZV) und Schlagvolumen (SV) sich während HG nicht signifikant veränderten.[28] Diese Beobachtungen legen nahe, dass erhöhter Nachlast im Rahmen von HG-Belastung eher durch eine Erhöhung der HF, als durch eine Verstärkung der kontraktilen Leistung des Myokards begegnet wird.

Mit der Messung von Strain haben kardiale Bildgebungsmethoden die direkte Quantifizierung von myokardialer Kontraktilität möglich gemacht.[29] Einige Studien mit unterschiedlichen Bildgebungs- und Stressmodalitäten untersuchten in der Vergangenheit die Auswirkungen erhöhter Nachlast auf myokardialen Strain und kamen zu divergierenden Ergebnissen. Fredholm et al. verabreichten 21 PatientInnen nach einem herzchirurgischen Eingriff Phenylephrin zur Steigerung der Nachlast und konnten mittels *speckle tracking* Echokardiographie (STE) keine Änderung des LV Strain messen.[30] Stefani et al. untersuchten AthletInnen und Nicht-AthletInnen vor und während HG-Belastung. Bei Nicht-AthletInnen

fand sich keine Änderung des *longitudinal peak systolic strain* (LPSS) während HG, bei AthletInnen fand sich eine LPSS-Steigerung nur in den mittigen und apikalen Segmenten.[31]
Andere Studien, die Strain bei gesunden Freiwilligen mittels STE untersuchten, fanden hingegen reduzierten Strain während HG-Belastung.[32,33] Eine tierexperimentelle Studie, die Nachlasterhöhung mittels chirurgischem Aorten-Banding herbeiführte, kam zu ähnlichen Ergebnissen.[34]

5.3 Heterogene Strainänderung bei HI-PatientInnen in Folge von HG-Belastung

In unserer Studie, die sowohl Herzgesunde als auch HI-PatientInnen einschloss und sich mit Fast-SENC einer gut reproduzierbaren, neuartigen Methode bediente, fanden wir eine heterogene Strainänderung in Folge von HG-Belastung, die stark zwischen einzelnen StudienteilnehmerInnenn variierte und sowohl positiv als auch negativ sein konnte (Figur 4, Blum et al. 2020).[11,18] Dieses Muster ergab sich sowohl bei HI-PatientInnen als auch bei Herzgesunden. Frühere Studien hatten Strainänderung während HG ausschließlich in Form von Mittelwerten wiedergegeben und die Möglichkeit und Implikationen einer deutlich heterogenen Strainänderung nie ausdrücklich diskutiert, obwohl sie das Nebeneinander positiver und negativer Ergebnisse von Studien mit ähnlichem Ansatz teilweise erklären könnte. Unsere Ergebnisse deuten hingegen darauf hin, dass nicht das Vorzeichen, sondern der Betrag der Strainänderung während HG mit kardialer Dysfunktion assoziiert ist. Dieser nahm mit zunehmender systolischer Funktionseinschränkung deutlich zu und war zudem signifikant mit Surrogatparametern der HI-Schwere, namentlich NTproBNP und Sechs-Minuten-Gehstrecke, assoziiert.
Dennoch bleibt die Frage, welche Faktoren determinieren, ob Strain während HG ansteigt oder abnimmt. In Anbetracht der Tatsache, dass der Anstieg der HF eine wichtige Rolle bei der Anpassung an erhöhte Nachlast spielt, liegt die Vermutung nahe, dass eine übermäßige Strainzunahme die Kompensation einer insuffizenten Erhöhung der HF während HG darstellt. In einer explorativen Analyse fanden wir, dass bei HI-PatientInnen die LV GLS-Änderung tatsächlich invers mit der Änderung der HF korrelierte ($r = -0.31$, $p = 0.023$). Offensichtlich spielen hier jedoch auch noch andere Faktoren eine wichtige Rolle: Beta-Blocker-Therapie interferiert mit der Modulationsbreite der HF, LV-endiastolischer Druck hängt eng mit der Anpassungsfähigkeit an erhöhte Nachlast zusammen und variable PatientInnenmitarbeit stellt unter Umständen einen Störfaktor dar.[17] Aufgrund all dieser Faktoren und der Heterogenität der Strainänderung, die wir in unserem Experiment zeigen konnten, scheint der klinische Nutzen von Strainmessung während isometrischer Muskelbelastung mittels HG begrenzt.

5.4 Multilayer-Strain zur Diagnostik von HFpEF

Technische Innovationen ermöglichen heute die differenzierte Analyse von Strain in verschiedenen myokardialen Wandschichten. Unsere Multilayer-Strain Analyse mittels FT-CMR ergab, dass LV GLS bei HFpEF in allen Wandschichten herabgesetzt ist. LV GCS hingegen unterschied sich nicht signifikant zwischen HFpEF und gesunden Kontrollen. Diese Beobachtung bestätigt die Ergebnisse früherer Studien zu dieser Frage.[35] Gestörter LV GLS ist zudem stark mit negativer kardialer Prognose assoziiert.[36]

Die offensichtlich große klinische Bedeutung des LV GLS wird mit dem Schichtaufbau des Myokards in Verbindung gebracht. Frühere anatomische und pathologische Studien untersuchten mikroskopisch den Verlauf myokardialer Fasern und beschrieben dabei ein dreischichtiges Modell in dem subepikardiale Fasern diagonal, intra-myokardiale Fasern circumferentiell und subendokardiale Fasern longitudinal verlaufen.[19] Als Grund für die enge Assoziation von LV GLS und myokardialem Schaden wurde deshalb vermutet, dass subendokardiale Fasern, die longitudinal verlaufen, am vulnerabelsten für Minderversorgung sind, da sie die Endstrecke der myokardialen Perfusion darstellen.[37] Unsere Beobachtung, dass sich subepikardialer LV GLS noch mehr als subendokardialer LV GLS zur Differenzierung von HFpEF und Gesunden eignet, war daher unerwartet.

Jüngere Publikationen weisen jedoch darauf hin, dass Belege für diese Theorie über den Zusammenhang von subendokardialer Faseranordnung und LV GLS fehlen und argumentieren stattdessen, dass die hohe Aussagekraft des LV GLS eher technisch als physiologisch bedingt sei: Während circumferentieller und radialer Strain stark von der korrekten Erfassung subendo- und subepikardialer Strukturen abhängig sind, ist die Messung von GLS weniger untersucherabhängig und fehleranfällig.[37] Überlegungen zur technischen Erfassung von Strain liefern auch eine mögliche Erklärung für die Überlegenheit des subepikardialen LV GLS gegenüber Strainableitungen aus anderen Wandschichten: An der Grenze von Myokard und Perikard, beziehungsweise extrakardialem Gewebe ergibt sich ein besonders hoher T1-Kontrast, der eine bessere FT-Gewebenachverfolgung ermöglicht.[38]

In unserer vergleichenden Analyse konnte subepikardialer LV GLS signifikant zur Differenzierung von HFpEF und Herzgesunden beitragen, was diesen neuartigen Parameter zu einem vielversprechenden Kandidaten für HFpEF-Diagnostikalgorithmen wie den HFA-PEFF Score macht.[15] Zur eindeutigen Klärung des diagnostischen Nutzens und zur Festlegung eines allgemeingültigen Cut-Off-Wertes sind allerdings größere Studien notwendig.

5.5 Tissue-Mapping zur Gewebecharakterisierung bei HI

Tissue-Mapping ist ein relativ neu entwickeltes Verfahren, dass die Quantifizierung von Gewebeeigenschaften basierend auf CMR ermöglicht. Insbesondere PatientInnen mit HFmrEF, einer Entität, die erst in der letzten Iteration der ESC Leitlinien definiert wurde, wurden unseres Wissens nach noch nie systematisch mittels Tissue-Mapping untersucht. Sowohl native T1-Relaxationszeit als auch ECV korrelieren signifikant mit dem Ausmaß myokardialer Fibrose in histologischen Untersuchungen und haben überdies prognostische Bedeutung bei verschiedenen Formen der HI.[39,40]

Während in früheren Studien sowohl HFrEF als auch HFpEF PatientInnen signifikant angehobenes ECV zeigten, unterschied sich in unserer Studie das aus prä- und post-KM T1-Relaxationszeit und Hämatokrit berechnete ECV nicht signifikant zwischen HFrEF, HFmrEF und HFpEF.[41]

Die native T1-Relaxationszeit hingegen waren bei HFrEF und HFmrEF im Vergleich zu Herzgesunden signifikant angehoben, bei HFpEF jedoch nicht. Da die native T1-Relaxationszeit Rückschlüsse auf Gewebezusammensetzung und Prognose erlaubt, lässt sich in Bezug auf die schlecht charakterisierte Entität HFmrEF pathophysiologische Ähnlichkeit mit HFrEF vermuten. Im Lichte der Ergebnisse einiger randomisierter kontrollierter Studien, die eine gewisse Wirksamkeit von HFrEF-Therapien bei PatientInnen fanden, die heute HFmrEF zugerechnet würden, nicht jedoch bei PatientInnen mit LV EF ≥50%, erscheint diese Vermutung durchaus plausibel.[42] Angehobene native T1-Relaxationszeiten verweisen auf myokardialen Umbau und Fibrose als wichtigen Faktor in der Pathophysiologie von sowohl HFrEF als auch HFmrEF.

T2-Mapping ermöglicht die Quantifizierung von intramyokardialem Wasser, welches vor allem im Rahmen von Entzündungsprozessen, zum Beispiel bei Myokarditis, als myokardiales Ödem auftritt.[24] Da T2-Relaxationszeiten jedoch stark von technischen Aspekten der CMR-Durchführung wie der Feldstärke und interindividuellen Schwankungen abhängen, ist bei ihrer Interpretation Vorsicht geboten.[24] In unserem Experiment war die T2-Relaxationszeit bei HFrEF und HFmrEF im Vergleich zu Herzgesunden angehoben. HFrEF und HFmrEF unterschieden sich nicht signifikant voneinander, was einen weiteren Hinweis auf die pathophysiologische Ähnlichkeit der intramyokardialen Prozesse dieser beiden HI-Entitäten liefert. Obwohl entzündlichen Prozessen in der Pathogenese von HFpEF eine große Rolle beigemessen wird, wiesen HFpEF-PatientInnen keine höhere T2-Relaxationszeit auf als Herzgesunde. Eine mögliche Erklärung hierfür ist, dass das Entzündungsgeschehen bei HFpEF durch ein subtil proinflammatorisches metabolisches Milieu ausgelöst und auf die Mikrozirkulation und Endothel-Kardiomyozyten-Wechselwirkungen beschränkt ist, die zu einer Veränderung des myokardialen Expressionsmusters, nicht jedoch zu makroskopisch erfassbarem intramyokardialem Ödem führen.[5]

5.6 Limitationen

Die Aussagekraft der vorliegenden Studie ist aufgrund verschiedener Faktoren eingeschränkt: Unsere Experimente erfassen teilweise keine a priori definierten Endpunkte, Analysen wurden retrospektiv ausgeführt. Die Charakteristika der Subgruppen spiegeln die Unterschiede in Bezug auf Demographie, Komorbiditäten und Begleitmedikation wieder, die sich auch in der klinischen Praxis zwischen den HI-Entitäten finden. Dies erhöht zwar die Generalisierbarkeit unserer Ergebnisse auf reale PatientInnenkollektive, die Möglichkeit von *confounding* kann aber dadurch nicht ausgeschlossen werden. Insbesondere Beta-Blocker-Therapie könnte die kardiovaskuläre Anpassung an HG beeinflusst haben.

Ausschlusskriterien waren der Grund, dass PatientInnen mit Vorhofflimmern, ICD, CRT, höhergradigen Klappenvitien, Ruhedyspnoe und weiteren Symptomen und Diagnosen nicht in die Studie eingeschlossen werden konnten, obwohl diese einen signifikanten Teil der gesamten HI-Population ausmachen, weswegen sich unsere Ergebnisse nur begrenzt verallgemeinern lassen. Die ausgewählten experimentellen Ansätze sind in unterschiedlichem Ausmaße fehleranfällig. Insbesondere PatientInnenmitarbeit bei HG-Belastung könnte Messungen verfälscht haben.

Aus all diesen Gründen sollten die vorliegenden Ergebnisse mit Vorsicht interpretiert werden. Sie sollen nicht der definitiven Beantwortung von Forschungsfragen dienen, sondern Hypothesen generieren und zukünftige Studien informieren und anregen.

5.7 Fazit

Wie in den drei dargestellten Experimenten gezeigt, ermöglichen CMR-basierte Bildgebungsmethoden tiefe Einblicke in die Pathophysiologie der Herzinsuffizienz, sei es mit genauer Erfassung der myokardialen Kontraktilität mittels Strain während Stressuntersuchungen oder in unterschiedlichen Gewebeschichten oder mit Tissue-Mapping, das heute Aussagen über Gewebeeigenschaften erlaubt, die früher nur per Biopsie möglich gewesen wären. Unser Ziel war es, dieses Potential zu nutzen, um die Differenzialdiagnostik der HI zu verbessern. Nach Auswertung und Diskussion der vorliegenden Ergebnisse kommen wir zu folgenden Schlüssen:

Fast-SENC-basierte Strainmessung während HG-Belastung ist möglich; die Strainänderung ist jedoch sowohl bei HI-PatientInnen als auch bei Herzgesunden heterogen. Auch wenn diese Beobachtung zukünftige Diskussionen über die kardiovaskulären Auswirkungen erhöhter Nachlast bereichern kann, ist ihr diagnostischer Nutzen für die Klinik begrenzt. Zukünftige Versuche, Strain während körperlicher Belastung zu messen, sollten andere Belastungsmodalitäten heranziehen, die einheitlichere und größere kardiovaskuläre Effekte haben.[28]

Multilayer-Strainmessung mittels FT-CMR ermöglicht die differenzierte Erfassung von myokardialem Strain in unterschiedlichen Wandschichten. Insbesondere subepikardialem LV GLS differenziert hervorragend zwischen HFpEF und Herzgesunden, was diesen Parameter zu einem vielversprechenden Kandidaten für die klinische Anwendung macht. Größere Studien sind jedoch notwendig um diese Beobachtung zu bestätigen und belastbare Grenzwerte festzulegen.

Mittels Tissue-Mapping fanden wir deutliche Unterschiede in der Gewebezusammensetzung der verschieden HI-Entitäten. HFmrEF ähnelt mit erhöhter nativer T1- beziehungsweise T2-Relaxationszeit, die mit Fibrose beziehungsweise myokardialem Ödem assoziiert ist, dabei stark HFrEF. Dies weist auf eine gewisse pathophysiologische Verwandschaft hin, die jedoch nur durch weitere Studien, insbesondere histopathologischer Natur, wirklich etabliert werden kann.

6. Referenzen

1. Ponikowski, P., Voors, A. A., Anker, S. D., Bueno, H., Cleland, J. G. F., Coats, A. J. S., Falk, V., González-Juanatey, J. R., Harjola, V.-P., Jankowska, E. A., Jessup, M., Linde, C., Nihoyannopoulos, P., Parissis, J. T., Pieske, B., Riley, J. P., Rosano, G. M. C., Ruilope, L. M., Ruschitzka, F., Rutten, F. H., van der Meer, P. & ESC Scientific Document Group. 2016 ESC Guidelines for the diagnosis and treatment of acute and chronic heart failure: The Task Force for the diagnosis and treatment of acute and chronic heart failure of the European Society of Cardiology (ESC)Developed with the special contribution of the Heart Failure Association (HFA) of the ESC. *Eur. Heart J.* **37,** 2129–2200 (2016).
2. Jaarsma, T., Johansson, P., Agren, S. & Strömberg, A. Quality of life and symptoms of depression in advanced heart failure patients and their partners. *Curr. Opin. Support. Palliat. Care* **4,** 233–237 (2010).
3. Roger, V. L., Weston, S. A., Redfield, M. M., Hellermann-Homan, J. P., Killian, J., Yawn, B. P. & Jacobsen, S. J. Trends in heart failure incidence and survival in a community-based population. *JAMA* **292,** 344–350 (2004).
4. Redfield, M. M. Understanding 'diastolic' heart failure. *N. Engl. J. Med.* **350,** 1930–1931 (2004).
5. Paulus, W. J. & Tschöpe, C. A novel paradigm for heart failure with preserved ejection fraction: comorbidities drive myocardial dysfunction and remodeling through coronary microvascular endothelial inflammation. *J. Am. Coll. Cardiol.* **62,** 263–271 (2013).
6. Kirkpatrick, J. N., Vannan, M. A., Narula, J. & Lang, R. M. Echocardiography in heart failure: applications, utility, and new horizons. *J. Am. Coll. Cardiol.* **50,** 381–396 (2007).
7. Gonzalez, J. A. & Kramer, C. M. Role of Imaging Techniques for Diagnosis, Prognosis and Management of Heart Failure Patients: Cardiac Magnetic Resonance. *Curr. Heart Fail. Rep.* **12,** 276–283 (2015).
8. Smiseth, O. A., Torp, H., Opdahl, A., Haugaa, K. H. & Urheim, S. Myocardial strain imaging: how useful is it in clinical decision making? *Eur Heart J* **37,** 1196–207 (2016).
9. Hor, K. N., Baumann, R., Pedrizzetti, G., Tonti, G., Gottliebson, W. M., Taylor, M., Benson, D. W. & Mazur, W. Magnetic resonance derived myocardial strain assessment using feature tracking. *J Vis Exp* (2011). doi:10.3791/2356
10. Pan, L., Stuber, M., Kraitchman, D. L., Fritzges, D. L., Gilson, W. D. & Osman, N. F. Real-time imaging of regional myocardial function using fast-SENC. *Magn Reson Med* **55,** 386–95 (2006).

11. Giusca, S., Korosoglou, G., Zieschang, V., Stoiber, L., Schnackenburg, B., Stehning, C., Gebker, R., Pieske, B., Schuster, A., Backhaus, S., Pieske-Kraigher, E., Patel, A., Kawaji, K., Steen, H., Lapinskas, T. & Kelle, S. Reproducibility study on myocardial strain assessment using fast-SENC cardiac magnetic resonance imaging. *Sci. Rep.* **8,** 14100 (2018).
12. Bucius, P., Erley, J., Tanacli, R., Zieschang, V., Giusca, S., Korosoglou, G., Steen, H., Stehning, C., Pieske, B., Pieske-Kraigher, E., Schuster, A., Lapinskas, T. & Kelle, S. Comparison of feature tracking, fast-SENC, and myocardial tagging for global and segmental left ventricular strain. *ESC Heart Fail* **7,** 523–532 (2020).
13. Lapinskas, T., Zieschang, V., Erley, J., Stoiber, L., Schnackenburg, B., Stehning, C., Gebker, R., Patel, A. R., Kawaji, K., Steen, H., Zaliunas, R., Backhaus, S. J., Schuster, A., Makowski, M., Giusca, S., Korosoglou, G., Pieske, B. & Kelle, S. Strain-encoded cardiac magnetic resonance imaging: a new approach for fast estimation of left ventricular function. *BMC Cardiovasc Disord* **19,** 52 (2019).
14. Messroghli, D. R., Moon, J. C., Ferreira, V. M., Grosse-Wortmann, L., He, T., Kellman, P., Mascherbauer, J., Nezafat, R., Salerno, M., Schelbert, E. B., Taylor, A. J., Thompson, R., Ugander, M., van Heeswijk, R. B. & Friedrich, M. G. Clinical recommendations for cardiovascular magnetic resonance mapping of T1, T2, T2* and extracellular volume: A consensus statement by the Society for Cardiovascular Magnetic Resonance (SCMR) endorsed by the European Association for Cardiovascular Imaging (EACVI). *J. Cardiovasc. Magn. Reson. Off. J. Soc. Cardiovasc. Magn. Reson.* **19,** 75 (2017).
15. Pieske, B., Tschope, C., de Boer, R. A., Fraser, A. G., Anker, S. D., Donal, E., Edelmann, F., Fu, M., Guazzi, M., Lam, C. S. P., Lancellotti, P., Melenovsky, V., Morris, D. A., Nagel, E., Pieske-Kraigher, E., Ponikowski, P., Solomon, S. D., Vasan, R. S., Rutten, F. H., Voors, A. A., Ruschitzka, F., Paulus, W. J., Seferovic, P. & Filippatos, G. How to diagnose heart failure with preserved ejection fraction: the HFA-PEFF diagnostic algorithm: a consensus recommendation from the Heart Failure Association (HFA) of the European Society of Cardiology (ESC). *Eur Heart J* **40,** 3297–3317 (2019).
16. Lind, A. R., Taylor, S. H., Humphreys, P. W., Kennelly, B. M. & Donald, K. W. THE CIRCULATIORY EFFECTS OF SUSTAINED VOLUNTARY MUSCLE CONTRACTION. *Clin Sci* **27,** 229–44 (1964).
17. Helfant, R. H., De Villa, M. A. & Meister, S. G. Effect of sustained isometric handgrip exercise on left ventricular performance. *Circulation* **44,** 982–93 (1971).

18. Blum, M., Hashemi, D., Motzkus, L. A., Neye, M., Dordevic, A., Zieschang, V., Zamani, S. M., Lapinskas, T., Runte, K., Kelm, M., Kühne, T., Tahirovic, E., Edelmann, F., Pieske, B., Düngen, H.-D. & Kelle, S. Variability of Myocardial Strain During Isometric Exercise in Subjects With and Without Heart Failure. *Front. Cardiovasc. Med.* **7,** 111 (2020).
19. Greenbaum, R. A., Ho, S. Y., Gibson, D. G., Becker, A. E. & Anderson, R. H. Left ventricular fibre architecture in man. *Br. Heart J.* **45,** 248–263 (1981).
20. Ho, S. Y. Anatomy and myoarchitecture of the left ventricular wall in normal and in disease. *Eur. J. Echocardiogr. J. Work. Group Echocardiogr. Eur. Soc. Cardiol.* **10,** iii3-7 (2009).
21. Tanacli, R., Hashemi, D., Neye, M., Motzkus, L. A., Blum, M., Tahirovic, E., Dordevic, A., Kraft, R., Zamani, S. M., Pieske, B., Düngen, H.-D. & Kelle, S. Multilayer Myocardial Strain Improves the Diagnosis of Heart Failure With Preserved Ejection Fraction. *ESC Heart Failure* **7,** 3240–3245 (2020).
22. Doeblin, P., Hashemi, D., Tanacli, R., Lapinskas, T., Gebker, R., Stehning, C., Motzkus, L. A., Blum, M., Tahirovic, E., Dordevic, A., Kraft, R., Zamani, S. M., Pieske, B., Edelmann, F., Dungen, H. D. & Kelle, S. CMR Tissue Characterization in Patients with HFmrEF. *J Clin Med* **8,** (2019).
23. Messroghli, D. R., Radjenovic, A., Kozerke, S., Higgins, D. M., Sivananthan, M. U. & Ridgway, J. P. Modified Look-Locker inversion recovery (MOLLI) for high-resolution T1 mapping of the heart. *Magn. Reson. Med.* **52,** 141–146 (2004).
24. Baeßler, B., Schaarschmidt, F., Stehning, C., Schnackenburg, B., Maintz, D. & Bunck, A. C. Cardiac T2-mapping using a fast gradient echo spin echo sequence - first in vitro and in vivo experience. *J. Cardiovasc. Magn. Reson. Off. J. Soc. Cardiovasc. Magn. Reson.* **17,** 67 (2015).
25. Ugander, M., Oki, A. J., Hsu, L.-Y., Kellman, P., Greiser, A., Aletras, A. H., Sibley, C. T., Chen, M. Y., Bandettini, W. P. & Arai, A. E. Extracellular volume imaging by magnetic resonance imaging provides insights into overt and sub-clinical myocardial pathology. *Eur. Heart J.* **33,** 1268–1278 (2012).
26. Dabir, D., Child, N., Kalra, A., Rogers, T., Gebker, R., Jabbour, A., Plein, S., Yu, C.-Y., Otton, J., Kidambi, A., McDiarmid, A., Broadbent, D., Higgins, D. M., Schnackenburg, B., Foote, L., Cummins, C., Nagel, E. & Puntmann, V. O. Reference values for healthy human myocardium using a T1 mapping methodology: results from the International T1 Multicenter cardiovascular magnetic resonance study. *J. Cardiovasc. Magn. Reson. Off. J. Soc. Cardiovasc. Magn. Reson.* **16,** 69 (2014).

27. Dickstein, K., Cohen-Solal, A., Filippatos, G., McMurray, J. J. V., Ponikowski, P., Poole-Wilson, P. A., Strömberg, A., van Veldhuisen, D. J., Atar, D., Hoes, A. W., Keren, A., Mebazaa, A., Nieminen, M., Priori, S. G., Swedberg, K. & ESC Committee for Practice Guidelines (CPG). ESC guidelines for the diagnosis and treatment of acute and chronic heart failure 2008: the Task Force for the diagnosis and treatment of acute and chronic heart failure 2008 of the European Society of Cardiology. Developed in collaboration with the Heart Failure Association of the ESC (HFA) and endorsed by the European Society of Intensive Care Medicine (ESICM). *Eur. J. Heart Fail.* **10,** 933–989 (2008).
28. Runte, K., Brosien, K., Salcher-Konrad, M., Schubert, C., Goubergrits, L., Kelle, S., Schubert, S., Berger, F., Kuehne, T. & Kelm, M. Hemodynamic Changes During Physiological and Pharmacological Stress Testing in Healthy Subjects, Aortic Stenosis and Aortic Coarctation Patients-A Systematic Review and Meta-Analysis. *Front Cardiovasc Med* **6,** 43 (2019).
29. Greenberg, N. L., Firstenberg, M. S., Castro, P. L., Main, M., Travaglini, A., Odabashian, J. A., Drinko, J. K., Rodriguez, L. L., Thomas, J. D. & Garcia, M. J. Doppler-derived myocardial systolic strain rate is a strong index of left ventricular contractility. *Circulation* **105,** 99–105 (2002).
30. Fredholm, M., Jorgensen, K., Houltz, E. & Ricksten, S. E. Load-dependence of myocardial deformation variables - a clinical strain-echocardiographic study. *Acta Anaesthesiol Scand* **61,** 1155–1165 (2017).
31. Stefani, L., Pedrizzetti, G., De Luca, A., Mercuri, R., Innocenti, G. & Galanti, G. Real-time evaluation of longitudinal peak systolic strain (speckle tracking measurement) in left and right ventricles of athletes. *Cardiovasc. Ultrasound* **7,** 17 (2009).
32. Murai, D., Yamada, S., Hayashi, T., Okada, K., Nishino, H., Nakabachi, M., Yokoyama, S., Abe, A., Ichikawa, A., Ono, K., Kaga, S., Iwano, H., Mikami, T. & Tsutsui, H. Relationships of left ventricular strain and strain rate to wall stress and their afterload dependency. *Heart Vessels* **32,** 574–583 (2017).
33. Weiner, R. B., Weyman, A. E., Kim, J. H., Wang, T. J., Picard, M. H. & Baggish, A. L. The impact of isometric handgrip testing on left ventricular twist mechanics. *J Physiol* **590,** 5141–50 (2012).
34. Donal, E., Bergerot, C., Thibault, H., Ernande, L., Loufoua, J., Augeul, L., Ovize, M. & Derumeaux, G. Influence of afterload on left ventricular radial and longitudinal systolic functions: a two-dimensional strain imaging study. *Eur J Echocardiogr* **10,** 914–21 (2009).

35. Morris, D. A., Ma, X.-X., Belyavskiy, E., Aravind Kumar, R., Kropf, M., Kraft, R., Frydas, A., Osmanoglou, E., Marquez, E., Donal, E., Edelmann, F., Tschöpe, C., Pieske, B. & Pieske-Kraigher, E. Left ventricular longitudinal systolic function analysed by 2D speckle-tracking echocardiography in heart failure with preserved ejection fraction: a meta-analysis. *Open Heart* **4,** e000630 (2017).
36. Biering-Sørensen, T., Biering-Sørensen, S. R., Olsen, F. J., Sengeløv, M., Jørgensen, P. G., Mogelvang, R., Shah, A. M. & Jensen, J. S. Global Longitudinal Strain by Echocardiography Predicts Long-Term Risk of Cardiovascular Morbidity and Mortality in a Low-Risk General Population: The Copenhagen City Heart Study. *Circ. Cardiovasc. Imaging* **10,** (2017).
37. Rademakers, F. & Nagel, E. Is Global Longitudinal Strain a Superior Parameter for Predicting Outcome After Myocardial Infarction? *JACC Cardiovasc. Imaging* **11,** 1458–1460 (2018).
38. Schuster, A., Hor, K. N., Kowallick, J. T., Beerbaum, P. & Kutty, S. Cardiovascular Magnetic Resonance Myocardial Feature Tracking: Concepts and Clinical Applications. *Circ. Cardiovasc. Imaging* **9,** e004077 (2016).
39. Duca, F., Kammerlander, A. A., Zotter-Tufaro, C., Aschauer, S., Schwaiger, M. L., Marzluf, B. A., Bonderman, D. & Mascherbauer, J. Interstitial Fibrosis, Functional Status, and Outcomes in Heart Failure With Preserved Ejection Fraction: Insights From a Prospective Cardiac Magnetic Resonance Imaging Study. *Circ. Cardiovasc. Imaging* **9,** (2016).
40. Bull, S., White, S. K., Piechnik, S. K., Flett, A. S., Ferreira, V. M., Loudon, M., Francis, J. M., Karamitsos, T. D., Prendergast, B. D., Robson, M. D., Neubauer, S., Moon, J. C. & Myerson, S. G. Human non-contrast T1 values and correlation with histology in diffuse fibrosis. *Heart Br. Card. Soc.* **99,** 932–937 (2013).
41. Su, M.-Y. M., Lin, L.-Y., Tseng, Y.-H. E., Chang, C.-C., Wu, C.-K., Lin, J.-L. & Tseng, W.-Y. I. CMR-verified diffuse myocardial fibrosis is associated with diastolic dysfunction in HFpEF. *JACC Cardiovasc. Imaging* **7,** 991–997 (2014).
42. Solomon, S. D., Claggett, B., Lewis, E. F., Desai, A., Anand, I., Sweitzer, N. K., O’Meara, E., Shah, S. J., McKinlay, S., Fleg, J. L., Sopko, G., Pitt, B., Pfeffer, M. A. & TOPCAT Investigators. Influence of ejection fraction on outcomes and efficacy of spironolactone in patients with heart failure with preserved ejection fraction. *Eur. Heart J.* **37,** 455–462 (2016).

7. Eidesstattliche Versicherung und Anteilserklärung

7.1 Eidesstattliche Versicherung

„Ich, Moritz Blum, versichere an Eides statt durch meine eigenhändige Unterschrift, dass ich die vorgelegte Dissertation mit dem Thema „Über die Differenzierung verschiedener Herzinsuffizienzentitäten mittels neuer Bildgebungsparameter der kardialen Magnetresonanztomographie“ selbstständig und ohne nicht offengelegte Hilfe Dritter verfasst und keine anderen als die angegebenen Quellen und Hilfsmittel genutzt habe.
Alle Stellen, die wörtlich oder dem Sinne nach auf Publikationen oder Vorträgen anderer Autoren/innen beruhen, sind als solche in korrekter Zitierung kenntlich gemacht. Die Abschnitte zu Methodik (insbesondere praktische Arbeiten, Laborbestimmungen, statistische Aufarbeitung) und Resultaten (insbesondere Abbildungen, Graphiken und Tabellen) werden von mir verantwortet.
Ich versichere ferner, dass ich die in Zusammenarbeit mit anderen Personen generierten Daten, Datenauswertungen und Schlussfolgerungen korrekt gekennzeichnet und meinen eigenen Beitrag sowie die Beiträge anderer Personen korrekt kenntlich gemacht habe (siehe Anteilserklärung). Texte oder Textteile, die gemeinsam mit anderen erstellt oder verwendet wurden, habe ich korrekt kenntlich gemacht.
Meine Anteile an etwaigen Publikationen zu dieser Dissertation entsprechen denen, die in der untenstehenden gemeinsamen Erklärung mit dem Erstbetreuer, angegeben sind. Für sämtliche im Rahmen der Dissertation entstandenen Publikationen wurden die Richtlinien des ICMJE (International Committee of Medical Journal Editors) zur Autorenschaft eingehalten. Ich erkläre ferner, dass ich mich zur Einhaltung der Satzung der Charité – Universitätsmedizin Berlin zur Sicherung Guter Wissenschaftlicher Praxis verpflichte.
Weiterhin versichere ich, dass ich diese Dissertation weder in gleicher noch in ähnlicher Form bereits an einer anderen Fakultät eingereicht habe.

Die Bedeutung dieser eidesstattlichen Versicherung und die strafrechtlichen Folgen einer unwahren eidesstattlichen Versicherung (§§156, 161 des Strafgesetzbuches) sind mir bekannt und bewusst.“

Datum Unterschrift

7.2 Anteilserklärung an den erfolgten Publikationen

Moritz Daniel Blum hatte folgenden Anteil an den folgenden Publikationen:

Publikation 1: *Blum, M., Hashemi, D., Motzkus, L. A., Neye, M., Dordevic, A., Zieschang, V., Zamani, S. M., Lapinskas, T., Runte, K., Kelm, M., Kühne, T., Tahirovic, E., Edelmann, F., Pieske, B., Düngen, H.-D. & Kelle, S. Variability of Myocardial Strain During Isometric Exercise in Subjects With and Without Heart Failure. Front. Cardiovasc. Med.* ***7,*** *111 (2020).*
Hilfestellung bei: Erstellung und Revision von Studienprotokoll und Ethikantrag.
Arbeitsteilig mit Ko-Doktorandin Laura Motzkus: Erstellung der Case-Report-Forms, Identifizierung, Rekrutierung von StudienteilnehmerInnen, Anamneseerhebung, körperliche Untersuchung, Blutentnahme, Durchführung von Sechs-Minuten-Gehtest und Minnesota-Living-With-Heart-Failure-Questionnaire, Betreuung der StudienteilnehmerInnen vor und nach der CMR, Erfassung und Management aller gesammelten Daten.
Selbstständig: Planung und Durchführung der statistischen Analyse, Erstellung aller Tabellen und Figuren, Verfassung des ersten Entwurfes einer Publikation, Überarbeitung des Entwurfes nach Rückmeldung der KoautorInnen, Einreichung der Publikation, Revision der Publikation im Peer-Review-Prozess.

Publikation 2: *Tanacli, R., Hashemi, D., Neye, M., Motzkus, L. A., Blum, M., Tahirovic, E., Dordevic, A., Kraft, R., Zamani, S. M., Pieske, B., Düngen, H.-D. & Kelle, S. Multilayer myocardial strain improves the diagnosis of heart failure with preserved ejection fraction. ESC Heart Fail. 7, 3240–3245 (2020).*
Hilfestellung bei: Erstellung und Revision von Studienprotokoll und Ethikantrag.
Arbeitsteilig mit Ko-Doktorandin Laura Motzkus: Erstellung der Case-Report-Forms, Identifizierung, Rekrutierung von StudienteilnehmerInnen, Anamneseerhebung, körperliche Untersuchung, Blutentnahme, Durchführung von Sechs-Minuten-Gehtest und Minnesota-Living-With-Heart-Failure-Questionnaire, Betreuung der StudienteilnehmerInnen vor und nach der CMR. Erfassung und Management aller gesammelten Daten.
Selbstständig: Kritische Überarbeitung des Manuskripts in der Rolle eines Koautors, insbesondere Anregung der Kombination von NTproBNP und subepikardialem LV GLS als zusätzlicher Parameter in der ROC-Analyse und der Einbindung von Spezifität als relevante Ergebnismetrik für diese Analyse.

Publikation 3: *Doeblin, P., Hashemi, D., Tanacli, R., Lapinskas, T., Gebker, R., Stehning, C., Motzkus, L. A., Blum, M., Tahirovic, E., Dordevic, A., Kraft, R., Zamani, S. M., Pieske, B., Edelmann, F., Dungen, H. D. & Kelle, S. CMR Tissue Characterization in Patients with HFmrEF. J Clin Med 8, (2019).*

Hilfestellung bei: Erstellung und Revision von Studienprotokoll und Ethikantrag.

Arbeitsteilig mit Ko-Doktorandin Laura Motzkus: Erstellung der Case-Report-Forms, Identifizierung, Rekrutierung von StudienteilnehmerInnen, Anamneseerhebung, körperliche Untersuchung, Blutentnahme, Durchführung von Sechs-Minuten-Gehtest und Minnesota-Living-With-Heart-Failure-Questionnaire, Betreuung der StudienteilnehmerInnen vor und nach der CMR. Erfassung und Management aller gesammelten Daten

Selbstständig: Kritische Überarbeitung des Manuskripts in der Rolle eines Koautors, insbesondere Hinweis auf Tukey's post-hoc Test im Rahmen einer ANOVA als Alternative zu wiederholten T-Tests und Korrektur des Methodenteils aus der Perspektive desjenigen, der die klinischen Untersuchungen durchgeführt hat.

Unterschrift, Datum und Stempel des/der erstbetreuenden Hochschullehrers/in

Unterschrift des Doktoranden/der Doktorandin

8. Druckexemplare der ausgewählten Publikationen

frontiers in Cardiovascular Medicine

CLINICAL TRIAL
published: 30 June 2020
doi: 10.3389/fcvm.2020.00111

Variability of Myocardial Strain During Isometric Exercise in Subjects With and Without Heart Failure

Moritz Blum[1], Djawid Hashemi[1,2], Laura Astrid Motzkus[1], Marthe Neye[1], Aleksandar Dordevic[1], Victoria Zieschang[3], Seyedeh Mahsa Zamani[3], Tomas Lapinskas[3,4], Kilian Runte[5,6], Marcus Kelm[5,6], Titus Kühne[2,5,6], Elvis Tahirovic[1,2], Frank Edelmann[1,2], Burkert Pieske[1,2,3], Hans-Dirk Düngen[1,2] and Sebastian Kelle[1,2,3*]

[1] Department of Internal Medicine/Cardiology, Charité–Universitätsmedizin Berlin, Berlin, Germany, [2] DZHK (German Center for Cardiovascular Research), Berlin, Germany, [3] Department of Internal Medicine/Cardiology, German Heart Center Berlin, Berlin, Germany, [4] Department of Cardiology, Medical Academy, Lithuanian University of Health Sciences, Kaunas, Lithuania, [5] Department of Congenital Heart Disease, German Heart Center Berlin, Berlin, Germany, [6] Institute for Imaging Science and Computational Modelling in Cardiovascular Medicine, Charité–Universitätsmedizin Berlin, Berlin, Germany

OPEN ACCESS

Edited by:
Matteo Cameli, University of Siena, Italy

Reviewed by:
Grigorios Korosoglou, Heidelberg University, Germany
Julian Vega Adauy, Pontificia Universidad Católica de Chile, Chile

***Correspondence:**
Sebastian Kelle
kelle@dhzb.de;
sebastian.kelle@charite.de

Specialty section:
This article was submitted to Cardiovascular Imaging, a section of the journal Frontiers in Cardiovascular Medicine

Received: *15 April 2020*
Accepted: *28 May 2020*
Published: *30 June 2020*

Citation:
Blum M, Hashemi D, Motzkus LA, Neye M, Dordevic A, Zieschang V, Zamani SM, Lapinskas T, Runte K, Kelm M, Kühne T, Tahirovic E, Edelmann F, Pieske B, Düngen H-D and Kelle S (2020) Variability of Myocardial Strain During Isometric Exercise in Subjects With and Without Heart Failure. Front. Cardiovasc. Med. 7:111. doi: 10.3389/fcvm.2020.00111

Background: Fast strain-encoded cardiac magnetic resonance imaging (cMRI, fast-SENC) is a novel technology potentially improving characterization of heart failure (HF) patients by quantifying cardiac strain. We sought to describe the impact of isometric handgrip exercise (HG) on cardiac strain assessed by fast-SENC in HF patients and controls.

Methods: Patients with stable HF and controls were examined using cMRI at rest and during HG. Left ventricular (LV) global longitudinal strain (GLS) and global circumferential (GCS) were derived from image analysis software using fast-SENC. Strain change $<$-0.5 and $>$ +0.5 was classified as increase and decrease, respectively.

Results: The study population comprised 72 subjects, including HF with reduced, mid-range and preserved ejection fraction and controls (HFrEF $n = 18$ HFmrEF $n = 18$, HFpEF $n = 17$, controls: $n = 19$). In controls, LV GLS remained stable in 36.8%, increased in 36.8% and decreased in 26.3% of subjects during HG. In HF subgroups, similar patterns of LV GLS response were observed (HFpEF: stable 41.2%, increase 35.3%, decrease: 23.5%; HFmrEF: stable 50.0%, increase 16.7%, decrease: 33.3%; HFrEF: stable 33.3%, increase 22.2%, decrease: 44.4%, $p = 0.668$). Mean change between LV GLS at rest and during HG ranged close to zero with broad standard deviation in all subgroups and was not significantly different between subgroups (+1.2 ± 5.4%, −0.6 ± 8.3%, −1.7 ± 10.7%, and −3.1 ± 19.4%, $p = 0.746$ in controls, HFpEF, HFmrEF and HFrEF, respectively). However, the absolute value of LV GLS change—irrespective of increase or decrease—was significantly different between subgroups with 4.4 ± 3.2% in controls, 5.9 ± 5.7% in HFpEF, 6.8 ± 8.3% in HFmrEF and 14.1 ± 13.3% in HFrEF ($p = 0.005$). The absolute value of LV GLS change significantly correlated with resting LVEF, NTproBNP and Minnesota Living with Heart Failure questionnaire scores.

Conclusion: The response to isometric exercise in LV GLS is heterogeneous in all HF subgroups and in controls. The absolute value of LV GLS change during HG exercise is elevated in HF patients and associated with measures of HF severity. The diagnostic utility of fast-SENC strain assessment in conjunction with HG appears to be limited.

Trial Registration: URL: https://www.drks.de; Unique Identifier: DRKS00015615.

Keywords: heart failure, cardiac magnetic resonance imaging, strain, fast SENC, isometric handgrip

INTRODUCTION

Heart Failure (HF) remains a significant burden for patients and health systems worldwide and, with high mortality despite optimal therapy, refinement of therapeutic and diagnostic strategies is needed (1). Different phenotypes in HF—namely HF with preserved, mid-range and reduced ejection fraction (HFpEF, HFmrEF, and HFrEF, respectively) (2)—respond differentially to medical therapy (3–6). Thus, accurate diagnosis and stratification of HF patients is of paramount importance.

Cardiac strain is an emerging diagnostic target in cardiac imaging, describing myocardial deformation throughout the cardiac cycle in three dimensions (7). Global longitudinal strain (GLS) and global circumferential strain (GCS) have been shown to be more sensitive in detecting myocardial dysfunctions than left ventricular (LV) ejection fraction (EF) and therefore promise earlier diagnosis and initiation of treatment (8, 9). Also, strain could facilitate accurate stratification of and consecutively appropriate therapy for HF patients (10). Cardiac magnetic resonance imaging (cMRI) represents the gold standard for cardiac imaging, especially for measuring volumes (2). Among other methods to quantify myocardial strain in cMRI, such as myocardial tagging, displacement encoding with stimulated echoes (DENSE) and feature tracking (FT) (11–13), fast strain-encoded cMRI (fast-SENC) is a relative novel approach which allows for reproducible and fast strain measurement (14, 15).

Physical stress testing can unmask myocardial dysfunction in early stages of HF—especially in HFpEF (16). For stress testing during cMRI, isometric handgrip exercise (HG) represents an accessible and reliable tool, potentially avoiding motion artifacts associated with dynamic exercise. The combination of strain analysis and HG has successfully been employed for detection of ischemia and could provide a new diagnostic approach for HF (17). HG represents an acute increase in afterload which physiologically is met by an elevation in HR and an increase of cardiac output. In patients with a poor cardiac reserve a rise in the left ventricular end-diastolic pressure can be expected (18). Also an effect on myocardial performance indices such as global strain might therefore be conceivable. Therefore, in this study we sought to characterize the impact of HG stress testing on cardiac strain assessed by fast-SENC, in HF patients and healthy controls.

METHODS

Study Population

The *Analysis of parameters of external and internal cardiac power, output and aortal compliance using cardiac MRI in patients with HF study* (EMPATHY-HF) was an investigator-initiated, prospective, cross-sectional study (German Clinical Trials Register ID: DRKS00015615). The study was performed in compliance with the Declaration of Helsinki and the study protocol was approved by the local institutional review board (Ethikausschuss 4 am Campus Benjamin Franklin, Charité Universitätsmedizin Berlin). All patients provided written informed consent before entering the study. A dedicated analysis of specific resting cMRI parameters derived from this study population has been published previously (19).

We included patients with stable chronic HF. Inclusion criteria are described in detail elsewhere (20). In brief, dyspnea NYHA class II or more and NTproBNP $\geq$ 220 ng/l were required for all HF patients, while specific imaging requirements applied for HFpEF (LV EF $\geq$ 50%, E/e' $\geq$ 13 or left atrial volume index $>$34 mL/m^2 or LV septum thickness $>$12 mm), HFmrEF (LV EF 40–49%) and HFrEF (LV EF $\leq$ 40%), as per European Society of Cardiology guidelines (2). All patients had to receive medical therapy as recommended in current guidelines. Additionally, we included controls without HF.

Exclusion criteria included atrial fibrillation (AF), high-grade valvular disease or a history of valve replacement, and cMRI contraindications such as implanted cardioverter-defibrillator (ICD) or pacemaker, BMI $>$38 kg/m^2 as well as a history of adverse contrast-medium reaction.

Study Procedures

All subjects underwent comprehensive clinical work-up including physical examination laboratory evaluation, ECG, 6-min walk test and quality of life assessment using the Minnesota Living with Heart Failure Questionnaire (MLHFQ). Medical history, current diagnoses and medication were extracted from electronic health records.

CMRI was performed using a clinical 1.5 Tesla MRI scanner (Achieva, Philips Healthcare, Best, The Netherlands) with a cardiac five-element phased array coil. Cine images were acquired using a retrospectively gated cine-cMRI in cardiac short-axis, vertical long-axis and horizontal long-axis orientations using a steady-state free precession sequence at rest. Fast-SENC was acquired at rest and during HG in real-time free breathing technique, as described previously (14). In brief, this SENC method generates temporary markers within the myocardium based on the unique MRI properties of tissue. The deformation of the myocardium during the cardiac phases changes the density of the markers, which when captured using an MRI spiral acquisition produces a cine sequence of SENC images (**Figure 1**).

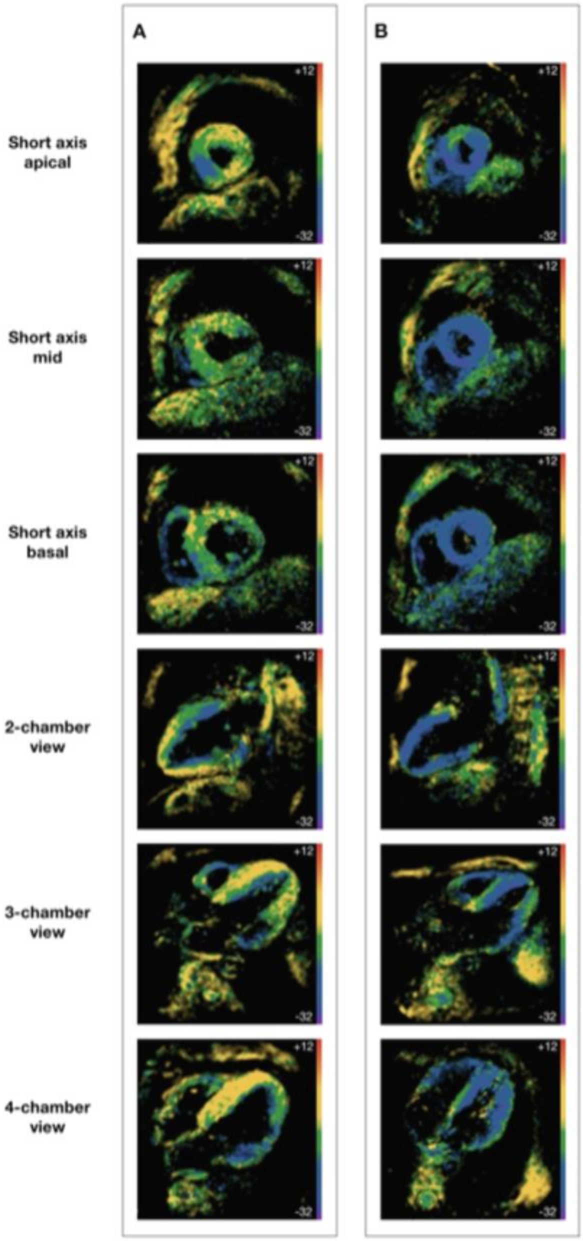

FIGURE 1 | Fast strain-encoded cardiac magnetic resonance imaging. **(A)** 62 year-old male with heart failure with reduced ejection fraction; **(B)** 62 year-old male without heart disease; all subjects were at physical rest during image acquisition; all images were acquired at end-systole; global longitudinal strain is derived from short axis views at apical, mid and basal level; global circumferential strain is derived from two-, three-, and for-chamber views.

Three short-axis planes (apical, mid, and basal level) as well as two-, three- and for-chamber planes were assessed.

After 15 min of supine rest, resting blood pressure and heart rate were obtained, followed by resting cMRI sequences. For HG exercise testing, a MRI-safe hand dynamometer was used (Stoelting, Wood Dale, Illinois). After determination of maximum voluntary contraction using the dominant hand, subjects were instructed to sustain 30% of maximum voluntary contraction for ~3 min, avoiding Valsalva maneuver by continued breathing. Continuing HG exercise, blood pressure, heart rate and stress cMRI sequences were recorded under stress conditions.

Image Analysis

Image analysis was performed using the software Medis® Suite 3.1.16.8 (Medis medical imaging systems, Leiden, The Netherlands) for left ventricular volume, mass and function measurements and the software MyoStrain 5.0 (Myocardial Solutions, Inc., Morrisville, North Carolina, USA) for fast-SENC strain measurements.

Trained operators manually traced endocardial and epicardial borders at end-systole and end-diastole. For quantitative assessment of global longitudinal strain (GLS), 3 short-axis planes (apical, mid and basal level) were analyzed using MyoStrain. Strain was calculated for each myocardial segment and then averaged. For quantitative global circumferential strain (GCS) assessment, three long-axis planes (two-, three-, and for-chamber view) were analyzed using the same software. Strain was calculated for each myocardial segment and then averaged. Myocardial shortening during systole translates to negative strain values. When communicating comparisons of strain values (e.g., strain decrease or increase) we will refer to the absolute value of strain, as recommended elsewhere (7).

We classified strain response to HG as *stable*, *increase* or *decrease*. In a recent study, our group investigated intra-observer reliability for LV GLS assessment employing fast-SENC in very similar cohort of healthy subjects and HF patients and found limits of agreement of −0.6 and +0.5 (15). Based on this observation, we decided that in order to classify as *increase* or *decrease*, LV GLS change must exceed <-0.5 or > +0.5, respectively. Accordingly, LV GLS change between ≥-0.5 and ≤+0.5 was classified as *stable*.

Statistical Analysis

Continuous variables are reported as mean (standard deviation), while categorical variables are reported as percentage. After testing for non-normality in distribution of continuous variables using the Shapiro-Wilk test, independent sample *t*-test, paired sample *t*-test and analysis of variance (ANOVA) for continuous response variables and Chi-square test for categorical response variables were used, as appropriate. For post-hoc analysis of intergroup differences in ANOVA we used Tukey's test. Pearson's coefficients were used to assess correlations between two continuous variables. For logarithmic transformations, the natural logarithm of variables of interest was utilized. Two-sided $p < 0.05$ were considered statistically significant. Sample size was chosen pragmatically based on similar previous studies and available research capacities (15, 21–23). Power calculation demonstrated that with the achieved sample size of $n = 18$ per subgroup and a standard deviation in LV GLS percentage change of ±12 overall, we were able to detect a subgroup difference of ±5 in LV GLS percentage change in ANOVA at a significance level of 0.05 yielding a statistical power of 0.83 (24).

Statistical analysis was performed using R version 3.5.1 (2018-07-02) (R Foundation for Statistical Computing, Vienna, Austria).

RESULTS

Study Population

The final analysis comprised 72 subjects, 18 HFrEF patients, 18 HFmrEF patients, 17 HFpEF patients and 19 controls.

Baseline characteristics varied widely between subgroups (**Table 1**). HFpEF patients were the oldest, most likely to be female and had the highest prevalence of hypertension and diabetes mellitus. HFmrEF patients had the highest prevalence of coronary artery disease but had the least severe dyspnea symptoms according to New York Heart Association (NYHA) classification. HFrEF patients were most likely to be men, had the highest BMI the most smoking pack years on average.

On laboratory examination, HFpEF patients had lowest levels of N-terminal pro-brain natriuretic peptide (NTproBNP), hemoglobin and red blood cells, but the highest levels of low-density-lipoprotein cholesterol, high-sensitivity Troponin T, high-sensitivity C-reactive protein, compared to other HF patients.

Almost all HFrEF patients received beta blockers (BB), and a majority also received angiotensin-converting enzyme inhibitors (ACEI) and mineralocorticoid antagonists (MRA). 22% of HFrEF patients received an angiotensin receptor blocker / neprilysin inhibitor (ARNI). HFmrEF patients were less likely to receive BB, ACEI or ARB and MRA compared to HFrEF patients. Among HFpEF patients, a majority received BB and either ACEI or ARB, 17.6% received MRA and one patient received off-label ARNI.

Hemodynamic Features at Rest and During Exercise

Hemodynamic features at rest and during HG are reported in **Table 2** and **Figure 2**. We report change as percentage change to account for subgroup differences at baseline. Numeric differences between rest and HG are reported in **Supplementary Table 1**. At rest, there were no differences between subgroups in regard of systolic blood pressure (BP), diastolic BP, pulse pressure (PP) or heart rate (HR).

In response to HG exercise, systolic and diastolic BP, HR and PP increased in all subgroups. Changes in BP, HR, and PP from rest to HG was not significantly different between subgroups. During HG exercise, we observed a stepwise decrease of systolic BP from controls to subjects with HFpEF, HFmrEF, and HFrEF with 163.2 ± 20.1, 156.2 ± 18.8, 147.8 ±17.3, and 140.7 ± 22.8 mmHg, respectively ($p = 0.006$). A similar pattern was found in PP during HG. Meanwhile, diastolic BP during HG was not different across subgroups.

Strain at Rest and During Isometric Exercise

At rest, LV strain was highest in healthy controls and decreased stepwise with HF category (**Table 2**, **Figure 3**). This held true for both LV GLS) and LV GCS. During HG exercise, we found mean LV strain to be largely unchanged. Correspondingly, there was a stepwise decrease with HF category in both LV GLS and LV GCS. A *post-hoc* analysis of subgroup differences in strain and hemodynamic parameters is detailed in **Supplementary Table 2**.

Mean percentage change between LV GLS at rest and during isometric exercise ranged close to zero with broad standard deviation in all subgroups (**Table 2**) and was not significantly different between subgroups (+1.2 ± 5.4%, −0.6 ± 8.3%, −1.7 ± 10.7%, and −3.1 ± 19.4%, $p = 0.746$ in controls, HFpEF, HFmrEF, and HFrEF, respectively). LV GLS change and LV GCS change in response to HG exercise were not correlated ($r = -0.02$, $p = 0.865$).

On subject level, strain response could be stable, as well as negative or positive (**Figure 4**). Strain change between ≥-0.5 and ≤+0.5 was classified as stable as specified above. In controls, LV GLS remained stable in 36.8%, increased in 36.8% and decreased in 26.3% of subjects in response to HG. In HFpEF, HFmrEF and HFrEF patients, similar distributions of LV GLS response to HG were observed (**Table 3**). The distribution of LV GLS response to HG did not vary significantly between subgroups ($p = 0.668$). There were no differences with regard to baseline characteristics between subjects with increase, decrease and no change of LV GLS in response to HG (**Supplementary Table 3**). LV GCS response to HG did not vary significantly between subgroups, either ($p = 0.831$).

Of note, the range of LV GLS change was narrow in controls (minimum: −11.0%, maximum: +10.0%), but wide in HFrEF (minimum: −42.0%, maximum: +32.0%). This led us to hypothesizing, that the absolute value of strain percentage change, rather than the direction of strain change (i.e., increase or decrease), was associated with presence of HF.

Absolute Value of Strain Change in Response to Isometric Exercise

Analyzing the absolute i.e., non-negative value of percentage change in strain as a measure of variability rather than increase or decrease in response to HG, we found substantial differences between subgroups (**Table 4**). In controls, the absolute value of LV GLS change was 4.4 ± 3.2%, in HFpEF it was 5.9 ± 5.7%, in HFmrEF it was 6.8 ± 8.3% and in HFrEF it was 14.1 ± 13.3% ($p = 0.005$). The absolute value of percentage change in LV GCS, again, was lowest in controls (8.6 ± 6.6%) followed by HFpEF (9.8 ± 6.6%), and HFrEF (14.7 ± 10.2%), and highest in HFmrEF (28.3 ± 40.4%, $p = 0.028$).

Plotting strain change against various surrogate parameters associated with HF illustrates that the absolute, non-negative value of LV GLS percentage change rather than the direction of this change (i.e., increase or decrease) was associated with disease severity (**Figure 5**). We further investigated different modes of expressing strain response (i.e., percentage change and the absolute value of percentage change) and their association with clinical, laboratory and imaging parameters. LV GCS change was not correlated with any parameter of HF severity — neither percentage change nor the absolute value of percentage change. Similarly, LV GLS percentage change was not correlated with

TABLE 1 | Baseline characteristics.

	Controls $n = 19$	HFpEF $n = 17$	HFmrEF $n = 18$	HFrEF $n = 18$	*p*-value
Female Sex–no. (%)	9 (47.4)	8 (47.1)	6 (33.3)	3 (16.7)	0.176
Age–years	61.5 ± 8.1	77.9 ± 8.0	67.9 ± 9.2	65.4 ± 10.5	<0.001
BMI–kg/m^2	25.1 ± 3.2	27.6 ± 3.8	27.3 ± 4.6	28.1 ± 3.8	0.104
CAD–no. (%)	0 (0.0)	11 (64.7)	15 (83.3)	13 (72.2)	<0.001
Hypertension–no. (%)	7 (36.8)	15 (88.2)	14 (77.8)	15 (83.3)	0.002
Previous MI–no. (%)	0 (0.0)	7 (41.2)	14 (77.8)	8 (44.4)	<0.001
Previous PCI–no. (%)	0 (0.0)	9 (52.9)	14 (77.8)	12 (66.7)	<0.001
Diabetes mellitus–no. (%)	2 (10.5)	5 (29.4)	3 (16.7)	5 (27.8)	0.441
LBBB on ECG–no. (%)	0 (0.0)	0 (0.0)	1 (5.6)	2 (11.1)	0.281
Ever Smoked–no. (%)	4 (21.1)	8 (47.1)	15 (83.3)	13 (72.2)	0.001
Packyears–years	2.0 ± 4.3	3.9 ± 6.8	29.8 ± 32.1	34.7 ± 52.7	0.003
NYHA Class II–no. (%)	0 (0.0)	10 (58.8)	15 (83.3)	15(72.2)	<0.001
III–no. (%)	0 (0.0)	7 (41.2)	3 (16.7)	3 (27.8)	
Leg Edema–no. (%)	3 (15.8)	12 (70.1)	14 (77.8)	12 (66.7)	<0.001
6 min walk distance–m	523.0 ± 118.6	344.4 ± 118.3	411.7 ± 86.0	417.4 ± 122.8	<0.001
MLHFQ QOL Score	4.7 ± 5.7	31.0 ± 23.1	25.2 ± 21.0	30.6 ± 25.8	<0.001
CONCOMITANT MEDICATION					
Beta-Blocker–no. (%)	6 (31.6)	11 (64.7)	14 (77.8)	17 (94.4)	<0.001
ACE-Inhibitor - no. (%)	2 (10.5)	3 (17.6)	6 (33.3)	10 (55.6)	0.015
ARB–no. (%)	4 (21.1)	12 (70.6)	7 (38.9)	8 (44.4)	0.027
MRA–no. (%)	0 (0.0)	3 (17.6)	4 (22.2)	11 (61.1)	<0.001
ARNI–no. (%)	0 (0.0)	1 (5.9)	0 (0.0)	4 (22.2)	0.026
Statin–no. (%)	2 (10.5)	9 (52.9)	15 (83.3)	11 (61.1)	<0.001
Loop Diuretic–no. (%)	0 (0.0)	3 (17.6)	6 (33.3)	7 (38.9)	0.02
HCT–no. (%)	4 (21.1)	4 (23.5)	2 (11.1)	1 (5.6)	0.401
LABORATORY					
Hb–g/dl	14.0 ± 1.1	13.0 ± 1.3	13.7 ± 1.1	14.9 ± 1.2	<0.001
RBC–/pl	4.7 ± 0.4	4.4 ± 0.5	4.5 ± 0.5	4.9 ± 0.5	0.007
WBC–/nl	6.1 ± 1.5	7.2 ± 2.4	8.5 ± 2.4	8.3 ± 2.3	0.003
Platelets–/nl	263.4 ± 65.9	265.8 ± 74.9	266.9 ± 74.0	209.7 ± 48.2	0.03
Hematocrit	0.40 ± 0.03	0.38 ± 0.03	0.41 ± 0.03	0.43 ± 0.04	0.001
Cholesterol–mg/dl	203.5 ± 33.5	172.5 ± 35.4	154.2 ± 44.3	156.1 ± 37.3	<0.001
LDL–mg/dl	133.0 ± 39.4	106.8 ± 29.5	92.2 ± 39.2	87.8 ± 30.4	0.001
HDL–mg/dl	66.5 ± 25.3	52.6 ± 12.8	49.4 ± 14.7	51.6 ± 18.3	0.029
Triglycerides–mg/dl	130.4 ± 79.6	129.7 ± 50.2	137.9 ± 81.1	173.3 ± 153.1	0.508
HbA1c –%	5.4 ± 0.5	5.9 ± 0.8	5.9 ± 0.7	5.8 ± 0.82	0.215
NTproBNP–ng/l	88.7 ± 61.1	459.1 ± 470.3	543.7 ± 385.5	2413.1 ± 3417.3	0.001
logNTproBNP–ng/l	4.26 ± 0.73	5.72 ± 1.13	6.06 ± 0.73	7.01 ± 1.20	<0.001
Hs TroponinT– ng/l	7.1 ± 3.4	19.9 ± 18.2	18.2 ± 19.67	19.4 ± 12.4	0.029
CRP–mg/l	1.3 ± 1.4	2.9 ± 2.7	3.1 ± 4.2	1.1 ± 0.7	0.029
CARDIAC MRI PARAMETERS					
LVEF –%	61.6 ± 5.4	61.6 ± 6.1	45.1 ± 2.7	33.5 ± 4.9	<0.001
LV EDV–ml	148.0 ± 34.5	130.3 ± 35.5	175.9 ± 28.8	261.8 ± 59.4	<0.001
LV ESV–ml	56.1 ± 18.4	50.9 ± 18.5	96.8 ± 17.7	175.6 ± 48.5	<0.001
LV SV–ml	90.1 ± 17.4	79.3 ± 20.1	79.1 ± 12.7	86.2 ± 16.6	0.144

ARB, angiotensin receptor blocker; ARNI, angiotensin receptor blocker–neprilysin inhibitor; BP, blood pressure EDV, end-diastolic volume; EF, ejection fraction; ECG, electrocardiogram; ESV, end-systolic volume; GCS, global circumferential strain; GLS, global longitudinal strain; HF, heart failure; HFpEF, HF with preserved EF; HFmrEF, HF with mid-range EF; HFrEF, HF with reduced EF; LBBB, left bundle branch block; MI, myocardial infarction; MLHFQ, Minnesota living with heart failure questionnaire; MRA, mineralocorticoid receptor antagonist, PCI, percutaneous coronary intervention; QOL, quality of life; RBC, red blood cells; WBC, white blood cells.

TABLE 2 | Hemodynamic characteristics and strain at rest and during isometric exercise.

		Controls $n = 19$	HfpEF $n = 17$	HfmrEF $n = 18$	HfrEF $n = 18$	p-value
Heart rate (/min)	Rest	59.9 ± 8.5	63.6 ± 9.8	64.3 ± 7.1	65.2 ± 7.0	0.231
	HG	69.4 ± 10.9*	71.5 ± 10.6*	71.7 ± 8.5*	74.2 ± 8.1*	0.514
	% Change	+16.2 ± 11.8	+12.9 ± 9.4	+11.6 ± 7.1	+14.3 ± 9.7	0.531
Systolic BP (mmHg)	Rest	129.8 ± 14.9	126.5 ± 19.2	119.9 ± 17.8	118.6 ± 17.7	0.165
	HG	163.2 ± 20.2*	156.2 ± 18.8*	147.8 ± 17.3*	140.7 ± 22.8*	0.006
	% Change	+26.3 ± 13.5	+24.8 ± 16.4	+24.1 ± 10.6	+18.9 ± 9.7	0.343
Diastolic BP (mmHg)	Rest	70.5 ± 6.6	67.8 ± 9.7	67.9 ± 8.8	68.8 ± 8.6	0.757
	HG	86.7 ± 8.6*	84.7 ± 11.9*	82.2 ± 8.3*	82.7 ± 13.1*	0.562
	% Change	+23.3 ± 11.5	+25.7 ± 13.7	+22.1 ± 13.3	+20.6 ± 14.7	0.714
Pulse pressure (mmHg)	Rest	59.4 ± 13.4	58.8 ± 13.2	51.9 ± 12.6	49.7 ± 11.9	0.06
	HG	76.5 ± 18.5*	71.5 ± 11.4*	65.6 ± 13.7*	58.1 ± 13.9*	0.002
	% Change	+30.0 ± 22.2	+24.9 ± 25.3	+28.2 ± 18.1	+17.3 ± 11.7	0.238
LV GLS	Rest	−20.1 ± 1.7	−19.1 ± 1.2	−16.0 ± 2.8	−11.4 ± 4.0	<0.001
	HG	−20.2 ± 1.5	−19.0 ± 2.1	−15.6 ± 2.6	−11.0 ± 4.1	<0.001
	% Change	+1.2 ± 5.4	−0.6 ± 8.3	−1.7 ± 10.7	−3.1 ± 19.4	0.746
LV GCS	Rest	−18.7 ± 2.4	−16.9 ± 2.3	−13.0 ± 3.5	−11.2 ± 3.3	<0.001
	HG	−18.4 ± 2.5	−17.2 ± 2.0	−13.1 ± 2.6	−10.6 ± 2.8	<0.001
	% Change	−0.8 ± 11.0	+3.1 ± 11.6	10.8 ± 48.6	−2.4 ± 18.1	0.467

Difference between rest and HG significant ($p<0.05$), assessed with paired t-test. BP, blood pressure; EF, ejection fraction; GCS, global circumferential strain; GLS, global longitudinal strain; HF, heart failure; HFpEF, HF with preserved EF; HFmrEF, HF with mid-range EF; HFrEF, HF with reduced EF, HG, isometric handgrip; LV, left ventricle.

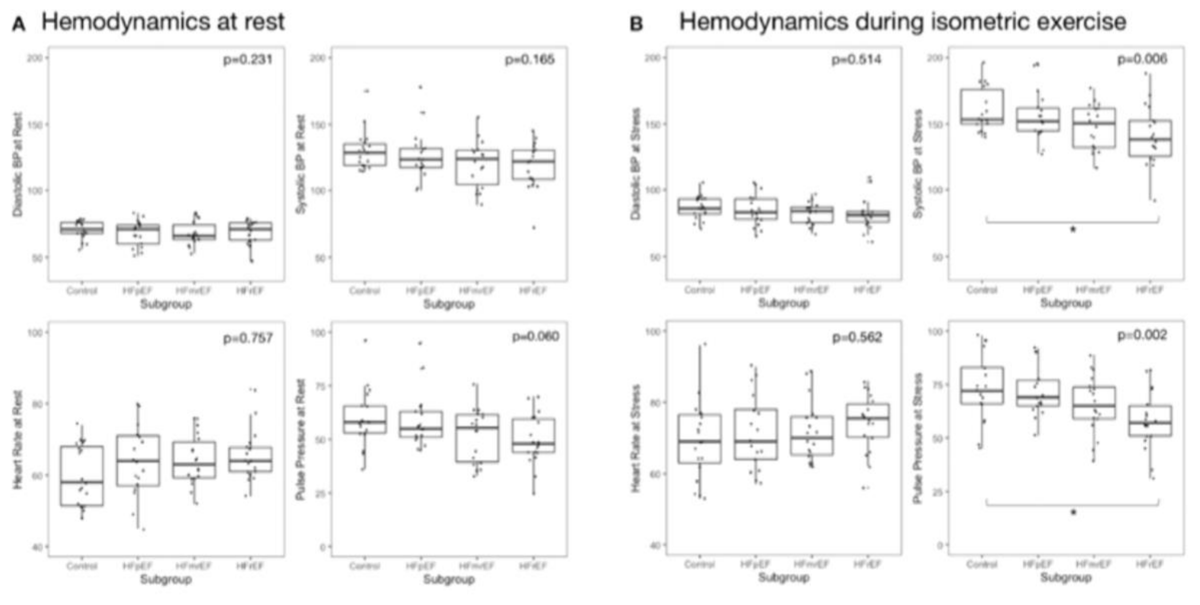

FIGURE 2 | Hemodynamic measurements at rest and during isometric exercise **(A)** at rest and **(B)** during isometric exercise. Reported are *p*-values from analysis of variance. Asterisks indicate significant inter-group difference in Tukey's *post-hoc* test of analysis of variance ($p < 0.05$). BP, blood pressure; EF, ejection fraction; HF, heart failure; HFpEF, HF with preserved EF; HFmrEF, HF with mid-range EF; HFrEF, HF with reduced EF.

surrogate parameters of HF severity. The absolute value of LV GLS percentage change, however, was moderately correlated with resting LV EF ($r = -0.37$, $p = 0.001$), NTproBNP ($r = 0.33$, $p = 0.004$), log-transformed NTproBNP ($r = 0.35$, $p = 0.002$), MLHFQ quality of life score ($r = 0.26$, $p = 0.028$), LV end-diastolic volume at rest ($r = 0.40$, $p = 0.006$), and LV end-systolic volume ($r = 0.43$, $p = 0.001$) at rest.

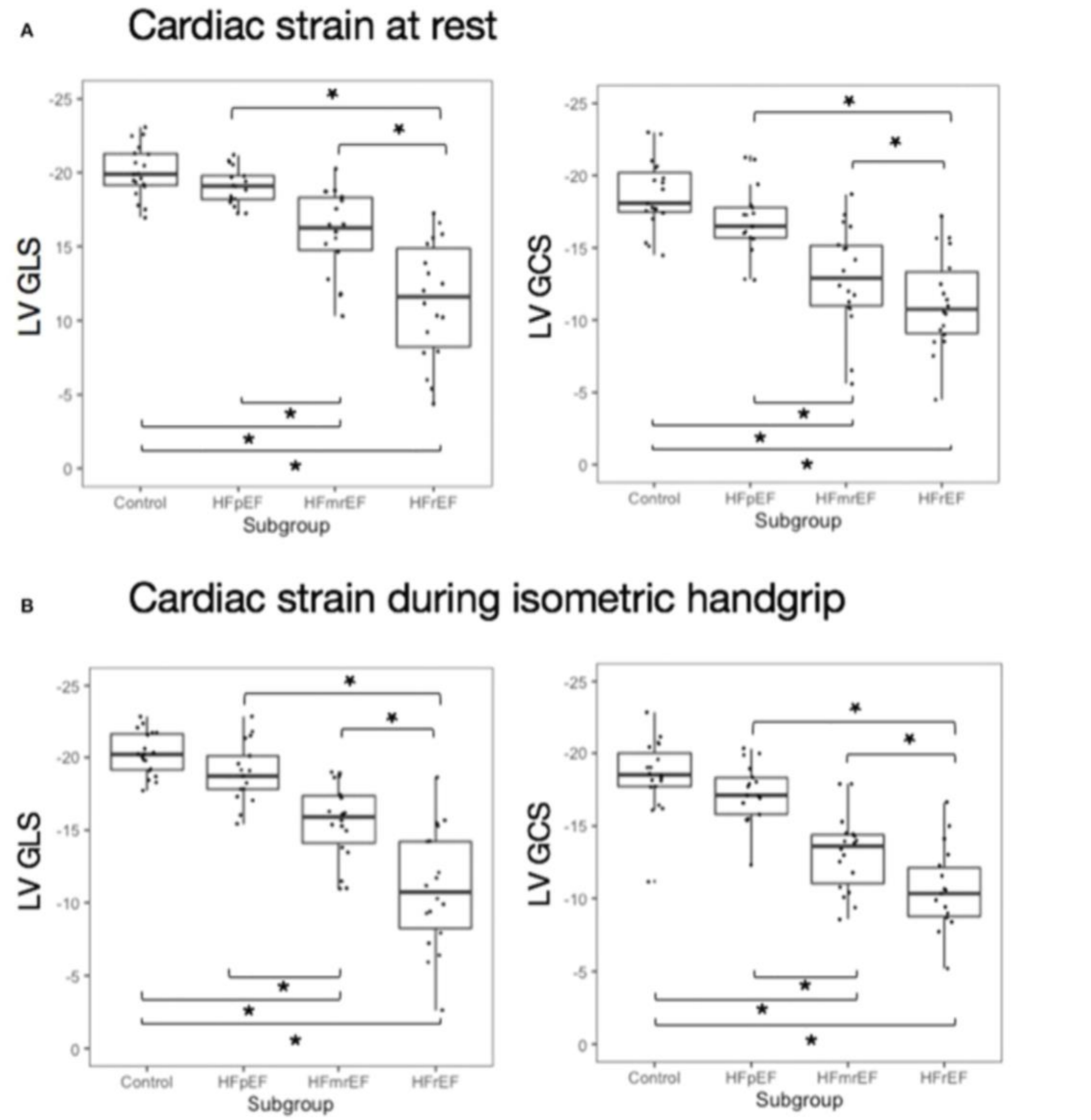

FIGURE 3 | Cardiac strain at rest and during isometric exercise **(A)** at rest and **(B)** during isometric exercise. Asterisks indicate significant inter-group difference in Tukey's *post-hoc* test of analysis of variance ($p < 0.05$). EF, ejection fraction; GCS, global circumferential strain; GLS, global longitudinal strain; HF, heart failure; HFpEF, HF with preserved EF; HFmrEF, HF with mid-range EF; HFrEF, HF with reduced EF; LV, left ventricle.

DISCUSSION

This study investigating cardiac strain in HF patients and controls undergoing cMRI paired with HG yielded the following findings:

1). The response to isometric exercise in LV GLS and GCS is heterogeneous, with increase and decrease in some subjects, and stable strain in others. This pattern was found in controls, as well as in all HF subgroups.

2). In HF patients, the extent of LV GLS change is elevated, regardless of whether strain increases or decreases, when compared to controls. This difference is most pronounced in patients with HFrEF.

3). The absolute value of LV GLS percentage change significantly correlates with surrogate parameters of HF severity.

Clinical Applications of Strain Assessment

Cardiac strain is a reliable and meaningful tool for detection of myocardial dysfunction in several diseases (2, 7). Multiple studies

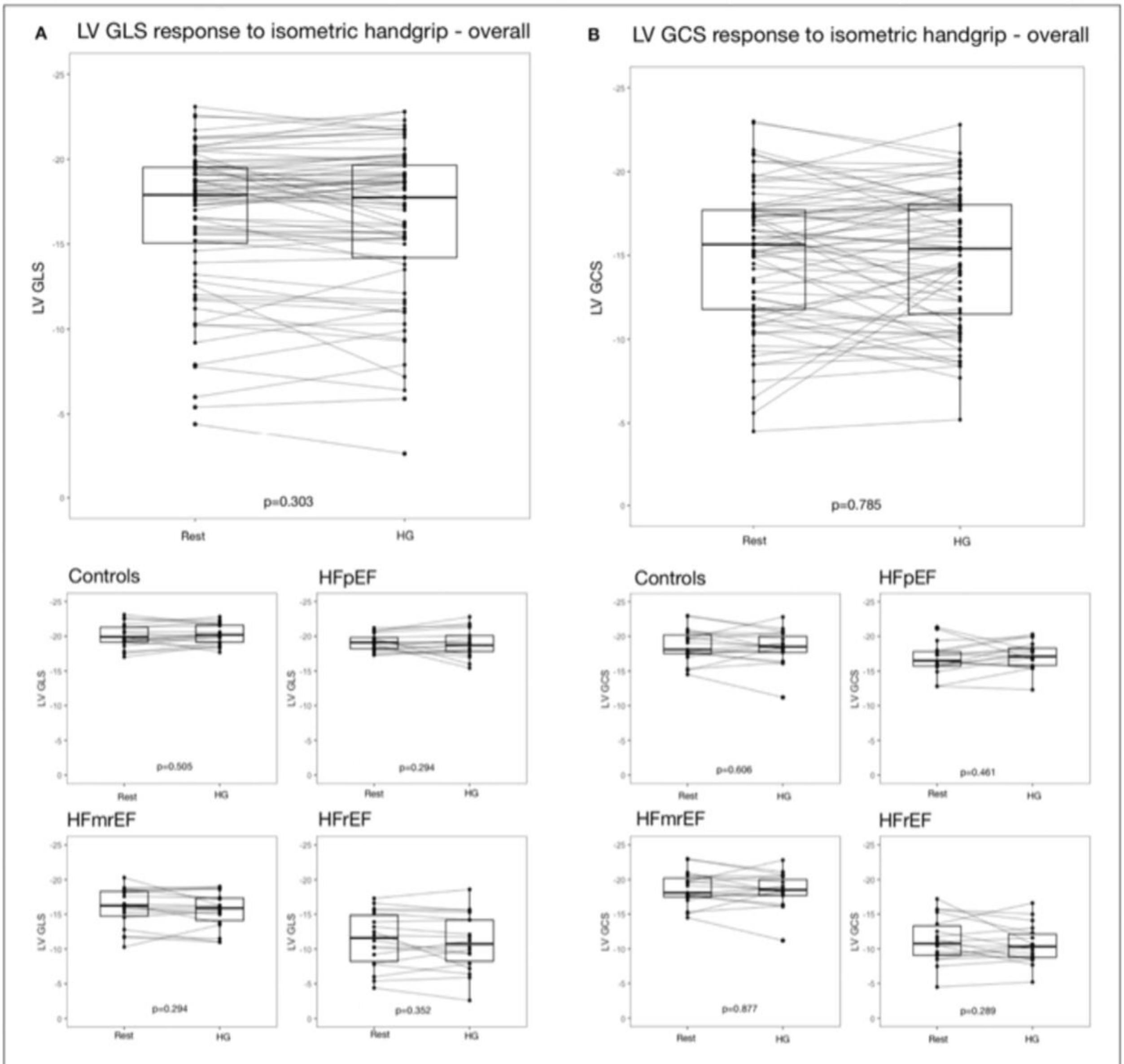

FIGURE 4 | Strain response to isometric exercise **(A)** LV GLS overall and in subgroups, **(B)** LV GCS overall and in subgroups. EF, ejection fraction; GCS, global circumferential strain; GLS, global longitudinal strain; HF, heart failure; HFpEF, HF with preserved EF; HFmrEF, HF with mid-range EF; HFrEF, HF with reduced EF; LV, left ventricle.

demonstrated its potential use for early detection of myocardial dysfunction, prognostic stratification and discrimination of different HF entities (8–10). A recent Heart Failure Association consensus recommendation for the diagnosis of HFpEF included impaired GLS into their HFA-PEFF score as a minor criterion (25). Especially in patients with borderline EF, assessment of cardiac strain could facilitate accurate diagnosis of HF, a possibility that future research has to investigate in depth.

The aim of this study, however, was to investigate the feasibility and diagnostic value of cardiac strain measured by fast-SENC in conjunction with HG exercise. Fast-SENC acquisition is rapid, within a single cardiac cycle, making the technique especially helpful for severely ill patients unable to hold breath as in typical cMRI exam (14, 26). It also requires minimal post-processing time to provide accurate and reproducible strain measurements. The SENC images can also be utilized for additional purposes, such as ultra-fast estimation of LV volumes and LV EF (15, 21).

To our best knowledge, our study was the first one to systematically evaluate the combined diagnostic approach of fast-SENC-based LV strain quantification and HG in HF patients and controls.

TABLE 3 | Categorization of change in strain during isometric exercise.

		Controls $n = 19$	HfpEF $n = 17$	HfmrEF $n = 18$	HfrEF $n = 18$	*p*-value
LV GLS	Increase–no. (%)	7 (36.8)	6 (35.3)	3 (16.7)	4 (22.2)	0.668
	No change–no. (%)	7 (36.8)	7 (41.2)	9 (50.0)	6 (33.3)	
	Decrease–no. (%)	5 (26.3)	4 (23.5)	6 (33.3)	8 (44.4)	
LV GCS	Increase– no. (%)	7 (36.8)	9 (52.9)	6 (33.3)	7 (38.9)	0.831
	No change– no. (%)	4 (21.1)	4 (23.5)	3 (16.7)	3 (16.7)	
	Decrease–no. (%)	8 (42.1)	4 (23.5)	9 (50.0)	8 (44.4)	

Increase: Δ LV GLS $<$ −0.5; No change: −0.5 $\leq$ Δ LV GLS $\leq$ +0.5; Increase: Δ LV GLS $>$ +0.5; Abbreviations: EF, ejection fraction; GCS, global circumferential strain; GLS, global longitudinal strain; HF, heart failure; HFpEF, HF with preserved EF; HFmrEF, HF with mid-range EF; HFrEF, HF with reduced EF; LV, left ventricle.

TABLE 4 | Change in strain during isometric exercise.

	Controls $n = 19$	HfpEF $n = 17$	HfmrEF $n = 18$	HfrEF $n = 18$	*p*-value
LV GLS					
% change	+1.2 ± 5.4	−0.6 ± 8.3	−1.7 ± 10.7	−3.1 ± 19.4	0.746
Absolute value of % change	4.4 ± 3.2	5.9 ± 5.7	6.8 ± 8.3	14.1 ± 13.3	0.005
LV GCS					
% change	−0.8 ± 11.0	+3.1 ± 11.6	+10.8 ± 48.6	−2.4 ± 18.1	0.467
Absolute value of % change	8.6 ± 6.6	9.8 ± 6.6	28.3 ± 40.4	14.7 ± 10.2	0.028

EF, ejection fraction; GCS, global circumferential strain; GLS, global longitudinal strain; HF, heart failure; HFpEF, HF with preserved EF; HFmrEF, HF with mid-range EF; HFrEF, HF with reduced EF, HG, isometric handgrip; LV, left ventricle.

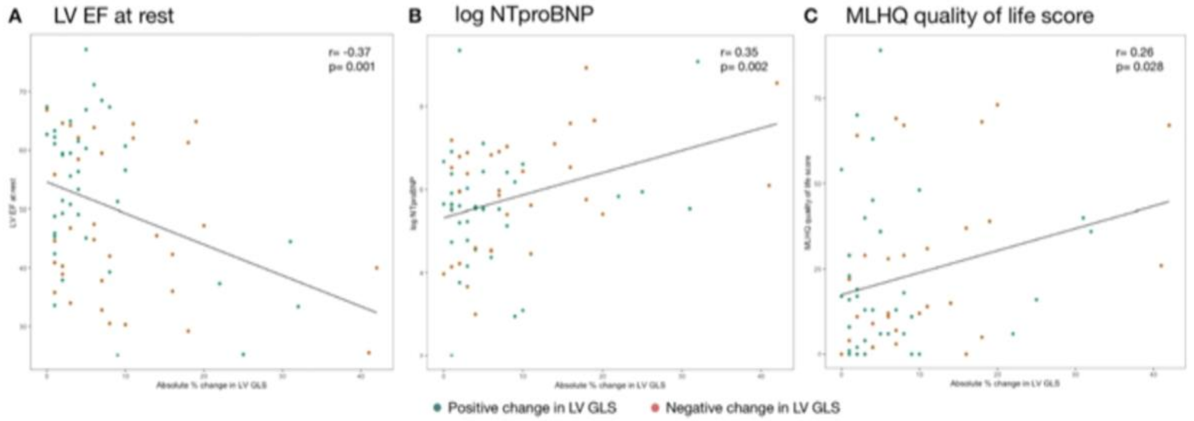

FIGURE 5 | Association of absolute change in strain during isometric exercise and **(A)** LV EF at rest, **(B)** log NTproBNP, and **(C)** MLHQ quality of life score. Reported are Pearson's *r* coefficients. NTproBNP was transformed by the natural logarithm function. EF, ejection fraction; GLS, global longitudinal strain; LV, left ventricle; MLHQ, Minnesota living with heart failure questionnaire; NTproBNP, N-terminal pro-brain natriuretic peptide.

Isometric Exercise, Afterload, and Contractility

In spite of only involving a relatively small group of muscles, HG exercise increases cardiac afterload, which has substantial effects on the cardiovascular system (18, 27): Systolic BP, diastolic BP and HR increase markedly which is believed to be due to a circulatory reflex serving to increase perfusion pressure in the contracting muscle groups (28). An early invasive study found that cardiac output (CO) increases during isometric handgrip exercise. However, this increase was mainly driven by a higher heart rate—LV systolic function even decreased slightly (18). A recent meta-analysis of imaging trials investigating the effects of HG on hemodynamic parameters confirmed that HR significantly increases, while SV and CO did not change significantly from rest to HG (29). All these studies support the notion, that the increase in cardiac afterload during HG is predominantly compensated by an increase in HR rather than in systolic myocardial contractility.

Strain has been postulated as the optimal measure of cardiac contraction and multiple studies demonstrated the close relation of strain with other measures of contractility (30–32). Thus, whether strain as a metric of contractility is an adequate measure to characterize the response to increased afterload, remains a question at issue.

Previous Studies on Strain Response to Increased Afterload

The dependency of myocardial strain on preload as implied by the principles of cardiac mechanics was already established by several early echocardiography studies (33–35). Conversely, the short-term impact of increased afterload on myocardial strain remains controversial.

Fredholm et al. examined 21 patients after cardiac surgery and found no change in strain in response to increased afterload after phenylephrine infusion (36). A study by Stefani et al. analyzed athletes and healthy controls undergoing speckle tracking echocardiography (STE) during HG. The authors found significant changes from baseline longitudinal strain exclusively in the medial to apical myocardial segments of athletes. In controls, no significant change in response to increased afterload was found, whatsoever (37).

On the contrary, a study by Donal et al. of 18 pigs employing open-chest echocardiography during graded aortic banding found a stepwise decrease in longitudinal strain with increasing afterload (38). The authors also found a differences between longitudinal strain, which already deteriorated after moderate increases in afterload (i.e. +10 mmHg) and radial strain, which was preserved during moderate increases in afterload and only deteriorated when afterload was further increased. This study indicates that the different vector components of myocardial strain, i.e. longitudinal, circumferential and radial strain, might react differentially to increased afterload. Of note, quantification of radial strain is technically not possible using fast-SENC (22). A study by Weiner et al. examining 18 healthy subjects undergoing STE found a significant decrease of LV longitudinal strain in response to HG. Simultaneously, parameters of LV twisting decreased significantly (39). Murai et al. observed decreased LV GLS in 41 young and healthy volunteers undergoing a similar STE + HG protocol (23). In addition, they measured ventricular wall stress in order to directly quantify afterload on the myocardium and found that the increase of wall stress and the decrease of strain during HG are inversely correlated. The authors also found that strain rate (SR) was less closely correlated to wall stress, suggesting that SR is less dependent on afterload than strain. All of the previous studies are limited by the shortcomings of hand-held echocardiography, namely angle-dependency of 2D image acquisition and intra-observer variability (7).

Heterogeneous Strain Response to Isometric Exercise in Controls and HF Patients

Our study expands this limited body of evidence employing a more accurate and reproducible fast-SENC acquisition-based approach to quantify strain and applying isometric HG exercise to increase afterload. Previous studies by our group demonstrated excellent inter-study, inter-observer and intra-observer reproducibility of fast-SENC based LV GLS assessment in both healthy controls and HF patients, providing evidence on the reliability of our strain measurements (15). Since the association of GLS and prognosis in HF is well established, we will focus on LV GLS changes in the following (9). In line with such previous evidence, we also found that the association with indices of HF severity is more pronounced with LV GLS compared to LV GCS.

We found a non-uniform LV GLS response to increased afterload with high variability between subjects. Investigating healthy controls, we found stable LV GLS as well as increase and decrease, with strain changes ranging from a −11.0 to +10.0%. In heart failure patients, strain changes ranged from −42.0 to +32.0%. Our findings imply that assessing strain response to HG based on whether strain increases or decreases might be misleading. Not only in HF patients, but also in healthy subjects, strain response appears to be heterogeneous.

Even though counter-intuitive at first glance, this finding appears to be in line with the preexisting literature: As lined out above, previous evidence on strain response to isometric exercise in non-HF subjects is equivocal with some studies reporting no change in longitudinal strain (36, 37), others reporting decreased GLS during HG (23, 38, 39). Most notably, none of these previous studies elaborated on the heterogeneity of strain response to afterload. Usually, only mean differences are reported. However, in some previous studies figures indicate a mixed response pattern with both increase and decrease of deformation indices present in some subjects (36, 39).

Thus, our observation of a non-uniform LV strain response in controls reconciles contradictory preliminary evidence and explicitly addresses a pattern already implicitly present in previous study reports.

Increased Absolute Value of Strain Change in HF Patients

In HF patients, LV GLS could be stable as well as increased or decreased in response to isometric exercise. This pattern did not significantly differ between HF patients and controls. However, the extent of strain change irrespective of whether strain increased or decreased was significantly elevated, particularly in HFrEF patients. In addition, the absolute value of LV GLS change was significantly associated with indicators for severity of symptoms. Patients with substantial change in strain—without regard to the direction of change– were more likely to have reduced LV EF, high levels of NTproBNP and to suffer from severe HF symptoms as quantified by MLHFQ. This association with HF severity also raises the question whether extreme strain changes in response to HG might have prognostic implications in HF patients. The significant correlation of the absolute value of LV GLS change and LV end-diastolic and LV end-systolic volumes also establishes a mechanical relationship to cardiac dilation and preload which stipulates further investigation.

The question remaining is what determine decrease or increase of strain in response to HG given that they occur in both healthy and HF subjects. Based on previous studies indicating that increased afterload was compensated by a rise in HR rather than an increase in myocardial contractility, we hypothesized that there might be an association between LV GLS change and with HR change to HG (18, 29). In fact, in an exploratory analysis including only HF patients, we found a significant inverse association between HR change and LV GLS change in response to HG ($r = -0.31$, $p = 0.023$, **Supplemental Figure 1**). This supports the notion that strain change and HR change are inversely related and excessive increase in LV GLS might be an expression of inability to adjust HR in response to isometric exercise. However, this association dissipated when including controls into this exploratory analysis ($r = -0.20$, $p = 0.095$).

Implications for Future Research Into Strain Response to Increased Afterload

The potential association of strain change and HR change again points toward SR, i.e. the temporal derivative of strain, as a promising measure for future studies into the effects of HG on myocardial contractility. SR depends on both strain and the length of the cardiac cycle (40). During HG exercise, HR physiologically increases leading to a shortening of myocardial contraction time per heartbeat. With strain decreasing while the cardiac cycle is shortening in response to increased afterload, SR which is a function of strain and contraction time might stay relatively stable. Murai et al. in fact demonstrated that SR is less dependent on afterload than strain in healthy subjects (23). Thus, significant changes in SR during HG could potentially reflect dysbalance regarding response of strain and HR to increased afterload in HF patients. However, due to software limitations we were not able to quantify SR in this study.

Furthermore, it is important to bear in mind that the LV is not operating mechanically in isolation. Both the right ventricle (RV) and the left atrium (LA) have been identified to play important roles in exercise hemodynamics (41, 42). Thus, further investigation into LA strain, RV strain and their relation to LV strain in exercise settings with increased afterload are necessary in order to fully understand cardiac deformation mechanics during HG.

Even though our findings elucidate cardiac adaption mechanisms in response to acute increase in afterload, our study suggests that the diagnostic utility of strain assessment in conjunction with HG is limited. With heterogeneous response patterns and dependency on heart rate variability and presumably other factors not yet fully understood, assessment of strain response to isometric exercise does not appear to provide substantial additional diagnostic value on top of strain assessment during physical rest. Other stress testing modalities such as pharmacological stress induction and dynamic exercise testing have more drastic effects on HR and stroke volume and might be better suited for diagnostic purposes (29).

Limitations

Several limitations of this study have to be addressed. We cannot rule out the possibility of confounding by unmeasured variables. While including more patients than previous studies investigating the impact of increased afterload on strain, our sample size was still relatively small. We had to exclude patients with implanted ICD and Pacemakers due to MRI contraindication. This limits the generalizability of our study to the general HF population, especially in patients with HFrEF. Concomitant medication, namely BB, might have influenced the hemodynamic response to isometric exercise, particularly regarding the physiological increase in HR. Similarly, left bundle branch block in particular is known to compromise cardiac adaption to increased afterload and different prevalence of LBBB within different subgroups might have impacted our findings (43). Also, we cannot rule out the possibility that ischemia-related motion abnormalities influenced our findings. Besides, HG exercise testing is prone to measurement errors due to lack of cooperation or Valsalva-maneuver during handgrip leading to elevated intrathoracic pressures. Diligent patient instruction and supervision during exercise by trained personnel was implemented to prevent such errors. However, our findings should only be considered hypothesis-generating.

CONCLUSION

In conclusion, we found that the strain response to isometric exercise quantified by fast-SENC is heterogeneous: LV GLS and GCS are stable in some patients, but decrease or increase in others, with no significant differences between controls and HF subgroups. However, the absolute value of strain change during isometric exercise—rather than increase or decrease—is elevated in HF patients and associated with measures of HF severity. Our observations indicate that the applicability of strain assessment in conjunction with HG for diagnostic purposes in HF seems to be limited.

DATA AVAILABILITY STATEMENT

The datasets presented in this article are not readily available because the informed consent given by study participants allows for data sharing only with parties which are explicitly mentioned in the consent form. Requests to access the datasets should be directed to Sebastian Kelle, kelle@dhzb.de.

ETHICS STATEMENT

The studies involving human participants were reviewed and approved by Ethikausschuss 4 am Campus Benjamin Franklin, Charité Universitätsmedizin Berlin. The patients/participants provided their written informed consent to participate in this study.

AUTHOR CONTRIBUTIONS

MB, DH, H-DD, and SK conceived and designed the study. MB, DH, LM, MN, AD, and KR acquired clinical data. VZ, SZ, TL, and SK acquired and analyzed imaging data. MB executed the statistical analysis and drafted the manuscript. MK, TK, ET, BP, FE, H-DD, and SK revised and amended critical parts of the manuscript. All authors contributed to the interpretation of the data and approved the final version of this manuscript.

FUNDING

The authors declare that this study received funding from Philips Healthcare, DZHK (German Centre for Cardiovascular Research), Partner Site Berlin, Germany and Myocardial Solutions. The authors also acknowledge support from the German Research Foundation (DFG) and the Open Access Publication Fund of Charité—Universitätsmedizin Berlin. The funders were not involved in the study design, collection, analysis, interpretation of data, and the writing of this article or the decision to submit it for publication.

ACKNOWLEDGMENTS

We would like to thank the study participants as well as the numerous individuals who contributed to this study, namely Robin Kraft, Radu Tanacli, Monica Post, Corinna Else, Gudrun Großer, Janina Dentzer, and Cosima Mattner.

SUPPLEMENTARY MATERIAL

The Supplementary Material for this article can be found online at: https://www.frontiersin.org/articles/10.3389/fcvm.2020.00111/full#supplementary-material

REFERENCES

1. Benjamin EJ, Muntner P, Alonso A, Bittencourt MS, Callaway CW, Carson AP, et al. Heart disease and stroke statistics-2019 update: a report from the american heart association. *Circulation.* (2019) 139:e56–e28. doi: 10.1161/CIR.0000000000000659
2. Ponikowski P, Voors AA, Anker SD, Bueno H, Cleland JG, Coats AJ, et al. (2016). ESC guidelines for the diagnosis treatment of acute chronic heart failure: the task force for the diagnosis treatment of acute chronic heart failure of the European Society of Cardiology (ESC). Developed with the special contribution of the Heart Failure Association (HFA) of the ESC. *Eur J Heart Fail.* (2016) 18:891–975. doi: 10.1002/ejhf.592
3. Yusuf S, Pfeffer MA, Swedberg K, Granger CB, Held P, McMurray JJ, et al. Effects of candesartan in patients with chronic heart failure and preserved left-ventricular ejection fraction: the CHARM-preserved trial. *Lancet.* (2003) 362:777–81. doi: 10.1016/S0140-6736(03)14285-7
4. Massie BM, Carson PE, McMurray JJ, Komajda M, McKelvie R, Zile MR, et al. Irbesartan in patients with heart failure and preserved ejection fraction. *N Engl J Med.* (2008) 359:2456–67. doi: 10.1056/NEJMoa0805450
5. Pieske B, Maggioni AP, Lam CSP, Pieske-Kraigher E, Filippatos G, Butler J, et al. Vericiguat in patients with worsening chronic heart failure and preserved ejection fraction: results of the soluble guanylate cyclase stimulator in heart failure patients with preserved ef (socrates-preserved) study. *Eur Heart J.* (2017) 38:1119–27. doi: 10.1093/eurheartj/ehw593
6. Pitt B, Pfeffer MA, Assmann SF, Boineau R, Anand IS, Claggett B, et al. Spironolactone for heart failure with preserved ejection fraction. *N Engl J Med.* (2014) 370:1383–92. doi: 10.1056/NEJMoa1313731
7. Smiseth OA, Torp H, Opdahl A, Haugaa KH, Urheim S. Myocardial strain imaging: how useful is it in clinical decision making? *Eur Heart J.* (2016) 37:1196–207. doi: 10.1093/eurheartj/ehv529
8. Thavendiranathan P, Poulin F, Lim KD, Plana JC, Woo A, Marwick TH. Use of myocardial strain imaging by echocardiography for the early detection of cardiotoxicity in patients during and after cancer chemotherapy: a systematic review. *J Am Coll Cardiol.* (2014) 63:2751–68. doi: 10.1016/j.jacc.2014.01.073
9. Kalam K, Otahal P, Marwick TH. Prognostic implications of global LV dysfunction: a systematic review and meta-analysis of global longitudinal strain and ejection fraction. *Heart.* (2014) 100:1673–80. doi: 10.1136/heartjnl-2014-305538
10. Kraigher-Krainer E, Shah AM, Gupta DK, Santos A, Claggett B, Pieske B, et al. Impaired systolic function by strain imaging in heart failure with preserved ejection fraction. *J Am Coll Cardiol.* (2014) 63:447–56. doi: 10.1016/j.jacc.2013.09.052
11. Zerhouni EA, Parish DM, Rogers WJ, Yang A, Shapiro EP. Human heart: tagging with MR imaging–a method for noninvasive assessment of myocardial motion. *Radiology.* (1988) 169:59–63. doi: 10.1148/radiology.169.1.3420283
12. Feng L, Donnino R, Babb J, Axel L, Kim D. Numerical and *in vivo* validation of fast cine displacement-encoded with stimulated echoes (DENSE) MRI for quantification of regional cardiac function. *Magn Reson Med.* (2009) 62:682–90. doi: 10.1002/mrm.22045
13. Hor KN, Baumann R, Pedrizzetti G, Tonti G, Gottliebson WM, Taylor M, et al. Magnetic resonance derived myocardial strain assessment using feature tracking. *J Vis Exp.* (2011) 12:2356. doi: 10.3791/2356
14. Pan L, Stuber M, Kraitchman DL, Fritzges DL, Gilson WD, Osman NF. Real-time imaging of regional myocardial function using fast-SENC. *Magn Reson Med.* (2006) 55:386–95. doi: 10.1002/mrm.20770
15. Giusca S, Korosoglou G, Zieschang V, Stoiber L, Schnackenburg B, Stehning C, et al. Reproducibility study on myocardial strain assessment using fast-SENC cardiac magnetic resonance imaging. *Sci Rep.* (2018) 8:14100. doi: 10.1038/s41598-018-32226-3
16. Obokata M, Kane GC, Reddy YN, Olson TP, Melenovsky V, Borlaug BA. Role of diastolic stress testing in the evaluation for heart failure with preserved ejection fraction: a simultaneous invasive-echocardiographic study. *Circulation.* (2017) 135:825–38. doi: 10.1161/CIRCULATIONAHA.116.024822
17. Ryo K, Tanaka H, Kaneko A, Fukuda Y, Onishi T, Kawai H, et al. Efficacy of longitudinal speckle tracking strain in conjunction with isometric handgrip stress test for detection of ischemic myocardial segments. *Echocardiography.* (2012) 29:411–8. doi: 10.1111/j.1540-8175.2011.01621.x
18. Helfant RH, De Villa MA, Meister SG. Effect of sustained isometric handgrip exercise on left ventricular performance. *Circulation.* (1971) 44:982–3. doi: 10.1161/01.CIR.44.6.982
19. Doeblin P, Hashemi D, Tanacli R, Lapinskas T, Gebker R, Stehning C, et al. CMR Tissue characterization in patients with HFmrEF. *J Clin Med.* (2019) 8:1877. doi: 10.3390/jcm8111877
20. *DRKS - Deutsches Register Klinischer Studien (German Clinical Trials Register).* (2018). Available from: https://www.drks.de/.
21. Lapinskas T, Zieschang V, Erley J, Stoiber L, Schnackenburg B, Stehning C, et al. Strain-encoded cardiac magnetic resonance imaging: a new approach for fast estimation of left ventricular function. *BMC Cardiovasc Disord.* (2019) 19:52. doi: 10.1186/s12872-019-1031-5
22. Bucius P, Erley J, Tanacli R, Zieschang V, Giusca S, Korosoglou G, et al. Comparison of feature tracking, fast-SENC, and myocardial tagging for global and segmental left ventricular strain. *ESC Heart Fail.* (2020) 7:523–32. doi: 10.1002/ehf2.12576

23. Murai D, Yamada S, Hayashi T, Okada K, Nishino H, Nakabachi M, et al. Relationships of left ventricular strain and strain rate to wall stress and their afterload dependency. *Heart Vessels.* (2017) 32:574–83. doi: 10.1007/s00380-016-0900-4
24. Cohen J. A power primer. *Psychol Bull.* (1992) 112:155–9. doi: 10.1037/0033-2909.112.1.155
25. Pieske B, Tschope C, de Boer RA, Fraser AG, Anker SD, Donal E, et al. How to diagnose heart failure with preserved ejection fraction: the HFA-PEFF diagnostic algorithm: a consensus recommendation from the Heart Failure Association (HFA) of the European Society of Cardiology (ESC). *Eur Heart J.* (2019) 40:3297–317. doi: 10.1093/eurheartj/ehz641
26. Osman NF, Sampath S, Atalar E, Prince JL. Imaging longitudinal cardiac strain on short-axis images using strain-encoded MRI. *Magn Reson Med.* (2001) 46:324–34. doi: 10.1002/mrm.1195
27. Lind AR, Taylor SH, Humphreys PW, Kennelly BM, Donald KW. The circulatiory effects of sustained voluntary muscle contraction. *Clin Sci.* (1964) 27:229–44.
28. MacDonald H, Sapru R, Taylor S, Donald K. Effects of intravenous propranolol (Inderal) on the systemic circulatory response to sustained handgrip. *Amer J Cardiol.* (1966) 18:333–44. doi: 10.1016/0002-9149(66)90051-8
29. Runte K, Brosien K, Salcher-Konrad M, Schubert C, Goubergrits L, Kelle S, et al. Hemodynamic changes during physiological and pharmacological stress testing in healthy subjects, aortic stenosis and aortic coarctation patients-a systematic review and meta-analysis. *Front Cardiovasc Med.* (2019) 6:43. doi: 10.3389/fcvm.2019.00043
30. Mirsky I, Parmley WW. Assessment of passive elastic stiffness for isolated heart muscle and the intact heart. *Circ Res.* (1973) 33:233–43. doi: 10.1161/01.RES.33.2.233
31. Greenberg NL, Firstenberg MS, Castro PL, Main M, Travaglini A, Odabashian JA, et al. Doppler-derived myocardial systolic strain rate is a strong index of left ventricular contractility. *Circulation.* (2002) 105:99–105. doi: 10.1161/hc0102.101396
32. Weidemann F, Jamal F, Sutherland GR, Claus P, Kowalski M, Hatle L, et al. Myocardial function defined by strain rate and strain during alterations in inotropic states and heart rate. *Am J Physiol Heart Circ Physiol.* (2002) 283:H792–9. doi: 10.1152/ajpheart.00025.2002
33. Urheim S, Edvardsen T, Torp H, Angelsen B, Smiseth OA. Myocardial strain by Doppler echocardiography. Validation of a new method to quantify regional myocardial function. *Circulation.* (2000) 102:1158–64. doi: 10.1161/01.CIR.102.10.1158
34. Rosner A, Bijnens B, Hansen M, How OJ, Aarsaether E, Muller S, et al. Left ventricular size determines tissue doppler-derived longitudinal strain and strain rate. *Eur J Echocardiogr.* (2009) 10:271–7. doi: 10.1093/ejechocard/jen230
35. Burns AT, La Gerche A, D'Hooge J, MacIsaac AI, Prior DL. Left ventricular strain and strain rate: characterization of the effect of load in human subjects. *Eur J Echocardiogr.* (2010) 11:283–9. doi: 10.1093/ejechocard/jep214
36. Fredholm M, Jorgensen K, Houltz E, Ricksten SE. Load-dependence of myocardial deformation variables - a clinical strain-echocardiographic study. *Acta Anaesthesiol Scand.* (2017) 61:1155–65. doi: 10.1111/aas.12954
37. Stefani L, Pedrizzetti G, De Luca A, Mercuri R, Innocenti G, Galanti G. Real-time evaluation of longitudinal peak systolic strain (speckle tracking measurement) in left and right ventricles of athletes. *Cardiovasc Ultrasound.* (2009) 7:17. doi: 10.1186/1476-7120-7-17
38. Donal E, Bergerot C, Thibault H, Ernande L, Loufoua J, Augeul L, et al. Influence of afterload on left ventricular radial and longitudinal systolic functions: a two-dimensional strain imaging study. *Eur J Echocardiogr.* (2009) 10:914–21. doi: 10.1093/ejechocard/jep095
39. Weiner RB, Weyman AE, Kim JH, Wang TJ, Picard MH, Baggish AL. The impact of isometric handgrip testing on left ventricular twist mechanics. *J Physiol.* (2012) 590:5141–50. doi: 10.1113/jphysiol.2012.236166
40. D'Hooge J, Heimdal A, Jamal F, Kukulski T, Bijnens B, Rademakers F, et al. Regional strain and strain rate measurements by cardiac ultrasound: principles, implementation and limitations. *Eur J Echocardiogr.* (2000) 1:154–70. doi: 10.1053/euje.2000.0031
41. Telles F, Nanayakkara S, Evans S, Patel HC, Mariani JA, Vizi D, et al. Impaired left atrial strain predicts abnormal exercise haemodynamics in heart failure with preserved ejection fraction. *Eur J Heart Fail.* (2019) 21:495–505. doi: 10.1002/ejhf.1399
42. Sugimoto T, Bandera F, Generati G, Alfonzetti E, Bussadori C, Guazzi M. Left atrial function dynamics during exercise in heart failure: pathophysiological implications on the right heart and exercise ventilation inefficiency. *JACC Cardiovasc Imaging.* (2017) 10:1253–64. doi: 10.1016/j.jcmg.2016.09.021
43. Aalen J, Storsten P, Remme EW, Sirnes PA, Gjesdal O, Larsen CK, et al. Afterload hypersensitivity in patients with left bundle branch block. *JACC Cardiovasc Imaging.* (2019) 12:967–77. doi: 10.1016/j.jcmg.2017.11.025

Conflict of Interest: SK reports grants and other support by the DZHK (German Center for Cardiovascular Research), Partner Site Berlin, Philips Healthcare, BioVentrix, Berlin-Chemie, Merck/Bayer, Novartis, Astra Zeneca, Siemens and Myocardial Solutions outside of the submitted work. SK was also on the advisory board for Merck/Bayer, BioVentrix, and Myocardial Solutions. BP has provided steering committee and advisory board services for Bayer Healthcare and MSD; and has received steering committee and advisory board/speaker honoraria from Novartis.

The remaining authors declare that the research was conducted in the absence of any commercial or financial relationships that could be construed as a potential conflict of interest.

ESC HEART FAILURE
ESC Heart Failure 2020; **7**: 3240–3245
Published online 21 June 2020 in Wiley Online Library (wileyonlinelibrary.com) **DOI:** 10.1002/ehf2.12826

SHORT COMMUNICATION

Multilayer myocardial strain improves the diagnosis of heart failure with preserved ejection fraction

Radu Tanacli[1,2*], Djawid Hashemi[2,3], Marthe Neye[1], Laura Astrid Motzkus[2], Moritz Blum[2], Elvis Tahirovic[2], Aleksandar Dordevic[2], Robin Kraft[2], Seyedeh Mahsa Zamani[1], Burkert Pieske[1,2,3], Hans-Dirk Düngen[2,3] and Sebastian Kelle[1,2,3]

[1]*Department of Internal Medicine/Cardiology, German Heart Center Berlin, Berlin, 13353, Germany;* [2]*Department of Internal Medicine/Cardiology, Charité Campus Virchow Klinikum, Berlin, 13353, Germany;* [3]*DZHK (German Center for Cardiovascular Research), Partner Site Berlin, Berlin, 10115, Germany*

Abstract

Aims The diagnostic and treatment of patients with heart failure with preserved ejection fraction (HFpEF) are both hampered by an incomplete understanding of the pathophysiology of the disease. Novel imaging tools to adequately identify these patients from individuals with a normal cardiac function and respectively patients with HF with reduced EF are warranted. Computing multilayer myocardial strain with feature tracking is a fast and accurate method to assess cardiac deformation. Our purpose was to assess the HFpEF diagnostic ability of multilayer strain parameters and compare their sensitivity and specificity with other established parameters.

Methods and results We included 20 patients with a diagnosis of HFpEF and, respectively, 20 matched controls. We assessed using feature-tracking cardiac magnetic resonance longitudinal and circumferential myocardial strain at three distinct layers of the myocardium: subendocardial (Endo-), mid-myocardial (Myo-), and subepicardial (Epi-). Comparatively, we additionally assessed various others clinical, imaging, and biochemical parameters with a putative role in HFpEF diagnostic: left ventricular end-diastolic volume (LVEDV), left ventricular mass (LVM), interventricular septum (IVS) wall thickness and free wall thickness, left atrial volume and strain, septal and lateral mitral annular early diastolic velocity (e\`), E/e´ ratio, and plasma levels of N-terminal pro-B-type natriuretic peptide (NT-proBNP). Global longitudinal strain (GLS) is significantly impaired at Endo (-20.8 ± 4.0 vs. -23.2 ± 3.4, $P = 0.046$), Myo- (-18.0 ± 3.0 vs. -21.0 ± 2.5, $P = 0.002$), and Epi- (-12.2 ± 2.0 vs. -16.2 ± 2.5, $P < 0.001$) levels. Compared with any other imaging parameter, an Epi-GLS lower than 13% shows the highest ability to detect patients with HFpEF [area under the curve (AUC) = 0.90 (0.81–1), $P < 0.001$] and in tandem with NT-proBNP can diagnose with maximal sensibility (93%) and specificity (100%), patients with HFpEF from normal, composed variable [AUC = 0.98 (0.95–1), $P < 0.001$]. In a logistic regression model, a composite predictive variable taking into account both GLS Epi and NT-proBNP values in each individual subject reached a sensitivity of 89% and a specificity of 100% with an AUC of 0.98 (0.95–1), $P < 0.001$, to detect HFpEF.

Conclusions Epi-GLS is a promising new imaging parameter to be considered in the clinical assessment of HFpEF patients. Given its excellent specificity, in tandem with a highly sensitive parameter such as NT-proBNP, Epi-GLS holds the potential to greatly improve the current diagnostic algorithms.

Keywords Multilayer myocardial strain; Heart failure with preserved ejection fraction; NT-proBNP; Cardiac magnetic resonance; Feature tracking

Received: 29 January 2020; Revised: 8 May 2020; Accepted: 21 May 2020
**Correspondence to: Radu Tanacli, MD, Department of Internal Medicine/Cardiology, German Heart Center Berlin, Augustenburger Platz 1, 13353 Berlin, Germany. Tel: + 49 30 4593-2459. Email: tanacli@dhzb.de*
German Clinical Trials Register (ID: DRKS00015615)

Background

Approximately half of the patients diagnosed with heart failure (HF) maintain a normal ejection fraction (HFpEF) despite increased left ventricular (LV) filling pressure and lusitropic stiffness.[1] In contrast with HF with reduced EF (HFrEF), in HFpEF, elevated inflammation levels determining microvascular disease, reconfiguration of structural proteins such as titin and interstitial collagen deposition, are the main pathophysiological effectors.[2] Such heterogeneity in pathophysiology is putatively responsible for the difficulty of finding a unifying and accessible imaging marker of disease severity. EF is *ipso facto* within the normal range, and global longitudinal strain (GLS), a powerful and robust prognostic factor in HFrEF,[3] is only inconstantly decreased in HFpEF patients.[4] Echocardiography-derived indexes of severity of diastolic dysfunction such as E/e` correlate only moderately with invasively measured LV filling pressure,[5] and, even so, up to one-third of patients diagnosed with HFpEF have a normal diastolic function.[4]

Aims

We hypothesized that benefiting from a superior spatial resolution and complete 3D coverage of the myocardial volume provided by the cine sequences, cardiac magnetic resonance (CMR) feature tracking (FT) can assess longitudinal and circumferential myocardial strain at multiple layer level and potentially augment the accuracy to detect deformation abnormalities in patients with HFpEF.

Methods

To establish this, we included 20 patients with a diagnosis of HFpEF and, respectively, 20 age-matched and gender-matched controls. Diagnosis of HF should have been older than 30 days, the patients were required to be in a stable state with no changes in their HF medication and no HF hospitalization within the previous 7 days, HFpEF was defined in agreement with recent ESC guidelines,[6] as presence of signs and symptoms of HF and LVEF ≥50% at the time of study inclusion plus the existence of one of the following echocardiographic criteria: left atrial volume index > 34 mL/m^2, E/e′ > 13 (medial or lateral mitral anulus), LV hypertrophy: septal wall thickness or posterior wall thickness ≥ 13 mm. Exclusion criteria were as follows: atrial fibrillation, symptomatic significant coronary artery disease, co-existence of any inherited cardiomyopathy or amyloidosis, myocarditis, pulmonary disease, and anaemia. Demographic and baseline characteristics of the study population are presented in *Table 1*. All subjects underwent clinical, comprehensive CMR and echocardiographic examinations and a 6 min walking test. All CMR images were acquired using a 1.5 T (Achieva, Philips Healthcare, Best, The Netherlands) MRI scanner with a five-channel cardiac surface coil in a supine position. Cine images were acquired using electrocardiogram-gated bSSFP sequence with multiple breath holds at end-expiration in three LV long-axis [two-chamber (2Ch), three-chamber (3Ch), and four-chamber (4Ch)] planes. The ventricular two-chamber and four-chamber planes were used to plan a stack of short-axis slices covering the entire LV. The following imaging parameters were used: repetition time (TR) = 3.3 ms, echo time (TE) = 1.6 ms, flip angle = 60°, voxel size = 1.8 × 1.7 × 8.0 mm^3 and 50 phases per cardiac cycle in accordance with standards of procedure established in our unit and described previously.[7] Using commercially available software (Medis Suite, version 3.1 and QStrain RE version 2.0, Leiden, The Netherlands) we derived the values of myocardial strain at three distinct layers of the myocardium: subendocardial (Endo-), mid-myocardial (Myo-), and subepicardial (Epi-) for GLS and circumferential (GCS) strain as previously reported (*Figure 1A*).[8] To compare the diagnostic accuracy, we additionally assessed various others clinical, imaging, and biochemical parameters with a putative role in HFpEF diagnostic: LV end-diastolic volume (LVEDV), LV mass (LVM), interventricular septum (IVS) wall thickness and free wall thickness, LA volume and strain, septal and lateral mitral anular early diastolic velocity (e`), E/e′ ratio, and plasma levels of N-terminal pro-B-type natriuretic peptide (NT-proBNP).[9] All the statistical analyses were performed with IBM SPSS v26 with the exception of comparative receiver operating characteristic analysis, which was performed with Medcalc v19.1.5, using the DeLong formula.

Results

Global longitudinal strain is significantly impaired at Endo- (−20.8 ± 4.0 vs. −23.2 ± 3.4, $P = 0.046$), Myo- (−18.0 ± 3.0 vs. −21.0 ± 2.5, $P = 0.002$), and Epi- (−12.2 ± 2.0 vs. −16.2 ± 2.5, $P < 0.001$) levels (*Figure 1B*). In contrast, in keeping with previously published meta-analysis,[5] GCS was similar at any level of myocardium in HFpEF patients (*Table S1*.). In a comparative receiver operating characteristic analysis, GLS Epi has the best ability to detect between HFpEF with an area under the curve (AUC) of 0.90 (0.81–1), $P < 0.001$, compared with 0.80 (0.66–0.94), $P = 0.002$, for GLS Myo and 0.69 (0.53–0.86), $P = 0.046$, for GLS Endo (*Figure 1C*). Additionally, this performance is higher than of any other parameter included in our analysis, excepting only NT-proBNP that is borderline better with an AUC of 0.91(0.79–1), $P < 0.001$ (*Figure 1C*).[9] In particular, a threshold value of Epi-GLS $< -13.0\%$ demonstrated an excellent diagnostic specificity (100%) for HFpEF. According to our data, a complementary threshold value for NT-proBNP > 203 ng/mL was able to detect all but two HFpEF patients, showing very good

ESC Heart Failure 2020: **7**; 3240–3245
DOI: 10.1002/ehf2.12826

Table 1 Demographics, Baseline Characteristics

	Control (N = 20)	HFpEF (N = 20)	*P* value
Demographics			
Male	12/20 (60%)	12/20 (60%)	0.75
Age, y	68.2 ± 8.1	73.3 ± 8.2	0.62
LVEF, %	62.5 ± 5.1	61.7 ± 7.2	0.84
LVM index (g/m^2)	43.5 ± 13.7	47.2 ± 8.5	0.21
LVEDV index (mL/m^2)	78 ± 12	70 ± 14	0.77
IVS thickness (mm)	9.2 ± 1.7	11.4 ± 2.0	0.03§
LA area index (cm^2/m^2)	20.4 ± 4.1	23.7 ± 5.1	0.046
LA volume index (mL/m^2)	37.3 ± 7.8	44.1 ± 13.9	0.068
LA strain (%)	31.3 ± 6.3	21.7 ± 8.2	<0.001§
Any LGE	0 (0%)	9 (45%)	<0.001§
Transmural LGE	4 (20%)		
Coronary artery disease	0 (0%)	11 (55%)	<0.001§
Peripheric artery disease	0 (0%)	6 (30%)	0.008§
Hypertension	7 (35%)	14 (70%)	0.027§
Diabetes	2 (10%)	5 (25%)	0.21
Hypercholesterolaemia	5 (25%)	13 (65%)	0.011§
COPD	0 (0%)	1 (5%)	0.31
Smokers	6 (30%)	8 (40%)	0.51
6 min walking test (m)	523 ± 119	352 ± 124	<0.001§
NYHA Class II	0 (0%)	11 (55%)	<0.001§
Class III	0 (0%)	9 (45%)	<0.001§
Quality of Life Score	5.2 ± 5.5	26.3 ± 21.8	<0.001§
Borg Score	7.4 ± 1.7	12.2 ± 2.4	<0.001§
Laboratory values			
Haemoglobin (g/dL)	13.9 ± 1.1	12.8 ± 1.2	0.86
Haematocrit	0.40 ± 0.03	0.38 ± 0.03	0.94
Creatinine (mg/dL)	0.87 ± 0.20	0.92 ± 0.18	0.88
GFR (mL/min)	81 ± 10	71 ± 16	0.34
NT-proBNP (ng/L)	89 ± 61	502 ± 497	<0.001§
Troponin T (ng/L)	7 ± 3	16 ± 12	<0.001§
CRP (mg/dL)	1.3 ± 1.4	2.9 ± 2.7	0.08
WBC (/nL)	6.1 ± 1.6	7.2 ± 2.4	0.19
Medication			
ACE inhibitors	3 (12%)	4 (20%)	0.68
Angiotensin receptor blocker	5 (25%)	11 (55%)	0.05
Calcium antagonist	4 (20%)	3 (12%)	0.68
Mineralocorticoid receptor antagonist	0 (0%)	2 (10%)	0.15
Angiotensin receptor-neprilysin inhibitor	0 (0%)	0 (0%)	n/a
Beta-blocker	6 (30%)	10 (50%)	0.20
Statin	4 (20%)	8 (40%)	0.17
Thiazide diuretic	5 (25%)	4 (20%)	0.71
Loop diuretic	0 (0%)	3 (15%)	0.07

Abbreviations: ACE, angiotensin-converting-enzyme; COPD, chronic obstructive pulmonary disease; CRP, C-reactive protein; GFR, glomerular filtration rate; IVS, interventricular septum; LA, left atrium; LGE, late gadolinium enhancement; LVEDV, left ventricular end-diastolic volume; LVEF, left ventricular ejection fraction; LVM, left ventricular mass; NT-proBNP, N-terminal pro-B-type natriuretic peptide; NYHA, New York Heart Association; WBC, white blood cell count; Quality of Life Score, Minnesota Living with Heart Failure Questionnaire. Discrete values given as absolute number and percentage of respective HF group. Continuous values given as mean and standard deviation.

sensitivity (*Figure 1D*). All numerical data are included in Supporting Information *Table S1*. In a logistic regression model, a composite predictive variable taking into account both GLS Epi and NT-proBNP values in each individual subject reached a sensitivity of 89% and a specificity of 100% with an AUC of 0.98 (0.95–1), $P < 0.001$, to detect HFpEF (*Figures 1C and S1*.)

Discussion

In line with previous studies, our findings confirmed a decrease of longitudinal strain in patients with HFpEF.[10] Additionally, we showed that, measured selectively at the level of the subepicardial layer, GLS has an increased potential to diagnose HFpEF and discriminate early phases of contractile impairment.

These results may be surprising. It has been previously proposed that a more pronounced vulnerability to ischaemia of subendocardial small-calibre vasculature irrigating predominantly longitudinally distributed fibres found at this level is responsible for a significant decrease in long-axis contraction. However, so far, there are no clear clinical evidences to substantiate this assumption and such a model is theoretically flawed.[11] In contrast, several possible explanations for the increased sensitivity of FT Epi-GLS could be proposed:

FIGURE 1 (A) CMR feature tracking multilayer segmentation principle exemplified in a long-axis four-chamber end-diastolic view in a patient with HFpEF. (B) Sub-endocardial (Endo-), mid-myocardial (Myo-), and sub-epicardial (Epi-) global longitudinal strain (GLS) in control and HFpEF patients. (C) Forest Plot of area under curve values: comparison between Endo-, Myo-, and Epi-GLS to detect patients with HFpEF and other parameters with a significant ability to discriminate between HFpEF and control. (D) Scatter Plot with Epi-GLS and NT-proBNP values in the two groups, dotted lines represent the cut-off values (GLS Epi = −13%, NT-proBNP = 220 ng/L) $^{*}P < 0.05$, $^{***}P < 0.001$, for all the comparisons a P value <0.05 was considered statistically significant. Abbreviations: CMR, cardiac magnetic resonance; Endo, Myo, and Epi, multilayer myocardial strain; FT, feature tracking; HFpEF, heart failure with preserved ejection fraction; LA, left atrium; LVM, left ventricular mass; LVEDV, left ventricular end-diastolic volume; e′ septal, lateral, peak early diastolic velocity at the septal and lateral mitral annular sites; E/e′, ratio between early trans-mitral flow velocity and average peak early diastolic velocity; NT-proBNP, N-terminal prohormone of brain natriuretic peptide.

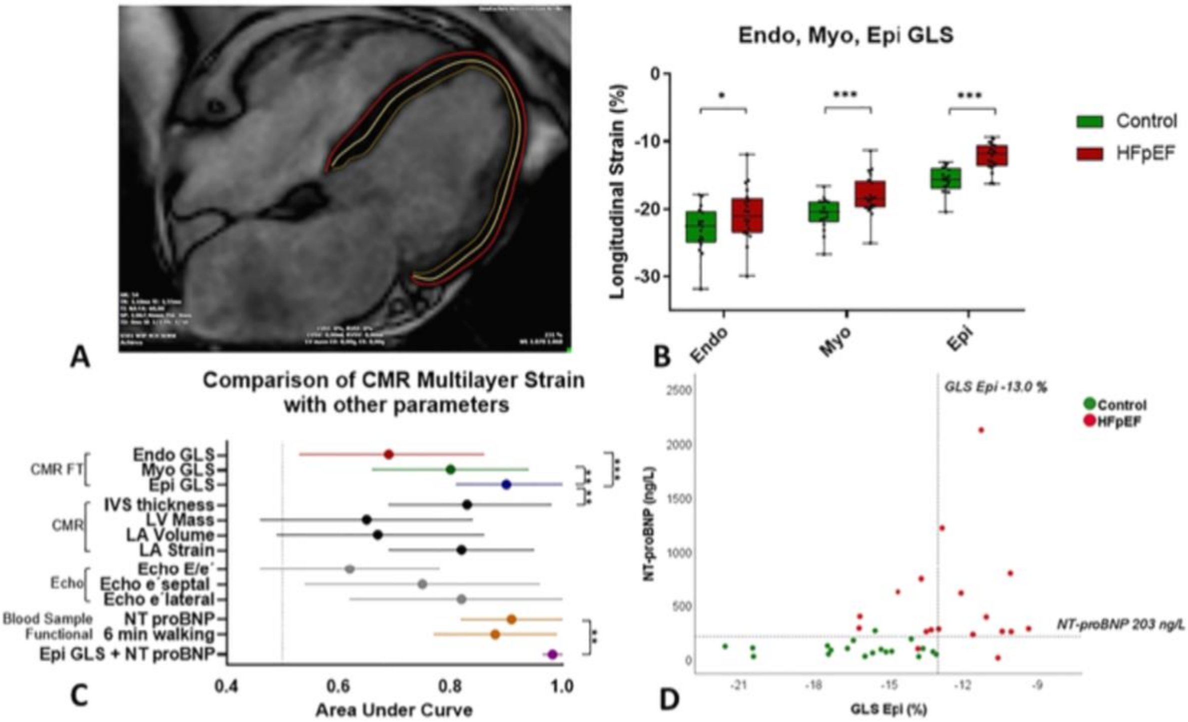

1 Pericardium is a rigid membrane that contains the movements of the heart towards exterior, and thus, the confounding effect of shear strain is absent at this level.[12]

2 Also due to pericardial containment, subepicardial deformation is in a tighter connection with a long axis descend of the mitral valve plane showed also to be an additional index of severity in HFpEF.[13]

3 Left ventricular hypertrophy, observed in up to one-half of patients with HFpEF,[14] leads to a decrease EDV and thus a false positive increase in strain assessment.

4 Feature tracking relies on adequate contour identification and tracking over the cardiac cycle phases, subepicardial longitudinal benefits from a high contrast difference between T1 values of myocardium, pericardium, and surrounding extracardiac space.[15]

In contrast with GLS, and confirming previous studies, GCS is not different at any level of the myocardium between HFpEF and controls.[8] NT-proBNP has been recently proposed by the most recent guidelines as a major diagnostic criteria for HFpEF.[9]

Our findings confirmed that NT-proBNP is generically a good discriminator of HFpEF from control subjects. However, NT-proBNP exponentially increase in the restrictive phase of diastolic dysfunction; thus, it might be particularly inefficient in identifying HFpEF patients without or with an earlier stage of diastolic dysfunction.[9] Additionally, NT-proBNP is not efficient to separate HFpEF from HFrEF.[16] In contrast, we showed previously an excellent specificity for Endo-GCS, which is normal in HFpEF patients but significantly decreased in HFrEF, to separate HFpEF from HFrEF[8] with various degrees of severity. With this current study, we brought new evidence that Epi-GLS is specifically decreased in HFpEF patients compared with control and thus, in tandem with Endo-GCS, constitutes an excellent diagnostic tool to optimally identify patients with HFpEF from both healthy individuals and patients with HFrEF.

DOI: 10.1002/ehf2.12826

Heart failure with preserved ejection fraction is particularly difficult to treat; important therapeutic tools such as β blockers, angiotensin-converting enzyme inhibitors or angiotensin-receptor antagonists, and mineralocorticoid-receptor antagonist, efficient in improving morbidity and mortality in HFrEF patients, all failed to show any benefits in HFpEF.[17] In these conditions, prompt diagnostic and progression monitoring are key factors to direct a salvaging adjuvant therapy such as decreasing an excessive preload or symptoms control. Our study suggests that recent advances in image processing such as multilayer CMR FT potentially increase the diagnostic accuracy in patients suspected of having HFpEF.

Conflicts of Interest

Sebastian Kelle is supported by a grant from Philips Healthcare and received lecture honoraria from Medis. Sebastian Kelle and Burkert Pieske received funding from the DZHK (German Centre for Cardiovascular Research) and by the BMBF (German Ministry of Education and Research). Burkert Pieske reports having received consultancy and lecture honoraria from Bayer Daiichi Sankyo, MSD, Novartis, sanofi-aventis, Stealth Peptides, and Vifor Pharma and editor honoraria from the Journal of the American College of Cardiology. Radu Tanacli and the other co-authors report no conflict of interest.

Supporting information

Additional supporting information may be found online in the Supporting Information section at the end of the article.

Table S1. ROC Analysis: Multilayer Myocardial Strain and other parameters to detect patients with HFpEF. GLS – global longitudinal strain, GCS – global circumferential strain, LVM left ventricular mass, LVEDV – left ventricular end-diastolic volume, LA – left atrium, e´ septal, lateral – peak early diastolic velocity at the septal and lateral mitral annular sites, E/e´ – ration between early trans-mitral flow velocity and average peak early diastolic velocity, NT-proBNP - N-terminal prohormone of brain natriuretic peptide. § $P < 0.05$ (for all the comparisons a P value < 0.05 was considered statistically significant)

Figure S1. ROC Analysis to detect patients with heart failure with preserved ejection fraction (HFpEF) from control: GLS Epi – subepicardial global longitudinal strain, NT-proBNP - N-terminal prohormone of brain natriuretic peptide, Combined – logistic regression composite predictor to detect HFpEF. AUCs were respectively: 0.90 (0.81–1), $P < 0.001$ for GLS Epi, 0.91(0.79–1), $P < 0.001$ for NT-proBNP, 0.98 (0.95–1), $P < 0.001$ for Combined. For all the comparisons a P value < 0.05 was considered statistically significant.

References

1. Redfield MM. Heart failure with preserved ejection fraction. *N Engl J Med* 2017; **376**: 897.
2. Paulus WJ, Tschope C. A novel paradigm for heart failure with preserved ejection fraction: comorbidities drive myocardial dysfunction and remodeling through coronary microvascular endothelial inflammation. *J Am Coll Cardiol* 2013; **62**: 263–271.
3. Sengelov M, Jorgensen PG, Jensen JS, Bruun NE, Olsen FJ, Fritz-Hansen T, Nochioka K, Biering-Sorensen T. Global longitudinal strain is a superior predictor of all-cause mortality in heart failure with reduced ejection fraction. *JACC Cardiovasc Imaging* 2015; **8**: 1351–1359.
4. Shah AM, Claggett B, Sweitzer NK, Shah SJ, Anand IS, Liu L, Pitt B, Pfeffer MA, Solomon SD. Prognostic importance of impaired systolic function in heart failure with preserved ejection fraction and the impact of spironolactone. *Circulation* 2015; **132**: 402–414.
5. Sharifov OF, Schiros CG, Aban I, Denney TS, Gupta H. Diagnostic accuracy of tissue Doppler index E/e' for evaluating left ventricular filling pressure and diastolic dysfunction/heart failure with preserved ejection fraction: a systematic review and meta-analysis. *J Am Heart Assoc* 2016; **5**.
6. Ponikowski P, Voors AA, Anker SD, Bueno H, Cleland JGF, Coats AJS, Falk V, Gonzalez-Juanatey JR, Harjola VP, Jankowska EA, Jessup M, Linde C, Nihoyannopoulos P, Parissis JT, Pieske B, Riley JP, Rosano GMC, Ruilope LM, Ruschitzka F, Rutten FH, van der Meer P, Group ESCSD. 2016 ESC Guidelines for the diagnosis and treatment of acute and chronic heart failure: The Task Force for the diagnosis and treatment of acute and chronic heart failure of the European Society of Cardiology (ESC). Developed with the special contribution of the Heart Failure Association (HFA) of the ESC. *Eur Heart J* 2016; **37**: 2129–2200.
7. Lapinskas T, Schnackenburg B, Kouwenhoven M, Gebker R, Berger A, Zaliunas R, Pieske B, Kelle S. Fatty metaplasia quantification and impact on regional myocardial function as assessed by advanced cardiac MR imaging. *MAGMA* 2018; **31**: 75–85.
8. Tanacli R, Hashemi D, Lapinskas T, Edelmann F, Gebker R, Pedrizzetti G, Schuster A, Nagel E, Pieske B, Dungen HD, Kelle S. Range variability in CMR feature tracking multilayer strain across different stages of heart failure. *Sci Rep* 2019; **9**: 16478.
9. Pieske B, Tschope C, de Boer RA, Fraser AG, Anker SD, Donal E, Edelmann F, Fu M, Guazzi M, Lam CSP, Lancellotti P, Melenovsky V, Morris DA, Nagel E, Pieske-Kraigher E, Ponikowski P, Solomon SD, Vasan RS, Rutten FH, Voors AA, Ruschitzka F, Paulus WJ, Seferovic P, Filippatos G. How to diagnose heart failure with preserved ejection fraction: the HFA-PEFF diagnostic algorithm: a consensus recommendation from the Heart Failure Association (HFA) of the European Society of Cardiology (ESC). *Eur Heart J* 2019; **40**: 3297–3317.
10. Morris DA, Ma XX, Belyavskiy E, Aravind Kumar R, Kropf M, Kraft R, Frydas A, Osmanoglou E, Marquez E, Donal E,

Edelmann F, Tschope C, Pieske B, Pieske-Kraigher E. Left ventricular longitudinal systolic function analysed by 2D speckle-tracking echocardiography in heart failure with preserved ejection fraction: a meta-analysis. *Open Heart* 2017; **4**: e000630.

11. Rademakers F, Nagel E. Is global longitudinal strain a superior parameter for predicting outcome after myocardial infarction? *JACC Cardiovasc Imaging* 2018; **11**: 1458–1460.
12. Lee JM, Boughner DR. Mechanical properties of human pericardium. Differences in viscoelastic response when compared with canine pericardium. *Circ Res* 1985; **57**: 475–481.
13. Wenzelburger FW, Tan YT, Choudhary FJ, Lee ES, Leyva F, Sanderson JE. Mitral annular plane systolic excursion on exercise: a simple diagnostic tool for heart failure with preserved ejection fraction. *Eur J Heart Fail* 2011; **13**: 953–960.
14. Shah AM, Shah SJ, Anand IS, Sweitzer NK, O'Meara E, Heitner JF, Sopko G, Li G, Assmann SF, McKinlay SM, Pitt B, Pfeffer MA, Solomon SD, Investigators T. Cardiac structure and function in heart failure with preserved ejection fraction: baseline findings from the echocardiographic study of the Treatment of Preserved Cardiac Function Heart Failure with an Aldosterone Antagonist trial. *Circ Heart Fail* 2014; **7**: 104–115.
15. Schuster A, Hor KN, Kowallick JT, Beerbaum P, Kutty S. Cardiovascular magnetic resonance myocardial feature tracking: concepts and clinical applications. *Circ Cardiovasc Imaging* 2016; **9**: e004077.
16. Salah K, Stienen S, Pinto YM, Eurlings LW, Metra M, Bayes-Genis A, Verdiani V, Tijssen JGP, Kok WE. Prognosis and NT-proBNP in heart failure patients with preserved versus reduced ejection fraction. *Heart* 2019; **105**: 1182–1189.
17. Fernandez-Ruiz I. The search for an effective HFpEF treatment continues. *Nat Rev Cardiol* 2019; **16**: 647.

Journal of
Clinical Medicine

MDPI

Article

CMR Tissue Characterization in Patients with HFmrEF

Patrick Doeblin [1,2,*], Djawid Hashemi [2,3], Radu Tanacli [1], Tomas Lapinskas [1,4], Rolf Gebker [1], Christian Stehning [1,5], Laura Astrid Motzkus [3], Moritz Blum [3], Elvis Tahirovic [3], Aleksandar Dordevic [3], Robin Kraft [3], Seyedeh Mahsa Zamani [1], Burkert Pieske [1,2,3], Frank Edelmann [2,3], Hans-Dirk Düngen [2,3] and Sebastian Kelle [1,2,3,*]

1. Department of Internal Medicine/Cardiology, German Heart Center Berlin, 13353 Berlin, Germany; tanacli@dhzb.de (R.T.); Tomas.Lapinskas@lsmuni.lt (T.L.); gebker@dhzb.de (R.G.); christian.stehning@philips.com (C.S.); zamani@dhzb.de (S.M.Z.); pieske@dhzb.de (B.P.)
2. DZHK (German Center for Cardiovascular Research), Partner Site Berlin, 10115 Berlin, Germany; djawid.hashemi@charite.de (D.H.); frank.edelmann@charite.de (F.E.); hans-dirk.duengen@charite.de (H.-D.D.)
3. Department of Internal Medicine/Cardiology, Charité Campus Virchow Klinikum, 13353 Berlin, Germany; laura-astrid.motzkus@charite.de (L.A.M.); moritz.blum@charite.de (M.B.); elvis.tahirovic@charite.de (E.T.); aleksandar.dordevic@charite.de (A.D.); robin.kraft@charite.de (R.K.)
4. Department of Cardiology, Medical Academy, Lithuanian University of Health Sciences, 50161 Kaunas, Lithuania
5. Philips Healthcare, 22335 Hamburg, Germany

* Correspondence: doeblin@dhzb.de (P.D.); kelle@dhzb.de (S.K.)

Received: 11 September 2019; Accepted: 30 October 2019; Published: 5 November 2019

check for updates

Abstract: The characteristics and optimal management of heart failure with a moderately reduced ejection fraction (HFmrEF, LV-EF 40–50%) are still unclear. Advanced cardiac MRI offers information about function, fibrosis and inflammation of the myocardium, and might help to characterize HFmrEF in terms of adverse cardiac remodeling. We, therefore, examined 17 patients with HFpEF, 18 with HFmrEF, 17 with HFrEF and 17 healthy, age-matched controls with cardiac MRI (Phillips 1.5 T). T1 and T2 relaxation time mapping was performed and the extracellular volume (ECV) was calculated. Global circumferential (GCS) and longitudinal strain (GLS) were derived from cine images. GLS (-15.7 ± 2.1) and GCS (-19.9 ± 4.1) were moderately reduced in HFmrEF, resembling systolic dysfunction. Native T1 relaxation times were elevated in HFmrEF (1027 ± 40 ms) and HFrEF (1033 ± 54 ms) compared to healthy controls (972 ± 31 ms) and HFpEF (985 ± 32 ms). T2 relaxation times were elevated in HFmrEF (55.4 ± 3.4 ms) and HFrEF (56.0 ± 6.0 ms) compared to healthy controls (50.6 ± 2.1 ms). Differences in ECV did not reach statistical significance. HFmrEF differs from healthy controls and shares similarities with HFrEF in cardiac MRI parameters of fibrosis and inflammation.

Keywords: HFmrEF; T2 mapping; T1 mapping; ECV, fibrosis; inflammation; strain

1. Introduction

Heart failure is a clinical entity with a diverse spectrum of etiologies and phenotypes. Classification systems and diagnostic criteria have been established paralleling better understanding of its pathophysiology. Early on, the significance of the left ventricular ejection fraction (LV-EF) in the classification of heart failure was acknowledged. The European Society of Cardiology recently suggested to define heart failure with moderately reduced ejection fraction (HFmrEF, LV-EF 40–50%) as a distinct category between heart failure with preserved (HFpEF, LV-EF > 50%) and reduced (HFrEF, LV-EF < 40%) ejection fractions [1]. Patients with HFrEF exhibit functional, structural, cellular and interstitial changes that are summarized as left ventricular remodeling and treatments targeted against remodeling are a mainstay of HFrEF therapy [2]. Unfortunately, these treatments have shown markedly less benefits in patients with HFpEF [3]. Patients with HFmrEF have only recently been proposed as a distinct category, and while debate is still ongoing about whether it truly represents a distinct category or merely a transition zone between HFpEF and HFrEF, available data suggests a possible benefit from treatment against remodeling [4].

Cardiac magnetic resonance (CMR) imaging is a noninvasive method to assess cardiac function, structure, inflammation, and fibrosis. The development of T1 and T2 relaxation time mapping techniques has greatly improved the ability to detect changes in tissue composition, most notably fibrosis and edema [5]. The combination of pre-contrast (native) and post-contrast T1 relaxation time mapping allows an estimation of the extracellular volume (ECV) [6]. While elevations in ECV and native T1 relaxation time seem more related to fibrosis and are strong predictors of adverse outcome, the T2 relaxation time seems more sensitive for the diagnosis of edema and inflammation [7–9]. In addition, strain-analysis is a promising new method of functional analysis whose clinical significance is currently still under investigation and which might provide additional prognostic and diagnostic information in heart failure patients [10].

The purpose of our study was to further characterize HFmrEF patients in terms of advanced CMR imaging markers of adverse cardiac remodeling, with a focus on T2 mapping as a potential biomarker in heart failure.

2. Experimental Section

From a contemporary trial, a total of 52 well characterized patients with HFpEF, HFmrEF and HFrEF, along with 17 controls, were included in this analysis (EMPATHY-HF, German Clinical Trials Register ID: DRKS00015615) [11]. HFrEF, HFmrEF and HFpEF were defined according to the 2016 ESC guidelines [1]. The study complies with the declaration of Helsinki and was approved by the ethics committee of the Charité-Universitätsmedizin Berlin. All analyses and procedures are covered by the informed consent obtained prior to inclusion. All patients were >45 years, had signs and symptoms of heart failure NYHA II or III (at least 30 d prior to screening), had been stable for at least 7 d (defined as no i.v. diuretics or inotropics, no hospitalization and no medication change). The complete inclusion and exclusion criteria are accessible through the German Clinical Trials Register [11]. All patients received a screening-echocardiography, a cardiac MRI and a comprehensive laboratory evaluation as part of the main study protocol. Quality of life was assessed using the Minnesota Living with Heart Failure Questionnaire. For our analysis, the patients were reclassified based on the results of the cardiac MRI derived LV-EF, leading to 17 patients with HFpEF, 18 with HFmrEF and 17 with HFrEF. When comparing MRI-derived LV-EF to echocardiography-derived LV-EF, roughly one third of HFpEF patients were reclassified as HFmrEF and half of the HFmrEF patients were reclassified as HFrEF.

All patients were examined with a clinical 1.5 Tesla MRI scanner (Achieva, Philips Healthcare, Best, The Netherlands) equipped with a cardiac, five-element phased array coil. Cine images were acquired using a retrospectively gated cine-CMR in cardiac short-axis, vertical long-axis and horizontal long-axis orientations using a steady-state free precession (SSFP) sequence. Native and 15 min post contrast T1-mapping were performed using a modified Look-Locker (MOLLI) 5s(3s)3s-scheme [12]. Typical imaging parameters were as follows: Acquired voxel size = $2.0 \times 2.0 \times 10$ mm^3, reconstructed voxel size = $0.5 \times 0.5 \times 10$ mm^3, balanced SSFP readout, flip angle = 35°, parallel imaging (SENSE) factor = 2 and effective inversion times between 150 and 3382 ms. T2-mapping was performed before administration of contrast media using a black-blood-prepared, navigator-gated, free-breathing hybrid gradient (echo planar imaging, EPI) and a spin-echo multi-echo sequence (GraSE), as described previously, with the following typical imaging parameters: TR = 1 heartbeat, 9 echoes (TE_1 = 15 ms, delta TE = 7.7 ms), FA 90°, parallel imaging (SENSE = 2), EPI factor = 7, black-blood prepulse and breath-hold (scan duration about 14 s). [13] Patients received 0.15 mmol/kg of gadolinium-based contrast agent (Gadobutrol 1.0 mmol/mL, Gadovist®, Bayer AG, Leverkusen, Germany). Quantitative modified

DIXON-imaging (mDIXON) for late enhancement was performed using a black-blood prepared, T1-weighted, spoiled-gradient, multi-echo sequence with 6 echoes starting 10 min post contrast agent application. Typical imaging parameters were as follows: Acquired voxel size = $2.0 \times 2.0 \times 8$ mm^3, reconstructed voxel size = $1.1 \times 1.1 \times 8$ mm^3, flip angle = 15° and effective echo time 4.75 ms.

Image analysis was performed offline using commercially available software (Medis Suite version 3.1, Medis Medical Imaging Systems bv Leiden, The Netherlands, and Extended MR WorkSpace version 2.6.3.5, Philips Medical Systems Nederland B.V., Best, The Netherlands). Late gadolinium enhancement (LGE) was assessed visually from mDIXON images. Segments with LGE were excluded from analysis, resulting in a total of 659 analyzed segments using a 16-segment-model. Mapping parameters were measured using QMap RE version 2.0 (Medis Medical Imaging Systems bv, Leiden, the Netherlands). Pre and post-contrast MOLLI images were manually corrected for in-plane-motion. The T1 and T2 relaxation times were calculated using nonlinear fitting with a maximum likelihood estimator (MLE). Extracellular volume (ECV) was calculated from pre and post-contrast T1-maps and the hematocrit, as described previously [6]. Due to possible harm, healthy controls received no contrast agent and were, therefore, not included in the ECV analysis. For comparison, data from a previous study using the same scanner model and contrast agent were used [14]. Exemplary images of patients with HFpEF, HFmrEF and HFpEF, and controls, are given in Figure 1A–L. For T1 native, T2 and ECV, the median value of all segments without late enhancement was calculated for each patient and used for all further analyses. In case of extensive artifacts in an imaging sequence, the patient was excluded from the respective analysis at the discretion of the analyzing physician. Peak left ventricular endocardial global longitudinal (GLS) and circumferential (GCS) strain were analyzed in accordance with a recent consensus document for the quantification of LV function using CMR [15]. Strain analysis included 2-chamber, 3-chamber and 4-chamber cine images and three preselected slices from the LV short-axis stack to correspond to basal, mid-ventricular and apical levels. The endocardial contours were drawn on the long and short-axis cine images with QMass version 8.1 (Medis Medical Imaging Systems bv, Leiden, the Netherlands) and were subsequently transferred to QStrain RE version 2.0 (Medis Medical Imaging Systems bv, Leiden, the Netherlands), where endocardial and epicardial borders were detected throughout the whole cardiac cycle using a tissue tracking algorithm. From these, global longitudinal and circumferential endocardial strain curves were calculated and the maximal amplitude was considered as the respective peak global strain. The strain ratio (SR = GLS/GCS) was calculated to assess for possible differences between heart failure groups.

Statistical analysis was performed using SPSS 24 (IBM, Armonk, NY, USA) and R 3.5.1 (The R Foundation for Statistical Computing, Vienna, Austria) [7]. Baseline data were reported as means ± standard deviations (SD) for interval and ratio-scaled parameters and as numbers and percentages for nominal and ordinal-scaled parameters. For comparisons between groups, ANOVA with Tukey–Kramer post-hoc analysis was performed. Pearson correlation coefficients were calculated for correlations between continuous variables and were tested for significance under the null hypothesis of $r = 0$. For quality of life, Spearman correlation was used. p-values below 0.05 were considered statistically significant.

Sample size calculations were performed for the detection of significant differences in native T1 relaxation time, T2 relaxation time and ECV between groups with a power of 80%. For native T1 relaxation time, previous studies have shown standard deviations between 20 and 50 ms and effect sizes of 30 to 40 ms [14,16]. For T2 relaxation time, standard deviations ranged from 3 to 7 ms and effect sizes from 3 to 5 ms [17,18]. For ECV, previous studies have shown standard deviations of 3–4% with effect sizes of about 4% [19,20]. Assuming a ratio of effect size to standard deviation of 1 for all three parameters, the minimum sample size is 16 per group.

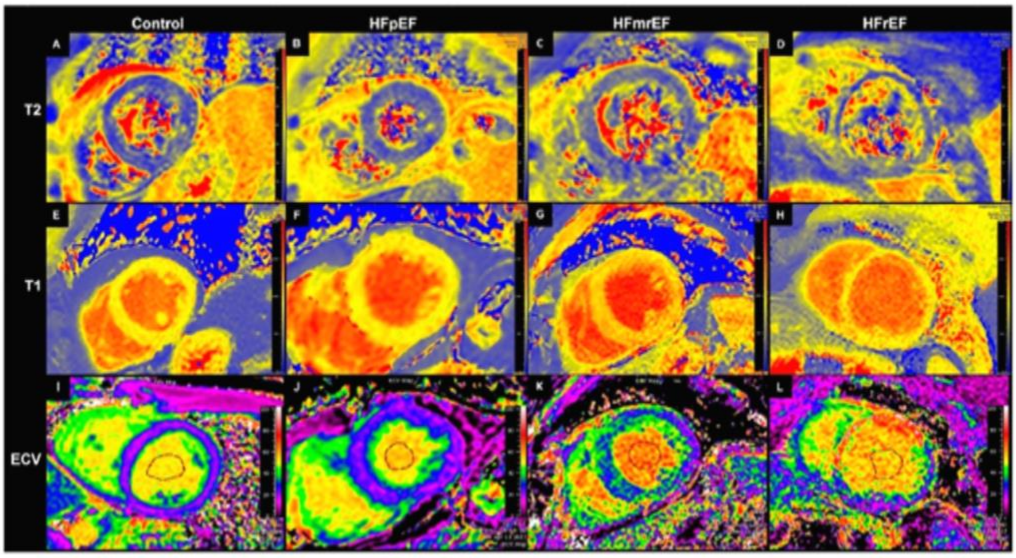

Figure 1. Exemplary medial short axis images of T2 relaxation time maps (first row, (**A**–**D**)), T1 relaxation time maps (second row, **E**–**H**) and extracellular volume (ECV) maps (third row, (**I**–**L**)). First column (**A**,**E**,**I**): Healthy control (ECV image from a patient from clinical routine, as no contrast agent was given to healthy controls in our study). Second column (**B**,**F**,**J**): Patient number 3 (HFpEF). Third column (**C**,**G**,**K**): Patient number 9 (HFmrEF). Fourth column (**D**,**H**,**L**): Patient number 11 (HFrEF). Segments with scars excluded from analysis. ECV = Extracellular volume. HFmrEF = Heart failure with moderately reduced Ejection fraction, HFpEF = Heart failure with preserved ejection fraction, HFrEF = Heart failure with reduced ejection fraction.

3. Results

3.1. Patients

17 patients with HFpEF, 18 with HFmrEF, 17 with HFrEF and 17 controls were included in the analysis. The baseline data of the patients and controls are given in Table 1. Overall, controls were healthier, younger and more likely to be female than HF patients. Between HF groups, there were relevant differences in sex, age, coronary artery disease, history of smoking, lab values (most notably hematocrit and N-terminal pro brain natriuritic peptide—NT-proBNP) and medication use. NT-proBNP was log-normally distributed and transformed to logarithmic for correlation analysis. A correlation matrix of all continuous baseline and imaging parameters is given in Figure S1.

Table 1. Baseline characteristics.

Clinical Data		Control	HFpEF	HFmrEF	HFrEF
Female		8/17 (47%)	9/17 (53%)	6/18 (33%)	3/17 (18%)
Age	Mean ± SD	61.7 ± 8.5	78.1 ± 8.2	67.8 ± 9.0	64.4 ± 10.3
LVEF	Mean ± SD	63.8 ± 5.4	61.7 ± 6.1	44.7 ± 2.9	33.1 ± 4.8
LA (cm^2)	Mean ± SD	19.5 ± 6.5	23.4 ± 4.9	22.8 ± 8.3	25.2 ± 6.6
RVEDD (mm)	Mean ± SD	31.5 ± 4.7	30.6 ± 3.8	29.6 ± 3.7	31.4 ± 5.4
Any LGE			7/17 (41%)	16/18 (89%)	15/17 (88%)
Transmural LGE			4/17 (24%)	7/18 (39%)	8/17 (47%)
Coronary Artery Disease		0/17 (0%)	11/17 (65%)	16/18 (89%)	11/17 (65%)
6 min Walking Test (m)	Mean ± SD	524 ± 126	345 ± 122	414 ± 88	414 ± 125
NYHA Class	2		9/17 (53%)	15/18 (83%)	12/17 (71%)
	3		8/17 (47%)	3/18 (17%)	5/16 (29%)
Quality of Life [1]	Mean ± SD	5.0 ± 5.9	27.3 ± 22.8	28.3 ± 22.8	28.5 ± 24.9
Borg Score	Mean ± SD	7.5 ± 1.7	12.4 ± 2.4	10.67 ± 2.3	10.9 ± 2.5

Table 1. *Cont.*

Clinical Data		Control	HFpEF	HFmrEF	HFrEF
Laboratory Values					
Hemoglobin (g/dL)	Mean ± SD	13.9 ± 1.1	12.8 ± 1.2	13.6 ± 1.1	15.0 ± 1.1
Hematocrit	Mean ± SD	0.40 ± 0.03	0.38 ± 0.03	0.40 ± 0.03	0.43 ± 0.04
Creatinin (mg/dL)	Mean ± SD	0.87 ± 0.20	0.92 ± 0.18	1.07 ± 0.33	1.09 ± 0.38
GFR (mL/min)	Mean ± SD	81 ± 10	71 ± 16	70 ± 18	72 ± 21
NT-proBNP (ng/L)	Mean ± SD	91 ± 62	614 ± 607	829 ± 1158	2257 ± 3447
Troponin T (ng/L)	Mean ± SD	7 ± 3	16 ± 12	19 ± 20	18 ± 12
CRP (mg/dL)	Mean ± SD	1.3 ± 1.4	2.9 ± 2.7	3.0 ± 4.2	1.0 ± 0.7
WBC (/nL)	Mean ± SD	6.1 ± 1.6	7.2 ± 2.4	8.5 ± 2.4	8.4 ± 2.3
Medication					
ACE-Inhibitors		2/17 (12%)	4/17 (24%)	7/18 (39%)	9/17 (53%)
Angiotensin-Receptor-Blocker		4/17 (24%)	11/17 (65%)	7/18 (39%)	8/17 (47%)
Calcium-Antagonist		4/17 (24%)	3/17 (18%)	3/18 (17%)	1/17 (6%)
Mineralocorticoid-Receptor-Antagonist		0/17 (0%)	2/17 (12%)	4/18 (22%)	11/17 (65%)
Angiotensin-Receptor-Neprilysin-Inhibitor		0/17 (0%)	0/17 (0%)	0/18 (0%)	4/17 (24%)
Beta-Blocker		6/17 (35%)	10/17 (59%)	14/18 (78%)	17/17 (100%)
Statin		2/17 (12%)	8/17 (47%)	15/18 (83%)	11/17 (65%)
Thiazide Diuretic		4/17 (24%)	4/17 (24%)	2/18 (11%)	1/17 (6%)
Loop Diuretic		0/17 (0%)	3/17 (18%)	7/18 (39%)	6/17 (35%)

Discrete values given as absolute number and percentage of respective HF group. Continuous values given as mean and standard deviation. ACE = angiotensin-converting-enzyme. CRP = C reactive protein. GFR = glomerular filtration rate. LA = left atrium. LGE = late gadolinium enhancement. LVEF = left ventricular ejection fraction. NT-proBNP = N-terminal pro brain natriuritic peptide. NYHA = New York Heart Association. RVEDD = right ventricular end diastolic diameter (MRI, three chamber view). WBC = white blood cell count. [1] Minnesota Living with Heart Failure Questionnaire.

3.2. CMR-Parameters

3.2.1. T2 Relaxation Time

One patient with HFpEF was excluded from analysis due to extensive artifacts. A boxplot of the measurements by group is given in Figure 2A. T2 relaxation times in HFmrEF and HFrEF patients were significantly elevated compared to healthy controls (Table 2). HFpEF patients did not differ significantly from healthy controls. Correlations of T2 with other MRI and baseline-parameters are given in Table 3. Scatter plots, and where appropriate, linear model parameter estimates are given in Figure 3 for the relationship between T2 and NT-proBNP, glomerular filtration rate (GFR), the 6 min walking test and quality of life.

Table 2. Group means and *p*-values for group-wise comparisons.

	Heart Failure Group				*p*-Value				
	Control	HFpEF	HFmrEF	HFrEF	Controls vs. HFpEF	Controls vs. HFmrEF	HFpEF vs. HFmrEF	HFpEF vs. HFrEF	HFmrEF vs. HFrEF
T2 (ms)	50.6 ± 2.1	52.6 ± 3.6	55.4 ± 3.4	56.0 ± 6.0	0.499	0.005 **	0.190	0.078	0.967
T1 native (ms)	972 ± 31	985 ± 32	1027 ± 40	1033 ± 54	0.776	0.001 **	0.023 *	0.005 **	0.954
ECV (%)	27 ± 4 †	27.3 ± 2.6	29.2 ± 2.6	29.3 ± 3.4	0.993	0.186	0.303	0.271	>0.999
GLS (%)	−23.0 ± 3.5	−20.8 ± 3.9	−15.7 ± 2.1	−11.0 ± 3.6	0.252	<0.001 **	<0.001 **	<0.001 **	<0.001 **
GCS (%)	−34.5 ± 6.2	−35.8 ± 6.7	−19.9 ± 4.1	−12.4 ± 4.6	0.902	<0.001 **	<0.001 **	<0.001 **	0.001 **
SR	0.68 ± 0.09	0.59 ± 0.11	0.82 ± 0.17	0.96 ± 0.33	0.600	0.159	0.007 **	<0.001 **	0.151

Data reported as means ± standard deviations. *p*-values calculated from one-way ANOVA with Tukey–Kramer post-hoc analysis. GCS = global circumferential strain, GLS = global longitudinal strain, ECV = extracellular volume, SR = strain ratio (GLS/GCS), T1 = T1 relaxation time and T2 = T2 relaxation time; other abbreviations as in Table 1.
* Significant at $\alpha = 0.05$. ** Significant at $\alpha = 0.01$. † Data from Dabir et al. 2014

Table 3. Correlations of parameters.

		T2	ECV	T1 Native	GLS	GCS	SR	LV-EF
ECV	Pearson r	0.353 **						
	p Value	0.010						
T1 native	Pearson r	0.660 **	0.472 **					
	p Value	<0.001	<0.001					
GLS	Pearson r	0.351 **	0.294 *	0.518 **				
	p Value	0.003	0.034	<0.001				
GCS	Pearson r	0.372 **	0.256	0.484 **	0.868 **			
	p Value	0.002	0.067	<0.001	<0.001			
SR	Pearson r	0.309 **	0.062	0.308 **	0.353 **	0.698 **		
	p Value	0.009	0.663	0.010	0.003	<0.001		
LV-EF	Pearson r	−0.422 **	−0.242	−0.518 **	−0.882 **	−0.929 **	−0.614 **	
	p Value	<0.001	0.090	<0.001	<0.001	<0.001	<0.001	
Age	Pearson r	0.234	−0.100	0.064	−0.199	−0.270 *	−0.202	0.246 *
	p Value	0.052	0.483	0.603	0.095	0.023	0.091	0.020
log(NT-proBNP)	Pearson r	0.642 **	0.287 *	0.601 **	0.544 **	0.544 **	0.234 *	−0.538 **
	p Value	<0.001	0.039	<0.001	<0.001	<0.001	0.050	<0.001
Glomerular filtration rate	Pearson r	−0.441 **	0.106	−0.123	−0.065	−0.057	−0.054	0.085
	p Value	<0.001	0.455	0.314	0.589	0.637	0.655	0.487
C-reactive protein (mg/dL)	Pearson r	0.105	−0.154	−0.006	−0.044	−0.087	−0.112	0.062
	p Value	0.393	0.281	0.961	0.715	0.473	0.357	0.614
Hematocrit	Pearson r	0.101	−0.180	0.150	0.330 **	0.405 **	0.343 **	−0.471 **
	p Value	0.407	0.201	0.219	0.005	<0.001	0.003	<0.001
6 min walking test	Pearson r	−0.345 **	0.273	-0.150	−0.102	0.014	0.138	0.037
	p Value	0.004	0.055	0.224	0.403	0.912	0.258	0.765
Quality of life	Spearman r	0.484 **	0.187	0.359 **	0.184	0.168	0.097	−0.230
	p Value	<0.001	0.185	0.002	0.124	0.162	0.420	0.058

p-values are given for the significance of the correlation coefficient. NT-proBNP was transformed to logarithmic scale. Abbreviations as in Tables 1 and 2. * Significant at $\alpha = 0.05$. ** Significant at $\alpha = 0.01$.

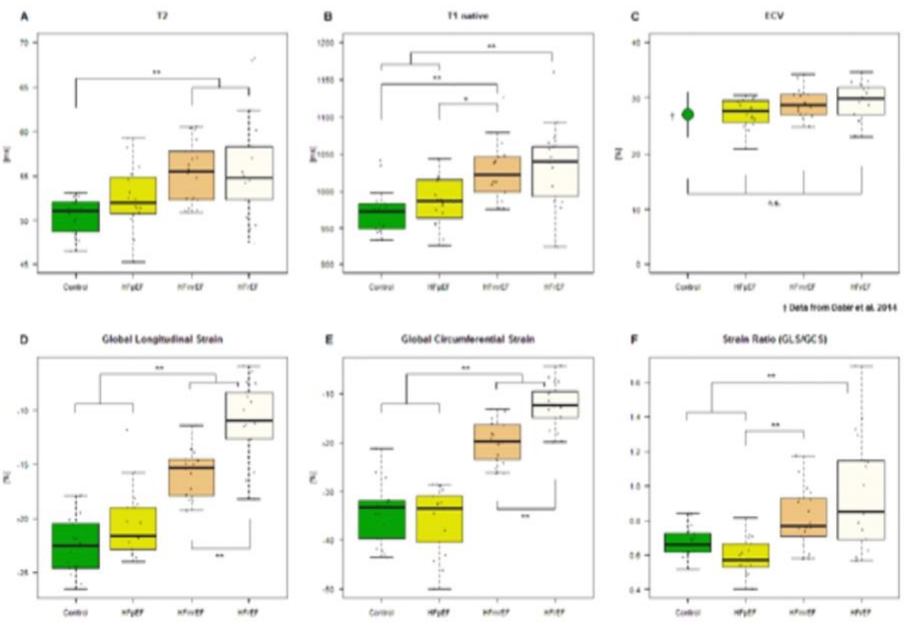

Figure 2. Boxplots of heart failure groups and controls versus (**A**) T2 relaxation time, (**B**) Native T1 relaxation time, (**C**) ECV (controls from Dabir et al. 2014) [14], (**D**) GLS, (**E**) GCS and (**F**) strain ratio (GLS/GCS). * Significant at $\alpha = 0.05$. ** Significant at $\alpha = 0.01$. n.s. = not significant at 0.05. GCS = global circumferential strain, GLS = global longitudinal strain. Other abbreviations as in Figure 1.

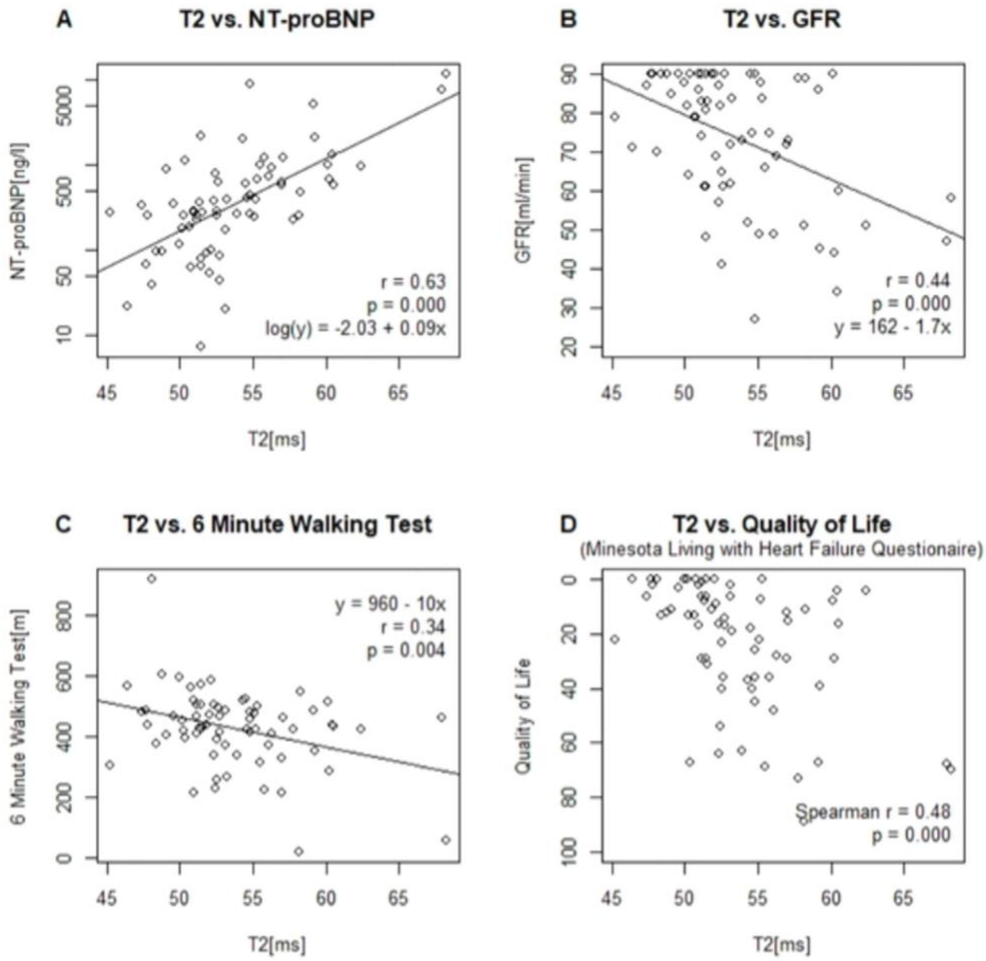

Figure 3. Scatter Plots and linear model parameters of T2 relaxation time versus (**A**) NT-proBNP (logarithmic scale), (**B**) glomerular filtration rate (GFR) and (**C**) 6 min walking test. (**D**) Scatter plot and Spearman's correlation coefficient of T2 relaxation time versus quality of life, as assessed by the Minnesota Living with Heart Failure Questionnaire.

3.2.2. T1 Relaxation Time

One patient with HFpEF and one patient with HFmrEF were excluded from analysis due to extensive artifacts. A boxplot of the measurements by group is given in Figure 2B. Patients with both HFmrEF and HFrEF showed significantly higher T1 relaxation times than controls and HFpEF patients (Table 2). The difference between HFrEF and HFmrEF patients and the difference between HFpEF patients and controls was not statistically significant. The correlations of the T1 relaxation time with MRI and baseline-parameters are given in Table 3.

3.2.3. Extracellular Volume (ECV)

The ECV was calculated for patients with HFpEF, HFmrEF and HFrEF. One patient with HFpEF and one with HFmrEF were excluded from analysis due to extensive artifacts in the T1 mapping sequences, from which ECV would be calculated. A boxplot of the measurements by group is given in Figure 2C and compared to historical data by Dabir et al. for volunteers [14]. None of the differences reached statistical significance (Table 2). The correlations of the ECV with MRI and baseline-parameters are given in Table 3.

3.2.4. Strain

Boxplots for the measurements of GCS, GLS and SR (GLS/GCS) are given in Figure 2D–F. There were no statistically significant differences between HFpEF and controls. Patients with HFmrEF showed significant impairment in both circumferential and longitudinal strain, with further impairment being present in HFrEF patients, reflecting systolic dysfunction. The SR in HFpEF was significantly lower than in HFmrEF and HFrEF. The correlations of the strain parameters with MRI and baseline-parameters are given in Table 3.

4. Discussion

Our study is the first to date to examine advanced imaging markers of remodeling in patients with HFmrEF.

Differences in ECV did not reach statistical significance. The ECV values in our HFpEF patients were lower than those reported in other studies, ranging from 28.3% to 32.9% (Table S1) [19–23]. The difference might be partly explained by differences in the applied scanners, sequences, contrast agents, image analysis, exclusion of LGE and LF-EF cut-off values for HFpEF. The lower ECV might also reflect our slightly healthier HFpEF group compared to previous studies. In our study, great effort was taken to manually adjust MOLLI-images for in-plane motion, thereby reducing artifacts by blood-signal. Blood has higher T1 and ECV values compared to myocardium, leading to falsely elevated myocardial ECV and T1 measurements in case of uncorrected in-plane motion. Additionally, while many studies used mid-ventricular septal measurements, our study measured the median value of all 16 myocardial segments, excluding segments with late enhancement. We chose our approach to be more representative of global left ventricular remodeling and less susceptible to artifacts and focal changes. One study comparing ECV in HFpEF versus HFrEF found a higher ECV in HFrEF, most likely representing advanced fibrosis in HFrEF [22]. Our study did not assess ECV in healthy volunteers. However, data from another study using the same scanner, mapping-sequence and contrast agent found a mean ECV of 27% ± 4% in healthy volunteers [14].

Native T1 relaxation times in HFmrEF were closer to HFrEF than HFpEF. A summary of studies examining native T1 relaxation times is given in Table S1. One study using the same field strength and MRI manufacturer found higher T1 relaxation times for both controls and HFpEF patients compared to our data [19]. Another study using the same field strength and a different MRI manufacturer found similar T1 relaxation times [21]. Yet another study of healthy volunteers found lower T1 relaxation times compared to our controls [14]. The reason for the difference might be attributable to the local setup, as T1 relaxation times are known to be highly setup dependent [24]. Assuming that elevations in native T1 relaxation times truly reflect fibrosis, our findings suggest that HFmrEF shares common pathophysiological changes with HFrEF, while HFpEF seems to resemble a different pathophysiological entity. The lower values for fibrosis markers in HFpEF compared to HFrEF might at least partly explain the lower effectiveness of renin-angiotensin-aldosterone system (RAAS) inhibitors in HFpEF [3,25]. On the other hand, if our findings were to be confirmed in further studies, patients with HFmrEF would be expected to benefit from RAAS inhibitors. This would be in line with the findings of the PARAGON-HF trial, which showed no overall benefit of angiotensin-neprilysin inhibition in all patients with an LV-EF > 45% but a possible benefit for the subgroup with an LV-EF below the median [26].

T2 relaxation times were significantly elevated in HFmrEF and HFrEF compared to healthy controls. Our values for T2 relaxation times in controls were within the published reference range for our mapping sequence [27]. To our knowledge, no studies examining T2 relaxation time in HFpEF and HFmrEF have been published to date. An increase in T2 relaxation time is likely to reflect increased myocardial water content, as it is commonly seen in inflammatory states and myocardial edema [9,28]. Elevated T2 relaxation times have also been found in dilated cardiomyopathy and acute myocardial infarction [29,30]. Current evidence suggests a coincidence of myocardial inflammation and heart failure, although the exact mechanism remains unclear [31]. Consequently, our observed increase in myocardial T2 relaxation times might reflect subclinical myocardial inflammation in heart failure. Of all MRI parameters, T2 relaxation time showed the highest correlation with NT-proBNP and quality of life, and was the only MRI parameter significantly correlated with the 6 min walking test and the GFR. The latter warrants further investigation and might reflect cardiac involvement in renal disease. Irrespective of the exact underlying mechanism, our findings provide further evidence for pathophysiological similarities between HFmrEF and HFrEF.

The observed increase in both longitudinal and circumferential strain in HFmrEF and HFrEF reflects the reduced ejection fraction. Our strain values for controls and patients with HFpEF were within previously published reference values for cardiac MRI-derived endocardial strain [10]. Impairment of both GCS and GLS has been reported in patients with HFpEF both for MRI and speckle tracking echocardiography (STE) derived strain values. [32,33] Of note, while STE and MRI-derived measurements for GLS and GCS generally show good correlations, the absolute values may differ depending on the technique applied [34].

In our study, GLS and GCS seem to increase at different rates as the LV-EF decreases, so that the ratio of longitudinal to circumferential strain (strain ratio, SR) differs in HFpEF compared to HFmrEF and HFrEF. To our knowledge, no previous study has examined the strain ratio as a cardiac parameter. The significance of this remains to be determined in future studies.

One limitation of all parametric mapping studies is the inherent dependence of the measurements on the local setup. Our study does not intend to provide diagnostic criteria but to characterize the heart failure subtypes in relation to each other in terms of pathophysiological targets.

Another obvious limitation of our study is its small sample size. Consequently, small differences between groups and correlations between parameters may have been missed. Yet, despite the small sample size, we found significant differences between heart failure subgroups and hope to contribute towards the characterization of HFmrEF. Our p-values were not corrected for multiple testing and should be confirmed in further studies.

The groups differed in baseline parameters, such as age, sex, comorbidities, laboratory values and medication use. The differences observed are mostly consistent with previous studies, showing intermediate values in HFmrEF compared to HFpEF and HFrEF for the parameters age, sex and NT-proBNP [35–37]. Our HFpEF group seems to be slightly healthier compared to previous studies in regard to mean NT-proBNP, GFR and diuretic use, which might explain some of the differences. Regarding the prevalence of coronary artery disease, previous studies have shown mixed results, with some showing the highest prevalence in HFmrEF, and others in HFrEF [36,38,39]. Mapping parameters were not influenced by the presence of transmural LGE in the excluded segments (Table S2). While mapping and strain parameters showed no relevant correlation with sex (Table S3), hematocrit and age (Table 3), they were indeed highly correlated with NT-proBNP (Table 3). Due to the small sample size, no multivariate analysis was performed and our results may be confounded by these differences, which might be inherent to the underlying pathology.

The high number of patients reclassified with MRI-derived LV-EF compared to echocardiography-derived LV-EF diminishes the comparability of our results with trials relying on echocardiography alone. Furthermore, the question arises as to how many HFpEF patients in the general population actually do have a moderate reduction in LV-EF that is missed by echocardiography.

5. Conclusions

Despite the small sample size, our study was able to show significant adverse remodeling beyond systolic functional impairment in patients with HFmrEF that resembles the changes seen in HFrEF.

Supplementary Materials: The following are available online at http://www.mdpi.com/2077-0383/8/11/1877/s1, Figure S1: Correlation matrix for all continuous baseline and imaging parameters. Table S1: Comparator studies for native T1 (ms) and ECV (%). Table S2: Differences in MRI-parameters by transmural LGE. Table S3: Differences in MRI-parameters between females and males.

Author Contributions: Conceptualization, D.H., F.E., H.-D.D. and S.K.; data curation, R.T., T.L., L.A.M., M.B., E.T., A.D., R.K. and S.M.Z.; formal analysis, P.D.; funding acquisition, S.K.; investigation, P.D., D.H., R.T. and T.L.; methodology, C.S.; project administration, F.E., H.-D.D. and S.K.; resources, R.G., B.P. and S.K.; supervision, S.K.; validation, S.M.Z.; visualization, P.D.; writing—original draft, P.D.; writing—review and editing, P.D., M.B., F.E., H.-D.D. and S.K.

Funding: This work was supported by an unrestricted grant of Philips Healthcare to S.K. T.L. received support from the Lithuanian University of Health Sciences. P.D., D.H., T.L., S.K., F.E., H.-D.D. and B.P. received support from the DZHK (German Center for Cardiovascular Research), Partner Site Berlin. C.S. is an employee of Philips Healthcare.

Acknowledgments: We thank all study participants, the MRI-technicians Gudrun Großer and Corinna Else and our study nurse Monica Post for their time and effort.

Conflicts of Interest: P.D. received a travel grant from Biotronic and owns stock of Siemens AG and Bayer AG. P.D., D.H., T.L., S.K., F.E., H.-D.D. and B.P. received support from the DZHK (German Centre for Cardiovascular Research). C.S. is an employee of Philips Healthcare. B.P. has received advisory board and lecture honoraria from Bayer Healthcare, Novartis, Merck Sharp and Dohme, Stealth Peptides, Sanofi and Servier. F.E. has received advisory board and lecture honoraria from Boehringer Ingelheim, Bayer Healthcare, Novartis, Merck Sharp and Dohme, Vifor, and Servier. H.-D.D. received advisory board honoraria from Bayer, Novartis, Stealt and Berlin Cures. S.K. was supported by an unrestricted research grant from Philips Health Care. All other authors declare that they have no financial or non-financial competing interest to disclose.

References

1. Ponikowski, P.; Voors, A.A.; Anker, S.D.; Bueno, H.; Cleland, J.G.; Coats, A.J.; Falk, V.; Gonzalez-Juanatey, J.R.; Harjola, V.P.; Jankowska, E.A.; et al. ESC Guidelines for the diagnosis and treatment of acute and chronic heart failure: The Task Force for the diagnosis and treatment of acute and chronic heart failure of the European Society of Cardiology (ESC). Developed with the special contribution of the Heart Failure Association (HFA) of the ESC. *Eur. J. Heart Fail.* **2016**, *18*, 891–975. [CrossRef]
2. Cohn, J.N.; Ferrari, R.; Sharpe, N. Cardiac remodeling—Concepts and clinical implications: A consensus paper from an international forum on cardiac remodeling. Behalf of an International Forum on Cardiac Remodeling. *J. Am. Coll. Cardiol.* **2000**, *35*, 569–582. [CrossRef]
3. Zheng, S.L.; Chan, F.T.; Nabeebaccus, A.A.; Shah, A.M.; McDonagh, T.; Okonko, D.O.; Ayis, S. Drug treatment effects on outcomes in heart failure with preserved ejection fraction: A systematic review and meta-analysis. *Heart* **2018**, *104*, 407–415. [CrossRef]
4. Altaie, S.; Khalife, W. The prognosis of mid-range ejection fraction heart failure: A systematic review and meta-analysis. *ESC Heart Fail.* **2018**, *5*, 1008–1016. [CrossRef]
5. Messroghli, D.R.; Moon, J.C.; Ferreira, V.M.; Grosse-Wortmann, L.; He, T.; Kellman, P.; Mascherbauer, J.; Nezafat, R.; Salerno, M.; Schelbert, E.B.; et al. Clinical recommendations for cardiovascular magnetic resonance mapping of T1, T2, T2* and extracellular volume: A consensus statement by the Society for Cardiovascular Magnetic Resonance (SCMR) endorsed by the European Association for Cardiovascular Imaging (EACVI). *J. Cardiovasc. Magn. Reson.* **2017**, *19*, 75. [CrossRef]
6. Ugander, M.; Oki, A.J.; Hsu, L.Y.; Kellman, P.; Greiser, A.; Aletras, A.H.; Sibley, C.T.; Chen, M.Y.; Bandettini, W.P.; Arai, A.E. Extracellular volume imaging by magnetic resonance imaging provides insights into overt and sub-clinical myocardial pathology. *Eur. Heart J.* **2012**, *33*, 1268–1278. [CrossRef]
7. Puntmann, V.O.; Carr-White, G.; Jabbour, A.; Yu, C.Y.; Gebker, R.; Kelle, S.; Hinojar, R.; Doltra, A.; Varma, N.; Child, N.; et al. T1-Mapping and Outcome in Nonischemic Cardiomyopathy: All-Cause Mortality and Heart Failure. *JACC* **2016**, *9*, 40–50. [CrossRef]
8. Schelbert, E.B.; Piehler, K.M.; Zareba, K.M.; Moon, J.C.; Ugander, M.; Messroghli, D.R.; Valeti, U.S.; Chang, C.C.; Shroff, S.G.; Diez, J.; et al. Myocardial Fibrosis Quantified by Extracellular Volume Is Associated With Subsequent Hospitalization for Heart Failure, Death, or Both Across the Spectrum of Ejection Fraction and Heart Failure Stage. *J. Am. Heart Assoc.* **2015**, *4*, e002613. [CrossRef]

9. Bohnen, S.; Radunski, U.K.; Lund, G.K.; Kandolf, R.; Stehning, C.; Schnackenburg, B.; Adam, G.; Blankenberg, S.; Muellerleile, K. Performance of t1 and t2 mapping cardiovascular magnetic resonance to detect active myocarditis in patients with recent-onset heart failure. *Circ. Cardiovasc. Imaging* **2015**, *8*, e003073. [CrossRef]
10. Scatteia, A.; Baritussio, A.; Bucciarelli-Ducci, C. Strain imaging using cardiac magnetic resonance. *Heart Fail. Rev.* **2017**, *22*, 465–476. [CrossRef]
11. DRKS-German Clinical Trials Register. DRKS00015615. Available online: https://www.drks.de (accessed on 10 September 2019).
12. Messroghli, D.R.; Radjenovic, A.; Kozerke, S.; Higgins, D.M.; Sivananthan, M.U.; Ridgway, J.P. Modified Look-Locker inversion recovery (MOLLI) for high-resolution T1 mapping of the heart. *Magn. Reson. Med.* **2004**, *52*, 141–146. [CrossRef] [PubMed]
13. Baessler, B.; Schaarschmidt, F.; Stehning, C.; Schnackenburg, B.; Maintz, D.; Bunck, A.C. Cardiac T2-mapping using a fast gradient echo spin echo sequence-first in vitro and in vivo experience. *J. Cardiovasc. Magn. Reson.* **2015**, *17*, 67. [CrossRef] [PubMed]
14. Dabir, D.; Child, N.; Kalra, A.; Rogers, T.; Gebker, R.; Jabbour, A.; Plein, S.; Yu, C.Y.; Otton, J.; Kidambi, A.; et al. Reference values for healthy human myocardium using a T1 mapping methodology: Results from the International T1 Multicenter cardiovascular magnetic resonance study. *J. Cardiovasc. Magn. Reson.* **2014**, *16*, 69. [CrossRef] [PubMed]
15. Suinesiaputra, A.; Bluemke, D.A.; Cowan, B.R.; Friedrich, M.G.; Kramer, C.M.; Kwong, R.; Plein, S.; Schulz-Menger, J.; Westenberg, J.J.; Young, A.A.; et al. Quantification of LV function and mass by cardiovascular magnetic resonance: Multi-center variability and consensus contours. *J. Cardiovasc. Magn. Reson.* **2015**, *17*, 63. [CrossRef]
16. aus dem Siepen, F.; Buss, S.J.; Messroghli, D.; Andre, F.; Lossnitzer, D.; Seitz, S.; Keller, M.; Schnabel, P.A.; Giannitsis, E.; Korosoglou, G.; et al. T1 mapping in dilated cardiomyopathy with cardiac magnetic resonance: Quantification of diffuse myocardial fibrosis and comparison with endomyocardial biopsy. *Eur. Heart J. Cardiovasc. Imaging* **2015**, *16*, 210–216. [CrossRef] [PubMed]
17. Lurz, P.; Luecke, C.; Eitel, I.; Fohrenbach, F.; Frank, C.; Grothoff, M.; de Waha, S.; Rommel, K.P.; Lurz, J.A.; Klingel, K.; et al. Comprehensive Cardiac Magnetic Resonance Imaging in Patients With Suspected Myocarditis: The MyoRacer-Trial. *J. Am. Coll. Cardiol.* **2016**, *67*, 1800–1811. [CrossRef] [PubMed]
18. Mordi, I.; Carrick, D.; Bezerra, H.; Tzemos, N. T1 and T2 mapping for early diagnosis of dilated non-ischaemic cardiomyopathy in middle-aged patients and differentiation from normal physiological adaptation. *Eur. Heart J. Cardiovasc. Imaging* **2016**, *17*, 797–803. [CrossRef]
19. Rommel, K.P.; von Roeder, M.; Latuscynski, K.; Oberueck, C.; Blazek, S.; Fengler, K.; Besler, C.; Sandri, M.; Lucke, C.; Gutberlet, M.; et al. Extracellular Volume Fraction for Characterization of Patients With Heart Failure and Preserved Ejection Fraction. *J. Am. Coll. Cardiol.* **2016**, *67*, 1815–1825. [CrossRef]
20. Roy, C.; Slimani, A.; de Meester, C.; Amzulescu, M.; Pasquet, A.; Vancraeynest, D.; Beauloye, C.; Vanoverschelde, J.L.; Gerber, B.L.; Pouleur, A.C. Associations and prognostic significance of diffuse myocardial fibrosis by cardiovascular magnetic resonance in heart failure with preserved ejection fraction. *J. Cardiovasc. Magn. Reson.* **2018**, *20*, 55. [CrossRef]
21. Duca, F.; Kammerlander, A.A.; Zotter-Tufaro, C.; Aschauer, S.; Schwaiger, M.L.; Marzluf, B.A.; Bonderman, D.; Mascherbauer, J. Interstitial Fibrosis, Functional Status, and Outcomes in Heart Failure With Preserved Ejection Fraction: Insights From a Prospective Cardiac Magnetic Resonance Imaging Study. *Circ. Cardiovasc. Imaging* **2016**, *9*, e005277. [CrossRef]
22. Su, M.Y.; Lin, L.Y.; Tseng, Y.H.; Chang, C.C.; Wu, C.K.; Lin, J.L.; Tseng, W.Y. CMR-verified diffuse myocardial fibrosis is associated with diastolic dysfunction in HFpEF. *JACC Cardiovasc. Imaging* **2014**, *7*, 991–997. [CrossRef] [PubMed]
23. Schelbert, E.B.; Fridman, Y.; Wong, T.C.; Abu Daya, H.; Piehler, K.M.; Kadakkal, A.; Miller, C.A.; Ugander, M.; Maanja, M.; Kellman, P.; et al. Temporal Relation Between Myocardial Fibrosis and Heart Failure With Preserved Ejection Fraction: Association With Baseline Disease Severity and Subsequent Outcome. *JAMA Cardiol.* **2017**, *2*, 995–1006. [CrossRef] [PubMed]
24. Kawel-Boehm, N.; Maceira, A.; Valsangiacomo-Buechel, E.R.; Vogel-Claussen, J.; Turkbey, E.B.; Williams, R.; Plein, S.; Tee, M.; Eng, J.; Bluemke, D.A. Normal values for cardiovascular magnetic resonance in adults and children. *J. Cardiovasc. Magn. Reson.* **2015**, *17*, 29. [CrossRef] [PubMed]

25. Butler, J.; Fonarow, G.C.; Zile, M.R.; Lam, C.S.; Roessig, L.; Schelbert, E.B.; Shah, S.J.; Ahmed, A.; Bonow, R.O.; Cleland, J.G.; et al. Developing therapies for heart failure with preserved ejection fraction: Current state and future directions. *JACC Heart Fail.* **2014**, *2*, 97–112. [CrossRef] [PubMed]
26. Solomon, S.D.; McMurray, J.J.V.; Anand, I.S.; Ge, J.; Lam, C.S.P.; Maggioni, A.P.; Martinez, F.; Packer, M.; Pfeffer, M.A.; Pieske, B.; et al. Angiotensin-Neprilysin Inhibition in Heart Failure with Preserved Ejection Fraction. *N. Engl. J. Med.* **2019**, *381*, 65–72. [CrossRef]
27. Baessler, B.; Schaarschmidt, F.; Stehning, C.; Schnackenburg, B.; Maintz, D.; Bunck, A.C. A systematic evaluation of three different cardiac T2-mapping sequences at 1.5 and 3T in healthy volunteers. *Eur. J. Radiol.* **2015**, *84*, 2161–2170. [CrossRef]
28. Thavendiranathan, P.; Walls, M.; Giri, S.; Verhaert, D.; Rajagopalan, S.; Moore, S.; Simonetti, O.P.; Raman, S.V. Improved detection of myocardial involvement in acute inflammatory cardiomyopathies using T2 mapping. *Circ. Cardiovasc. Imaging* **2012**, *5*, 102–110. [CrossRef]
29. Nishii, T.; Kono, A.K.; Shigeru, M.; Takamine, S.; Fujiwara, S.; Kyotani, K.; Aoyama, N.; Sugimura, K. Cardiovascular magnetic resonance T2 mapping can detect myocardial edema in idiopathic dilated cardiomyopathy. *Int. J. Cardiovasc. Imaging* **2014**, *30*, 65–72. [CrossRef]
30. Verhaert, D.; Thavendiranathan, P.; Giri, S.; Mihai, G.; Rajagopalan, S.; Simonetti, O.P.; Raman, S.V. Direct T2 quantification of myocardial edema in acute ischemic injury. *JACC Cardiovasc. Imaging* **2011**, *4*, 269–278. [CrossRef]
31. Dick, S.A.; Epelman, S. Chronic Heart Failure and Inflammation: What Do We Really Know? *Circ. Res.* **2016**, *119*, 159–176. [CrossRef]
32. Mordi, I.R.; Singh, S.; Rudd, A.; Srinivasan, J.; Frenneaux, M.; Tzemos, N.; Dawson, D.K. Comprehensive Echocardiographic and Cardiac Magnetic Resonance Evaluation Differentiates Among Heart Failure With Preserved Ejection Fraction Patients, Hypertensive Patients, and Healthy Control Subjects. *JACC Cardiovasc. Imaging* **2018**, *11*, 577–585. [CrossRef] [PubMed]
33. DeVore, A.D.; McNulty, S.; Alenezi, F.; Ersboll, M.; Vader, J.M.; Oh, J.K.; Lin, G.; Redfield, M.M.; Lewis, G.; Semigran, M.J.; et al. Impaired left ventricular global longitudinal strain in patients with heart failure with preserved ejection fraction: Insights from the RELAX trial. *Eur. J. Heart Fail.* **2017**, *19*, 893–900. [CrossRef] [PubMed]
34. Obokata, M.; Nagata, Y.; Wu, V.C.; Kado, Y.; Kurabayashi, M.; Otsuji, Y.; Takeuchi, M. Direct comparison of cardiac magnetic resonance feature tracking and 2D/3D echocardiography speckle tracking for evaluation of global left ventricular strain. *Eur. Heart J. Cardiovasc. Imaging* **2016**, *17*, 525–532. [CrossRef] [PubMed]
35. Hamatani, Y.; Nagai, T.; Shiraishi, Y.; Kohsaka, S.; Nakai, M.; Nishimura, K.; Kohno, T.; Nagatomo, Y.; Asaumi, Y.; Goda, A.; et al. Long-Term Prognostic Significance of Plasma B-Type Natriuretic Peptide Level in Patients With Acute Heart Failure With Reduced, Mid-Range, and Preserved Ejection Fractions. *Am. J. Cardiol.* **2018**, *121*, 731–738. [CrossRef]
36. Guisado-Espartero, M.E.; Salamanca-Bautista, P.; Aramburu-Bodas, O.; Conde-Martel, A.; Arias-Jimenez, J.L.; Llacer-Iborra, P.; Davila-Ramos, M.F.; Cabanes-Hernandez, Y.; Manzano, L.; Montero-Perez-Barquero, M.; et al. Heart failure with mid-range ejection fraction in patients admitted to internal medicine departments: Findings from the RICA Registry. *Int. J. Cardiol.* **2018**, *255*, 124–128. [CrossRef]
37. Lauritsen, J.; Gustafsson, F.; Abdulla, J. Characteristics and long-term prognosis of patients with heart failure and mid-range ejection fraction compared with reduced and preserved ejection fraction: A systematic review and meta-analysis. *ESC Heart Fail.* **2018**, *4*, 685–694. [CrossRef]
38. Choi, K.H.; Lee, G.Y.; Choi, J.O.; Jeon, E.S.; Lee, H.Y.; Cho, H.J.; Lee, S.E.; Kim, M.S.; Kim, J.J.; Hwang, K.K.; et al. Outcomes of de novo and acute decompensated heart failure patients according to ejection fraction. *Heart* **2018**, *104*, 525–532. [CrossRef]
39. Farmakis, D.; Simitsis, P.; Bistola, V.; Triposkiadis, F.; Ikonomidis, I.; Katsanos, S.; Bakosis, G.; Hatziagelaki, E.; Lekakis, J.; Mebazaa, A.; et al. Acute heart failure with mid-range left ventricular ejection fraction: Clinical profile, in-hospital management, and short-term outcome. *Clin. Res. Cardiol.* **2017**, *106*, 359–368. [CrossRef]

9. Lebenslauf

Mein Lebenslauf wird aus datenschutzrechtlichen Gründen in der elektronischen Version meiner Arbeit nicht veröffentlicht.

10. Publikationsliste

	Originalarbeiten in Zeitschriften mit Peer-Review-Verfahren	IF*
1.	**Blum, M.**, Hashemi, D., Motzkus, L. A., Neye, M., Dordevic, A., Zieschang, V., Zamani, S. M., Lapinskas, T., Runte, K., Kelm, M., Kühne, T., Tahirovic, E., Edelmann, F., Pieske, B., Düngen, H.-D. & Kelle, S. Variability of Myocardial Strain During Isometric Exercise in Subjects With and Without Heart Failure. *Frontiers in Cardiovascular Medicine* **7,** 111 (2020).	3.915
2.	**Blum, M.**, Cao, D., Chandiramani, R., Goel, R., Roumeliotis, A., Sartori, S., Beyhoff, N., Kelle, S., Kovacic, J. C., Krishnan, P., Sweeny, J., Barman, N., Baber, U., Dangas, G. D., Kini, A., Sharma, S. K. & Mehran, R. Prevalence and prognostic impact of hsCRP elevation are age-dependent in women but not in men undergoing percutaneous coronary intervention. *Catheterization and Cardiovascular Interventions* (2020). doi: 10.1002/ccd.29402	2.044
3.	Hashemi, D., **Blum, M.**, Mende, M., Störk, S., Angermann, C. E., Pankuweit, S., Tahirovic, E., Wachter, R., Pieske, B., Edelmann, F., Düngen, H.-D. & German Competence Network for Heart Failure. Syncopes and clinical outcome in heart failure: results from prospective clinical study data in Germany. *ESC Heart Failure* **7,** 942–952 (2020).	3.490
4.	Tanacli, R., Hashemi, D., Neye, M., Motzkus, L. A., **Blum, M.**, Tahirovic, E., Dordevic, A., Kraft, R., Zamani, S. M., Pieske, B., Düngen, H.-D. & Kelle, S. Multilayer myocardial strain improves the diagnosis of heart failure with preserved ejection fraction. *ESC Heart Failure* **7,** 3240–3245 (2020).	3.490

5. Chandrasekhar, J., Kalkman, D. N., Sartori, S., Baber, U., **Blum, M.**, Aquino, M. B., Woudstra, P., Beijk, M. A., Tijssen, J. G., Koch, K. T., Dangas, G. D., Colombo, A., de Winter, R. J., Mehran, R. & MASCOT and REMEDEE investigators. 2.044
   One-year clinical outcomes in patients with chronic kidney disease treated with COMBO stents: From the COMBO collaboration. *Catheterization and Cardiovascular Interventions* (2020). doi:10.1002/ccd.29270

6. Goel, R., Cao, D., Chandiramani, R., Roumeliotis, A., **Blum, M.**, Bhatt, D. L., Angiolillo, D. J., Ge, J., Seth, A., Saito, S., Krucoff, M., Kozuma, K., Makkar, R. M., Bangalore, S., Wang, L., Koo, K., Neumann, F.-J., Hermiller, J., Stefanini, G., Valgimigli, M. & Mehran, R. 2.044
   Comparative influence of bleeding and ischemic risk factors on diabetic patients undergoing percutaneous coronary intervention with everolimus-eluting stents. *Catheterization and Cardiovascular Interventions* (2020). doi:10.1002/ccd.29314

7. Chandiramani, R., Cao, D., Claessen, B. E., Sorrentino, S., Guedeney, P., **Blum, M.**, Goel, R., Roumeliotis, A., Krucoff, M., Kozuma, K., Ge, J., Seth, A., Makkar, R., Bangalore, S., Bhatt, D. L., Angiolillo, D. J., Ruster, K., Wang, J., Saito, S., Neumann, F.-J., Hermiller, J., Valgimigli, M. & Mehran, R. 4.660
   Sex-Related Differences in Patients at High Bleeding Risk Undergoing Percutaneous Coronary Intervention: A Patient-Level Pooled Analysis From 4 Postapproval Studies. *Journal of the American Heart Association* **9,** e014611 (2020).

8. Guedeney, P., Claessen, B. E., Baber, U., Camaj, A., Sorrentino, S., Aquino, M., **Blum, M.**, Chandiramani, R., Goel, R., Elsayed, S., Kovacic, J. C., Sweeny, J., Barman, N., Moreno, P., Dangas, G. D., Kini, A., Sharma, S. & Mehran, R. 2.570
   Temporal Trends in Statin Prescriptions and Residual Cholesterol Risk in Patients With Stable Coronary Artery Disease Undergoing Percutaneous

Coronary Intervention. *American Journal of Cardiology* **123,** 1788–1795 (2019).

9. Doeblin, P., Hashemi, D., Tanacli, R., Lapinskas, T., Gebker, R., Stehning, C., Motzkus, L. A., **Blum, M.**, Tahirovic, E., Dordevic, A., Kraft, R., Zamani, S. M., Pieske, B., Edelmann, F., Düngen, H.-D. & Kelle, S. 5.583
CMR Tissue Characterization in Patients with HFmrEF. *Journal of Clinical Medicine* **8,** (2019).

Übersichtarbeiten in Zeitschriften mit Peer-Review-Verfahren

1. **Blum, M.**, Cao, D. & Mehran, R. 2.200
Device profile of the Resolute Onyx Zotarolimus eluting coronary stent system for the treatment of coronary artery disease: overview of its safety and efficacy. *Expert Review Medical Devices* **17,** 257–265 (2020).

Ausgewählte Konferenzbeiträge

1. **Blum M.**, Chandiramani R., Mehran R., Cao D., Singleton R., Goel R., Roumeliotis A., Beyhoff A., Kapur V., Hasan C., Suleman J., Kesanakurthy S., Dangas G., Khan A. A, Krishnan P., Barman N., Kovacic J. C., Sweeny J., Sharma S. K. & Kini A.
Prevalence and Prognostic Value of Elevated High-Sensitivity C-reactive Protein Differ Between Races/Ethnicities Undergoing Percutaneous Coronary Intervention.
Poster präsentiert bei *American Heart Association's 2019 Scientific Sessions* (Abstract 14789); Publiziert in *Circulation* **140,** A14789–A14789 (2019).

2. **Blum M.**, Guedeney, P., Claessen, B., Aquino, M., Kalkman, D., Sorrentino, S., Chandiramani, R., Elsayed, S., Goel, R., Vogel, B., Barman, N., Sweeny, J., Kovacic, J., Kini, A., Dangas, G., Baber, U., Sharma, S. & Mehran, R.
Residual Inflammatory Risk in Patients with Chronic Kidney Disease Undergoing Percutaneous Coronary Intervention.

Poster präsentiert bei *The American College of Cardiology 68th Annual Scientific Session 2019*. Publiziert in *Journal of the American College of Cardiology* **73,** 1357 (2019)

3. **Blum M.**, Claessen, B., Mehran, R., Cao, D., Aquino, M., Chandiramani, R., Goel, R., Roumeliotis, A., Dangas, G., Baber, U., Khan, A., Krishnan, P., Barman, N., Sharma, S. & Kini, A.
Patients Who Do Not Receive Drug-Eluting Stent for In-Stent Restenosis: Characteristics and Outcomes.
Poster präsentiert beim *Thirty First Annual Symposium Transcatheter Cardiovascular Therapeutics 2019* (Abstract TCT-662). Publiziert in *Journal of the American College of Cardiology* **74,** B650 (2019).

4. **Blum M.**, Chandiramani, R., Mehran, R., Cao, D., Sartori, S., Goel, R., Roumeliotis, A., Beyhoff, N., Dangas, G., Baber, U., Khan, A., Krishnan, P., Barman, N., Sharma, S. & Kini, A..
Inflammatory Risk Status Is Age-Dependent in Women but Not in Men Undergoing Percutaneous Coronary Intervention.
Poster präsentiert beim *Thirty First Annual Symposium Transcatheter Cardiovascular Therapeutics* (Abstract TCT-833). Publiziert in *Journal of the American College of Cardiology* **74,** B816 (2019).

5. Hashemi, D., **Blum M.**, Kraft, R., Mende, M., Stoerk, S., Angermann, C. E., Pankuweit, S., Wachter, R., Edelmann, F., Pieske, B. & Duengen, H. D.
The history of syncope in heart failure. Mortality increases - but not in all. Poster präsentiert bei *European Society of Cardiology Congress 2017* (Abstract P1082). Publiziert in *European Heart Journal* **38,** (2017).

* Impact Factor im Erscheinungsjahr der Publikation

11. Danksagung

Mein Dank gilt als erstes Herrn Professor Sebastian Kelle, der mit seiner unermüdlichen Unterstützung diese Arbeit möglich gemacht hat und mich auf wissenschaftlicher, professioneller und menschlicher Ebene viel Wichtiges gelehrt hat.

Des Weiteren danke ich den Mitarbeiterinnen und Mitarbeitern der kardiologischen Studienambulanz der Charité Campus Virchowklinikum und der CMR am Deutschen Herzzentrum Berlin, namentlich Frau Monica Post, Frau Corinna Else, Frau Yvonne Saewe und Frau Franziska Jesuiter sowie Herrn Dr. Elvis Tahirovic für ihre praktische Hilfe bei der Durchführung der Studie. Herrn Dr. Djawid Hashemi danke ich für immer wieder guten wissenschaftlichen Austausch und eine langjährige Freundschaft. Meinen Ko-DoktorandInnen Frau Laura Motzkus und Herrn Aleksandar Dordevic danke ich für hervorragenden Teamgeist.

Zum Schluss gilt mein Dank von Herzen Cosima Mattner und meiner lieben Mutter Catharina Blum.